Master's degree thesis

Ship Machinery Configuration Analysis - An Open Source Web-based Simulation Environment

Azibodusi Osain

Aalesund, 20.12.2020

Norwegian University of Science and Technology
Department of Ocean Operations and Civil Engineering

Mandatory statement

Each student is responsible for complying with rules and regulations that relate to examinations and to academic work in general. The purpose of the mandatory statement is to make students aware of their responsibility and the consequences of cheating. **Failure to complete the statement does not excuse students from their responsibility.**

Please complete the mandatory statement by placing a mark ***in each box*** *for statements 1-6 below.*		
1.	**I/we herby declare that my/our paper/assignment is my/our own work, and that I/we have not used other sources or received other help than is mentioned in the paper/assignment.**	☒
2.	**I/we herby declare that this paper** 1. Has not been used in any other exam at another department/university/university college 2. Is not referring to the work of others without acknowledgement 3. Is not referring to my/our previous work without acknowledgement 4. Has acknowledged all sources of literature in the text and in the list of references 5. Is not a copy, duplicate or transcript of other work	Mark each box: 1. ☒ 2. ☒ 3. ☒ 4. ☒ 5. ☒
3.	**I am/we are aware that any breach of the above will be considered as cheating, and may result in annulment of the examination and exclusion from all universities and university colleges in Norway for up to one year, according to the Act relating to Norwegian Universities and University Colleges, section 4-7 and 4-8 and Examination regulations at NTNU.**	☒
4.	**I am/we are aware that all papers/assignments may be checked for plagiarism by a software assisted plagiarism check.**	☒
5.	**I am/we are aware that The Norwegian University of Science and Technology (NTNU) will handle all cases of suspected cheating according to prevailing guidelines.**	☒
6.	**I/we are aware of the University's rules and regulations for using sources.**	☒

Publication agreement

ECTS credits: 30

Supervisor: Henrique M. Gaspar

Co-Supervisor: Ícaro Aragão Fonseca

Agreement on electronic publication of master thesis

Author(s) have copyright to the thesis, including the exclusive right to publish the document (The Copyright Act §2).
All theses fulfilling the requirements will be registered and published in Brage with the approval of the author(s).

I/we hereby give NTNU the right to, free of charge, make the thesis available for electronic publication: ☒**yes** ☐**no**

Is there an agreement of confidentiality? ☐**yes** ☒**no**
(A supplementary confidentiality agreement must be filled in)

Date: 16.12.2020

Ship Machinery Configuration Analysis - An Open Source Web-based Simulation Environment

Introduction

During conceptual or early phase of ship design, some parameters of the vessel are required to be estimated which may include the machinery configuration, installed power, hull, type of propulsion system, etc. These estimations are usually based on analytical result or operational profile of the ship. In this stage of design phase, there are different software's and tools dedicated for simulation or analysis of these different sub-systems to estimate these result like hull, resistance, etc While no or few tools or software are dedicated for simulation or analyzing of machinery configuration.

Motivation

Ship with DE or Hybrid propulsion uses complex machinery configuration. these ships are also increasing in complexity therefore the need for a software or tools for simulation of these different machinery configuration become eminent in other to aiding in analysis of these different configuration. In addition to trend in open source software, the application will be an open source software.

Scope

The scope of this thesis is to develop the basis of an open source simulation environment where other system will be built upon or improve. The environment shall be develop based on ship propulsion machinery and using JavaScript as the major language.

Objectives

The main objective of this thesis is to:

- Use web technologies to develop simulation environment.
- How can this technologies be used to achieved the goal.
- Present machinery as a mathematical model and as Object which are then used in developing the software.

Milestones:

Tasks:

1. Literature review.
   a) State of the art; researching related works that has been done.
   b) Ship propulsion machinery; theories regarding propulsion machinery.
   c) Web-based technologies; researching and gaining more knowledge on technology needed to develop the application.
2. Methodology
   a) Creating method; developing the methodology for the thesis.
   b) Development of application; developing the open-source application.
3. Analysis
   c) Transit Case study.
   d) Engine dynamic case study.
4. Results and discussion.
5. Writing

Schedule

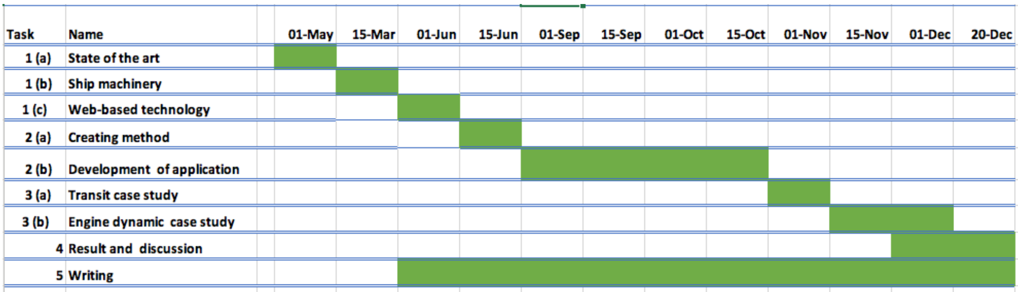

The thesis shall be written as a research report, following the template given in Inspera. During preparation of the text, the candidate should make efforts to create a well-arranged and well-written report. To ease the evaluation of the thesis, it is important to cross-reference text, tables and figures. For evaluation of the work a thorough discussion of results is needed. Discussion of research method, validation and generalization of results is also appreciated.

The thesis shall be submitted in electronic version according to standard procedures (.PDF or .ZIP files). Instructions are found on the NTNU website (Inspera) and on Blackboard. In addition to the specified tasks, an A3 poster should be prepared and delivered together with this proposal, and a conference paper will be handled at the end of the research.

After finalizing and delivering the thesis, it must be sent a copy to the supervisor(s).

Deliveries:
Final Thesis + Article (20th December)

Azibodusi Osain
Student - Master Program
PHONE (+47) 9730400
E-mail. azibodusiosain@gmail.com

Henrique Murilo Gaspar
Supervisor – IHB
E-mail: henrique.gaspar@ntnu.no

Ícaro Aragão Fonseca
CO-Supervisor: IHB
E-mail : icaro.a.fonseca@ntnu.no

Preface

This Research is part of the Master of Science degree in Product and System Design at the Norwegian University of Science and Technology (NTNU) in lesund, 2020. The workload corresponds to 30 ECTS. The research focuses on developing the basis of a open source simulation software for ship machinery configuration. The software was built by using different model which where used represent ship machinery and integrate this model into the software. where different functionalities where implement into the models to have the behaviours of a real system.

Acknowledgment

I will like to thank my project Supervisor Henrique M. Gaspar and my co-supervisor Ícaro Aragão Fonseca for their guidance. During the process of deciding a case study, I will like to thank Ícaro for suggesting Gunnerus vessel as a case study and also the back for fort movement of trying to get the corresponding data of the vessel and also the review and feedback.

I will also want to thank Håvard Vollset Lien for providing the area of the Bulbous bow cross sectional and the area of the wet transom of the vessel.

Abstract

In the conceptual design phase of a ship, some of the parameters of the ship are required to be estimated to allow engineers proceed to other stages of the design. A ship is a complex structure which can be divided into many areas, in the conceptual phase some engineers might be involved in the design of the hull (structure) while others might be involved in the machinery of the ship. There are many tools and software that aid engineers in designing the hull while only few tools are available for analysis of the machinery of the ship.

Therefore in this thesis, an application for ship machinery configuration analysis will be developed. The development of the software will be done with JavaScript programming language, where a concept in JavaScript called "Object-Oriented Programming " (OOP) will be used. The application that will be developed will use the concept of open-source software to allow a wide range of engineers to contribute to the development of the system.

To develop the application, the thesis uses the concept of OOP to represent the machinery as an object where methods are added to the object. These objects and methods for each machinery were then used to build the software. The application is divided into 7 modules which include resistance module for estimation of resistance, propeller module for propeller analysis, SFOC module for engine performance analysis, power source module for the different power source example diesel engine and battery storage, simulation module for performing different simulations (transit and DP), PMS module is an algorithm that is designed to performing the functions of a PMS on a vessel which is integrated into the software, and data insights module is used for the analysis of the data generated during simulation. With these modules, a complex simulation could be made where these modules interact with one another. The result of the thesis is a software that allows a user to perform analysis with different machinery configuration.

The software developed was used to perform an analysis case study with NTNU research Vessel Gunnerus. The first analysis of the vessel was a simulation in transit mode, where the vessel moves from Trondheim to Aalesund. The analysis from the data insight is the emission, fuel consumption and others. The second analysis is done to determine the dynamic load effects on gunnerus engine in a rough environment with different machinery configuration. One configuration is an hybrid (DE and battery pack) installed and other configuration is DE. The results of the two configurations were compared with each other, which shows that the result of the simulation with DE configuration will have large impact from the dynamic load on the gen-set which results in low efficiency of the gen-set and therefore resulting in higher emission and fuel consumption.

Table of Contents

List of Tables

List of Figures

Abbreviations

[H] **Symbol**	**definition**
$ITTC$:	International Towing Tank conference
$SFOC$:	Specific fuel oil consumption
RPM :	Rotation per minute
P :	Engine power
L :	Cylinder length
p_{mep} :	Mean effective pressure
A :	engine piston Area
N_e :	Numbers of rotation rpm
n_r :	Numbers of revolutions required to complete one engine
n_c :	Numbers of engine cylinder
V_d :	Displacement of the cylinder
P_L :	Load on the engine
EF ;	Emission factor
t :	Operating time
L_{WL} :	Waterline Length
B :	Molded beam
T:	Molded mean draught
$C_{B,WL}$:	Block coefficient
R_T :	Calm water ship Resistance
V :	Ship speed
S :	Hull wetted surface area
C_T :	Total resistance coefficient
C_F :	Frictional factor
R_F :	Frictional resistance
R_{APP} :	Appendage resistance
R_W :	Wave resistance
R_B :	Resistance due to bulbous bow near the water surface
R_{TR} :	Pressure resistance due to immersed transom
R_A :	Model-ship correlation
R_{AA} :	Air resistance
C_M :	Midship section coefficient
C_p :	Prismatic coefficient
C_{WP} :	Waterline area coefficient
L_R :	Is the Run
l_{cb} :	Longitudinal center of buoyancy
∇ :	molded volumetric displacement
F_n :	Floude number

R_e :	Reynolds number
$C_{D_{TH}}$:	Drag coefficient of the thruster
S_{APPi} :	iS the wetted area of the of individual appendage.
i_E :	Half angle of waterline entrance
D :	Diameter of the propeller
T_F :	Molded draft at forward perpendicular
T_A :	Molded draft at aft perpendicular
h_B :	Height of the center above A_{BT}, it is $< 0.6T_F$
A_{BT} :	Transverse area of the bulbous bow
w :	is the wake
t :	thrust deduction factor
P_D :	Power delivered to the propeller
R_{wave} :	Wave added resistance
R_{Awind} :	Wind resistance
C_W :	Wind resistance coefficient
A_F :	Is the frontal area
L_{pp} :	Length between perpendicular
$h_s = H_{1/3}$:	Significant wave height
L_{BWL} :	Distance from bow to 95% of the maximum breath on the waterline
P/D :	pitch diameter ration
A_E/A_0 :	expanded ratio
K_{Qo} :	Open water torque coefficient
K_{To} :	Open water thrust coefficient
K_T and K_Q :	Are general thrust and torque coefficient
J :	Advance coefficient
T_p :	Is the propeller thrust
Q :	Is the Torque
Z :	Is the number of blades
s, t, u, v :	Are are coefficient for propeller polynomials
$V_{0.7}$:	Undisturbed incident velocity to the propeller blade at radius
C_T :	Thrust coefficient for 4 quadrant
C_Q :	Torque coefficient for 4 quadrant
$(A_T(k)$ and $B_T(k)$:	Are are coefficient used for the Fourier series
P_E :	Effective power
P_T :	The thrust power
η_H :	Hull efficiency
η_D :	propulsion efficiency
P_B:	Is the break power
η_S :	Is the Shaft efficiency
η_T :	Is the total efficiency
Q_B :	Is the required Engine torque

Chapter 1

Introduction

In this section an overview of the thesis introduction will be described, which include the background, motivation, objective and research, scope and the thesis structure.

1.1 Problem

A ship is a complex system with different sub-systems and components which can be considered separately Tinga et al. [14]. During the conceptual or early phase of ship design, some parameters of these sub-systems are required to be estimated which may include the machinery configuration, installed power, hull, type of propulsion system, etc. These estimations are usually based on an analytical result or operational profile of the ship. In this stage of the design phase, there are different software and tools dedicated to simulation or analysis of these different sub-systems to estimate these results. A typical data required in the early stage is the ship resistance which is a major criterion used in estimating the required power of the ship. This is normally obtained at a later stage by creating a scaled model of the vessel and test it in towing to obtained the resistance.

As the requirement for energy efficiency and emission on vessel tightens, DE and hybrid propulsion are becoming increasing. These type of vessel required a complex machinery configuration system to be installed on the vessel Riviera [15]. Where the machinery configuration installed on the ship depends on the operational profile of the ship and other criteria like environmental, cost, etc. For the designer to be able to decide the machinery configuration to be installed on the ship, analysis or simulation is done with different configurations of the machinery to determine which configuration provides the optimal solution for the desired KPI. This is an important phase of the ship design since the machinery determines how the vessel will be operated, emission, cost, redundancy etc. In this phase, most of the sub-systems have dedicated software for that purpose, for example design of the hull, resistance estimation, have numerous of tools for analysis. While no or few tools/software are dedicated for machinery configuration analysis Solem et al. [16], Egil Christoffer [17].

In the maritime and offshore industry, some of the operation carried out on vessel are very complex and are done in rough weather condition, therefore it is important that these operations are well planned to ensure the operators are familiar with the process or know what is possible to be expected, these are usually achieved by running the operation in a simulated environment similar to where the operation will take place to ensure smooth operation. There are many companies specialized in offering these services, currently there are a limited number or no web-based simulation tools that are open-source for these operation simulation or capable to be used for optimization of a design process. Whereby the effect of any changes made on the sub-model will automatically be applied to the entire system. Most of the tools available works separately and their results are not automatically used by other sub-systems. for example, the changes made on the hull will not reflect on the resistance since they are usually done by separate tool exception of few software.

1.2 Motivation

Today cloud computing has become a trend within the software industry because of its capabilities to allow applications to be deployed on the web, thereby eliminating the need for installing these applications on the devices. this has given rise to complex applications to be deployed and used over the browser. One of the problems in the traditional software for large simulations is the large computational energy required which not all computer have. With cloud computing, a complex web-based applications could be accessed on the browser, a typical example of this is "SimScale".

Open sources projects have continued to gain momentum across industry ranging from building, robotics, and software industry. Recently, the maritime industry is joining the trend of Open source systems, for example Open Simulation Platform (OSP) and Veesel.js. The motivation of the thesis is to is due to different factors.

- The main motivation of this thesis is the limited numbers of ship machinery configuration analysis tools available for testing or analyzing different machinery as mentioned in section 1.1, this creates a motive for the thesis on developing ship machinery configuration analysis environment that will allows the changes on any of the sub-system to be applied to the entire system.

- Open source and web technologies hold great potential to allow the development of a complex systems and in this era of open source collaboration developers and engineers all over could joint hands to develop open-source tools that could be accessed in our browsers for machinery configuration.

Combining these two reasons the thesis will focus on developing an open source to allow different developers and engineers to develop an environment that allows ship machinery to be configured and test to see there effects on different KPI.

1.3 Objective and research question

The main objective of this thesis is to develop the basis of a web-based open-source software for ship machinery configuration analysis that will allow developers and engineers to improve on the system. The platform will be designed using JavaScript, CSS, HTML as the programming language and other open source visualization libraries. To achieved this, the corresponding models or mathematical equations that already been established in previous publications or report will be used. The thesis will answer these questions:

1. Can web Technologies be used to develop simulation environment ?

2. How can this technologies be used to achieved the goal?

3. Can vessel machinery be represented as mathematical model and as Object?

4. What are the necessary models that are required?

5. How can these model be combine with web technologies to develop simulation environment?

1.4 Scope

In order to design a tool for machinery configuration, the scope of the thesis is divided into ship machinery, web technologies and simulation environment as shown in Figure 1.

- **Ship machinery**; Since ship have many different machinery, therefore not all the machinery will be considered in this thesis. The machinery considered in this thesis are the required machinery for propulsion system, their theories and mathematical models that will be used to represent them.

- **Web technologies**; The web technologies refers the different technologies that will be used in developing the application and how machinery are represented with this technologies. The main technologies are JavaScript which is used for representing the machinery and how they function, CSS, HTML, and visualization libraries like plotly.js and Chart.js.

- **Simulation Environment**; The simulation environment is the result of the ship machinery which were represented by models and mathematical equations that have been computed using JavaScript and can be accessed with the browser.

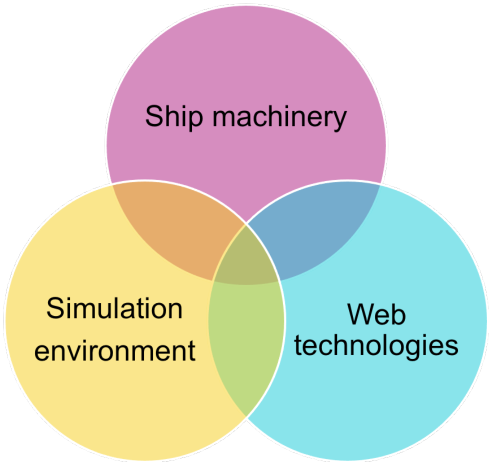

Figure 1: Scope

1.5 Structure of the thesis

The structure of the thesis is organized into 6 chapters as presented below.

Chapter 2
This chapter is divided into two main section, section 2.1 present and review some selected state of the art of different projects/reports that have been done related to the thesis while section 2.2 investigate different theories in ship machinery, how this machinery can be used to form different configuration, ship hull and its resistance, and web-based development. Where the machinery presented are battery pack, diesel engine, and propeller. The ship hull resistance is presented using Holtrop and Mennen‘s method. The web-based development presented is based on a method called ”object oriented” using JavaScript.

Chapter 3
This chapter presents the methodology and approach used in this thesis. It presents a flowchart of how the methodology is implemented. It also presents how machinery are represented as an object in JavaScript and showing how diesel engine are represented as an object, Power management system (PMS), the hierarchy of the application and present how different systems works using a block diagram. Finally, the steps needed to perform a simulation is presented using an example of a vessel.

Chapter 4
This chapter present the case study that was done using the application that was developed in this thesis. The case study involves NTNU vessel called “Gunnerus”. The analysis down with gunnerus involves simulation and analysis for calm water using DE propulsion , simulation and analysis of during a rough water condition and final analysis on the effect of installing a battery pack on the vessel.

Chapter 5

This chapter is the discussion section of the thesis. It is divided into Discussion regarding development of the application, the result of the analysis , other possible simulation that could be done on the application and conclusion.

Chapter 6

This chapter presented future of this thesis that should be done.

Chapter 2

Literature Review

This chapter will discuss and present theories that are related to the scope of the thesis and also review some state of the art research that have been done related to the thesis.

2.1 State of the art and selected works

2.1.1 Review A

Title: Simulation of marine hybrid machinery systems based on vessel operational data.
Author: Voldnes [18].
This review is about a master's thesis from NTNU Aalesund written by Bendik Voldnes. The main points in the thesis are simulation of hybrid ship machinery and a proposed method that could be developed into different programming for machinery configuration simulation. The machinery presented by Voldnes are the machinery required for propulsion of a ship, he focuses on hybrid propulsion power sources and its theory. The thesis considered two power sources which include Diesel engine and batteries storage. He presented the necessary theories of a diesel engine that are relevant to his scope of work, he classified engine into 2 stroke and 4 stroke engine and explained there difference.

To perform a simulation, the diesel engine is represented as a mathematical model. Where the engine was model to have to function to produce power, fuel consumption and SFOC since these are the only function needed for the scope of the thesis. The model he used to present the power uses the relationship between power,torque and revolution while the torque is related to mean effective pressure, numbers of strokes and cylinder displacement. One important factor to determine how an engine will performance is the SFOC and is a function of the percentage of load on the on the engine, in his thesis a third degree polynomia was used in estimating the SFOC at every given load. He also discussed the importance of battery pack on-board a ship, he focus on the used of battery pack on the ship for peaks saving to avoid turning on a new engine. He also presented an overview of a battery and how they work and other properties.

Furthermore, Voldnes created a methodology for calculating different machinery configurations with necessary equations and mathematical models in a block diagram showing the flow of data. He divided the procedure of the methodology into 5 categories as follows.

1. **Library**; the library in the context of his thesis represent the physical attribute of the component.
2. **Operation data**; He refers to this as the input parameter.
3. **Configuration**; this is the combination of different machinery at given operation.
4. **Simulation**; computation and evaluating the operational data and the given configuration to give an output.
5. **Evaluation**; this is analysing the output.

He then used the methodology procedure to perform a simulation of a case study. In his conclusion, he said that further studies should consider more accurate assumptions and decided if the methodology should be implemented into a real system. Hes also said that a more advance model for the physic system can be built upon this.

In summary, This thesis provide in-depth overview of an hybrid machinery configuration analysis with a detailed presentation of the methodology that can be developed into a program presented in block diagram.

2.1.2 Review B

Title: Virtual Prototyping and simulation of multi body marine operation using web-based technologies.
Author: Henrique M. et al. [19].
This is a publication that was published at proceeding of the ASME 2019 38th and was written at Norwegian University of Science and Technology NTNU Aalesund. The publication focuses on the capability and endless opportunities the web technologies have for vessel and maritime operations. The authors presented some importance of web-based application which include easy accessibility of any device with a web browser, avoiding compatibility issue, ability for the user to have complex interaction with a given system, etc. They are consistently working on developing web application for marine design and engineering application. The paper represented a case study of the capability of the web technologies with a JavaScript library called "Vessel.js" that is developed by the department of Ocean Operations and Civil Engineering in NTNTU Aalesund. It is a library dedicated for investigation of common problem during conceptual design of a ship or operation, the library uses object-oriented programming approach and it is also open source project. The library is used for simulation and for Prototyping, in **prototyping mode**, the Vessel.js uses object approach to represent the ships structure which comprises of hull, decks and bulkheads, etc. It uses empirical formulae to estimate the ship structure like hull. The ship is visualized by a web technology called webGL, which allows 3D visualization on the web. The application is expected to have an input from the user which allows to upload the ship details as an object in JSON format. In **Simulation mode**, Vessel.js can be used for simulating the behaviour of the designed prototype, this is achieved

by what they called a “state ” which is used to create constraint on the designed prototype, like floating point or resistance of the designed prototype to be simulated. The library also has the ability to be used for different simulations as presented in the publication which include:

- **Multibody Motion Response** simulation this function is designed to allow analysis of multiple ship hull subjected to regular wave.
- **Time-Dommain Simulation**,this is done by combining states (constraint) of the vessel are analyzed and calculated Continuously in synchronization with the visualization.
- **Time-Domain Response of Hull with Equations of Motion**
- **Time-Domain Response of Hull with Closed-Form Expressions**
- **Pendulum Motion of Lifted Load**
- **Time-Domain Response of Hull with Equations of Motion**

In their discussion they mentioned the importance of the using a web-based application and also they said “At this point, the web applications still present some limitations in scope and accuracy to account for the simulation of an entire marine operation”, however they also mentioned potential of the web-based approach to test and serve as a starting point for the forthcoming work.

In summary this publication shows the potential of web-based application in the maritime industry by using Vessel.js library and the example presented.

2.1.3 Review C

Title: Fundamentals of Ship Hydrodynamics: Fluid Mechanics, Ship Resistance and Propulsion.
Author: Birk [20].
This review is about a book written by Lothar Birk, at the University of New Orleans USA., according to the author, the book is aim at bridging the information gap between fluid mechanics and ship hydrodynamics fundamentals. Although this review is not directly related to development of web-based application but it presented useful methods that could be implemented into the systems.

As mentioned by the author, the book focuses on ship hydrodynamic and fluid mechanics with examples and solution in each chapter, but the review will focus on the aspect of the ship hydrodynamics. The author cover from ship resistance estimation, propeller analysis, power estimation, etc.

Estimation of ship resistance, the author limit the scope of the book to cover just the aspect of calm water resistance, he uses different methods in estimating the resistance. He discussed full scaled and test model resistance, where he presented the setup used by the

International Towing Tank conference (ITTC) for a modeled ship resistance and power prediction method to predict required power of a ship. For full scale ship, he uses different method for the propulsion analysis which include

- Guldhammer and Harvald's method, this method was developed in 60's and was later updated by 1983 and 1986, the method are based on regression method, the author also method that new update to the regression method has been made by Kristensen and Lutzen in 2012. The author uses this method perform extensive analysis from resistance to power estimation with detailed information and steps.
- Hollenbach's Method, The author presented an overview of the method and how the formulas which make up the method. He also presented the applicability, advantage and the limitation of the the method. To further demonstrate this, he uses the method to calculate different ship parameters ranging from resistance to power estimation.
- Holtrop and Mennen's Method; this is one of most used regression method using in estimation or calculating ship resistance and power estimation, the author created an in-depth overview of the method, and step by step procedure on how to implement this method. This method has wide range of regression equations to consider depending on the case. One of author‘s aim is to create a steps that allow users to easily implement this method into computer program.

Propeller analysis; the author spend a great deal on this topic, presented different theories in regarding propeller, from momentum theory of propeller, Hull and propeller interaction, propeller design process and hull matching, etc. He also presented model scale and full scaled propeller comparison. The author discussed the problem of cavitation process of preventing sing a design case study. To perform a propeller hull matching the author uses “Wageningen B series” in most of the propeller design process studies with detail steps and procedures.

In summary; this simplifies different theories in ship hydrodynamics, that makes it possible for a any person with basic engineering background to perform analysis using its guide or procedures. The book as mention by the author is design for this procedures to be easily implemented as a computer program or software.

2.1.4 Review D

Title: Control of Marine Propellers From Normal to Extreme Conditions.
Author: yvind Notland Smogeli [21]. This review is for a PhD thesis written by yvind Notland Smogeli at department of marine technology: Norwegian university of Science and technology NTNU. The PhD he did was on control of marine propellers. In his thesis, he focuses his research on developing controller system for the following

- Propeller performance measure that can be used to improve thrust allocation in extreme operating conditions is introduced.
- Propeller load torque and a torque loss estimation scheme which enable online monitoring.

- Anti-spin thruster control for torque and power in extreme operation using load observer.

- A combine power/torque controller and speed/torque/power controller which increase thrust and reduce wear and tear.

One of the areas he spend a great detail of time is modelling of a fixed pitched propeller (FPP). He discussed extensively on 4 quadrant of operation a propeller, where he analyzed the governing equations and compared the linear and quadratic form. One of the drawback of using open water equations is the singularity problem when n = 0, the open-water characteristic does not cover the 4 quadrant and therefore cant be used for all the 4 quadrant. This is probably the open-water equation was developed just for vessel in transit by Smogeli. To be able to capture quasi-static behaviour of all 4 quadrant a different equation was presented which was first define by Miniovich in (1960) and later used by Van et al. [22], this equation uses completely different parameters from the conventional open-water equation. Using this parameters which are mostly governed by the angle of attack of the propeller. Smogeli presented a equation that covers quasi static of the 4 quadrant of the propeller.

Propulsion control; in the propulsion section of his work he focused on controlling of thruster in normal and extreme conditions where his aims was thrust prediction in disturbance, reduced mechanical wear and tear due to dynamic of the oscillations of the motor and propeller, predict power consumption, and robust performance.

In summary, Smogeli publication has touches aspect of control system, from controlling a propeller and power management system (PMS). His works provided different ways of controlling thruster and propeller and also formulation for the 4 quadrant of the propeller.

2.2 Theory

2.2.1 Ship Machinery

A ship or vessel is a system with many different machinery needed to operate successfully, this machinery can range from boiler, deck machinery, etc. As mentioned earlier in the scope, the machinery that will be focus in thesis is the machinery necessary for propulsion .

2.2.1.1 Diesel Engine

Today diesel engine is one of the main source of power used on board a vessel. They are internal combustion engine in which the ignition occurs when a fuel is injected into a hot and high pressurized air chamber. They could either be used for AC power supply or to directly connect to the propeller. Diesel engine are grouped into 2 stroke and 4 stroke engine, where the 2 stroke are usually “slow-speed” with a speed less than 400 RPM and used to directly connected to the propeller, while the 4 stroke engine could be either be ”Medium-speed” with a speed range of about 400 to 1200 RPM or ”High-speed” with a speed of 1400 RPM or above Woodford [23], marinediesels [24], wartsila [25].

A “Stroke” represents the number of stages an engine cylinder/crankshaft has to take before a complete engine combustion is made to produced power. The 2 stroke engines are characterized by high power and usually found on larger ships, the main difference between 2 stroke engine and 4 stroke engine is the mode of operation and the design. 2 stroke engines are designed to be crosshead while 4 stoke engines are designed to be “trunk piston”. As the name implies, a 2 stroke engine complete its combustion in two stage, the principle of how it works can be seen in Figure 2a, where the first stage as shown comprise of ignition/compression, this is where the piston make upward move to draw the fuel and compress it while the second stage also comprises of Combustion/Exhaust, this is where the fuel is ignited and finally, the piston is pushed downward to release the air in the chamber through the exhaust power equipment direct [4], Woodford [23].

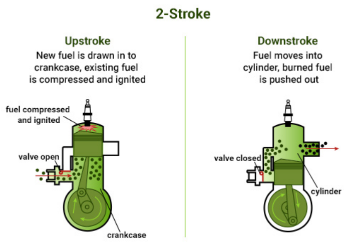

(a) 2 stroke engine working principle

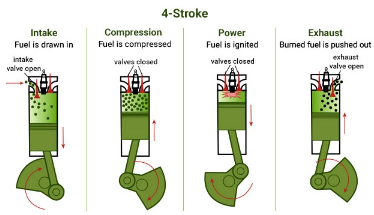

(b) 4 stroke engine working principle

Figure 2: 2 and 4 Stroke engine working principle [4]

The 4 stroke engine works in the same principle as the 2 stroke engine. The only difference is the number of revolution it takes to complete 1 power, for the 4 stroke engine, 4 stages are required as shown in Figure 2b. The first stage is where the fuel is drawn inside the chamber (intake), the second stage is where the fuel inside is compressed then the third stage is where the combustion occurs and the finally, the air sent out through the exhaust power equipment direct [4], Woodford [23].

2.2.1.2 Engine Power and performance curve

The power produced by any given diesel engine could be estimated using different methods or models. In this thesis, the power is consider based on the operation of the stroke and its internal components. Where the engine power P can be expressed as a function of the cylinder L, Area of piston A, mean effective pressure p_{mep}, engine speed RPM N_e, numbers of revolutions required to complete one engine circle n_r, for 2 stroke engine n_r = 1 while for 4 stroke engine n_r = 2 and n_c is the number of cylinders, V_d and is given in equation 1 or as a relationship between the engine torque and the rotation N_e as given in equation 2. The V_d is the displacement of the cylinder and can be expressed in equation 3.

$$P = \frac{p_{mep} \times V_d \times N_e \times n_c}{n_r \times 60} \tag{1}$$

$$P = \frac{2\pi \times T_e \times N_e}{60} \tag{2}$$

$$V_d = L \times A \tag{3}$$

While the engine torque is expressed in relation to the break mean effective pressure P_{BMEP} using equation 4 INNOVATIONS [26], x Engineer [27].

$$P_{BMEP} = \frac{2\pi \times T_e \times n_r}{n_c \times V_d} \tag{4}$$

Today, one of the focuses in the shipping industry is to reduced emission produced by ships, a key factor of the emissions produced by a ship is connected to the engine performance, one way of determining the engine performance is through specific fuel oil consumption (SFOC) of the engine, which is a function of the load on the engine. A typical engine performance curves are shown in Figure 4, where Figure 4a shows a relative SFOC curve for the three main diesel engine suppliers MAN, CAT, and Wartsila. The data used for the relative curve for MAN and CAT are based on three different 4 stroke engines while the data for Wartsila is based on 46F model engine . With this curve a regression analysis was made which result in second degree polynomial equation that can be used to estimate an approximated relative SFOC of the above mentioned engine at any given load, the equation for the three suppliers are given in equation 5 where EL is the fraction or percentage of the load on the engine IMO [3], Hassan and Hassan [5].

$$\begin{aligned} SFOC_{relative-W} &= 0.4613EL^2 - 0.7168EL + 1.28 \\ SFOC_{relative-M} &= 0.29334EL^2 - 0.432EL + 1.1565 \\ SFOC_{relative-C} &= 0.7024EL^2 - 0.97728EL + 1.35 \end{aligned} \tag{5}$$

The equation 5 mentioned above only gives the result of the relative value of the SFOC, to compute the actual SFOC a concept called “SFOC baseline”, which is a unique value for every engine is used to multiply the relative SFOC as shown in equation 6 while Figure 3 shows a table for different base lines which can be used to compute the actual SFOC using equation 6. For details about ”SFOC baseline” check IMO [3], Hassan and Hassan [5], Jalkanen et al. [6].

$$SFOC = SFOC_{Relative} \times SFOC_{Base_{l}ine} \tag{6}$$

Build year	2-stroke	4-stroke (>5000 kW)	4-stroke (1000–5000 kW)	4-stroke (<1000 kW)
1970–1983	180–200	190–210	200–230	210–250
1984–2000	170–180	180–195	180–200	200–240
2000–	165–175	175–185	180–200	190–230

Figure 3: Base line SFOC of different engine IMO [3], Hassan and Hassan [5]

As mentioned the method of estimation of SFOC presented in equation 5 and 6 are not valid for every engine.

In the shipping industry, only a few types of fuel are used which include LNG, MGO/MDO, and HFO, although H2 is gaining attention. The major engine suppliers can supply engines for any of this fuel or for dual fuel. The type of fuel to choose when designing a ship depends on the individual KPI like emissions, cost, etc. The emissions produced by a diesel engine also depends on the chosen fuel and the engine performance (SFOC) as mentioned. IMO has made different regulations which classified engines into Tier I, Tier II, and Tier III which determine the level of SFOC of the engine. The emission is a function of the fuel consumption FC, SFOC, load, and the emission factor of the given fuel, where the 5 major emission factors are (NO_X, SO_X, CO_2, PM, $NMVOC$) in a study done by IMO [3] are reconstructed in Annex A Table 8.

To calculate the emission of an engine during a given operation equation 7 could be used which take into account the load P_L, $SFOC$, the given emission factor EF, and the operating time t.

$$Emission_{type} = P_L \times SFOC \times EF \times t \tag{7}$$

While the fuel consumption of the operation can be estimated using equation 8.

$$FC = P_L \times SFOC \times t \tag{8}$$

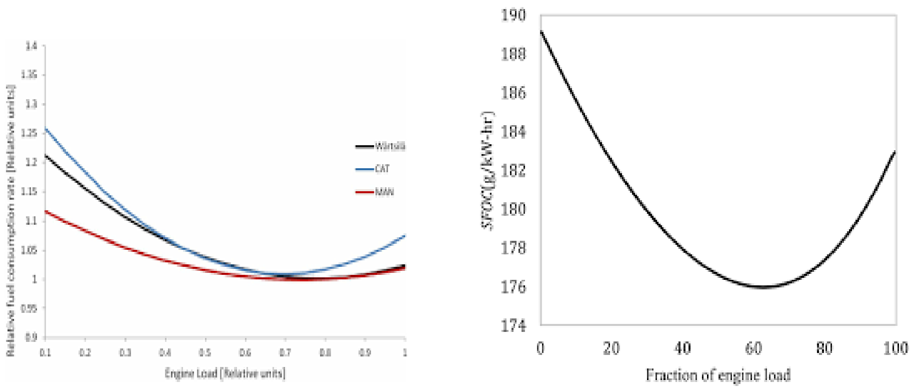

(a) relative SFOC and relative load **(b)** SFOC and percentage of load

Figure 4: different representation of engine load vs SFOC curve Jalkanen et al. [6]

2.2.2 Battery storage

Today the use of energy storage in form of battery on board a vessel continues to increase due to different reasons which vary from vessel owners to another, as the shipping industry continues to focus on reducing emissions, one of the main reasons for installing a battery back becomes to reduces emission NO_X, SO_X, CO_2. There are other reasons for installing a battery storage on board a vessel which includes fuel consumption, peak shaving, Risk , etc. Most battery storage found on vessels are used in combination with other sources of power like diesel engine where the battery pack is usually used for peak shaving of dynamic load, thereby eliminating the need for turning on a new engine which allows the engines to run on a predefined load that will give the engine a better performance in terms of SFOC. Although there are vessels which run on pure battery system and they are usually ferries that operate in a predefined voyage or route MO [28], E and Bergh [29].

There are basically four types battery storage, they are: Lead-Acid, Nickle-cadmium (NiCd), Nickle-metal-Hybride (NiMH), and Lithium-Iron (Li-Ion). Among these batteries Li-Ion has been the most used battery Olivier et al. [30]. The basic parameters and terms used to describe a battery are:

- Battery capacity, is the amount energy the battery can store in kWh.
- Depth of discharge (DOD), is the percentage of battery pack energy allowable to be used from a fully charged battery system. The DOD is an important parameter of the battery system because of its correlation with life cycle of the battery, a battery pack with a DOD of 60% will have a longer life cycle than DOD of 90%.
- State of Charge (SOC), is the level of the battery pack compared to its capacity, it is given in percentage or kWh.
- C-rating, C-rate is a number which tells the charging and discharging rate of the battery, 1C rated battery means that the battery will fully discharge or fully charge in 60 minutes, although some battery packs have peak C-rate and continue C-rate where the peak C-rate is use for short period of time, in maritime application it is common use for taking high peak load that last for just seconds.

2.2.2.1 Battery management system (BMS)

The BMS is an electronic device that is part of the battery pack system which is design to have an insights of the battery system by keeping track of all the battery parameters mentioned above. Some of the function of the BMS include Electropaedia [31]:

- Monitoring; the BMS can be used for monitoring and calculating necessary battery parameters like voltage, SOC, temperature, DOD, etc.
- protection of the battery pack; the BMS protects the battery pack by preventing over charging, discharged more than its DOD, control the charging power according to the C-rate.

For details of the functions of the BMS check Electropaedia [31], DNVGL [32].

2.2.2.2 Battery pack Sizing

The capacity of battery to be installed on a vessel depends on the purpose of installing the battery system, DNV GL have two sets of class notation and rules called “Battery(Power)” and “Battery(Safety)” used as guide or rule when planning battery pack installation. The class notation Battery(Power) is a requirement for vessels in which the battery is the only source of propulsion power. The requirement state that at least two independent battery systems shall be installed in separate locations, this means that for a vessel that required

1000kWh of energy for propulsion shall have two sets of 1000kWh installed, where each set is installed in separate compartment GL [33]. The class notation Battery(Safety) is required for vessels where the installed battery system is used for mainly additional power source, which is usually a battery hybrid system. For details of the rules check GL [33]. The battery capacity can be estimated using equation 9, where the $P_{Batt-capacity}$ is the battery capacity, $P_{required}$ is the required power, the DOD and the C-rate is not a constant value but varies with the individual criteria as mentioned, a typical value of the DOD is 80% depending on the intended life span of the battery while C-rate depends also on the operation and it can be estimated using equation 10.

$$P_{Batt-capacity} = \frac{P_{required}}{C - rate \times DOD} \tag{9}$$

$$C - rate = \frac{h_{60minutes}}{t} \tag{10}$$

2.2.3 Machinery Configuration

The machinery to be installed on a vessel vary, "machinery configuration" in this context refers to the set of machinery that is installed on a particular vessel. Almost every vessel has a different machinery configuration which depends on many factors ranging from the mission of the vessel, cost, environment, comfort, etc. The basic illustration of ship machinery configuration can be seen in Figure 5 which shows three main machinery configuration where Figure 5a is a Mechanical ME, Figure 5b is a Diesel electric DE, and Figure 5c is an Hybrid battery diesel electric. Each of these configurations as shown in the figure have the possibility for different configurations. For example, the ME can also be equipped with PTO and PTI.

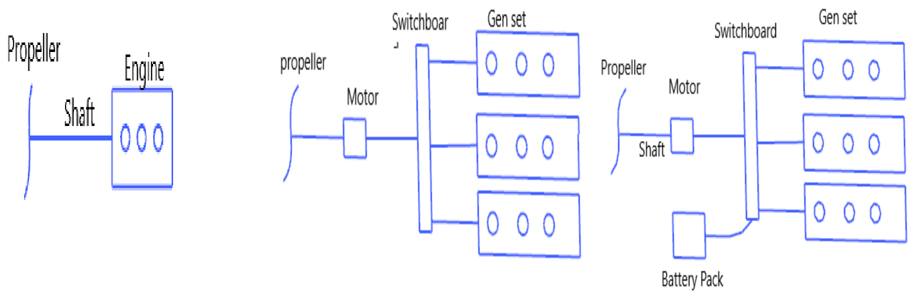

(a) ME propulsion **(b)** DE propulsion **(c)** Hybrid: DE-Battery propulsion

Figure 5: Ship machinery configuration

2.2.4 Ship Hull

The ship hull is designed to have a form such that its dimensions as shown in Figure 6 will cause a predefined displacement of volume of water ∇ which is governed by equation 11. Where L_{WL} is waterline Length, B is the moulded beam, T is the moulded mean draught, and $C_{B,WL}$ is the block coefficient as shown in the figure MAN [7], Anthony F. et al. [34]. Their are numerous possible combinations of the above mentioned dimensions to be chosen when designing a ship, for any given combination the parameters will influence the ship resistance, stability, efficiency therefore they are subjected to constraints depending on the ship type and efficiency of the hull Anthony F. et al. [34]. These parameters are used in the estimation of the ship resistance and other measures performance , for detail on how each parameter affect the ship hull check Anthony F. et al. [34].

$$\nabla = L_{WL} \times B \times T \times C_{B,WL} \tag{11}$$

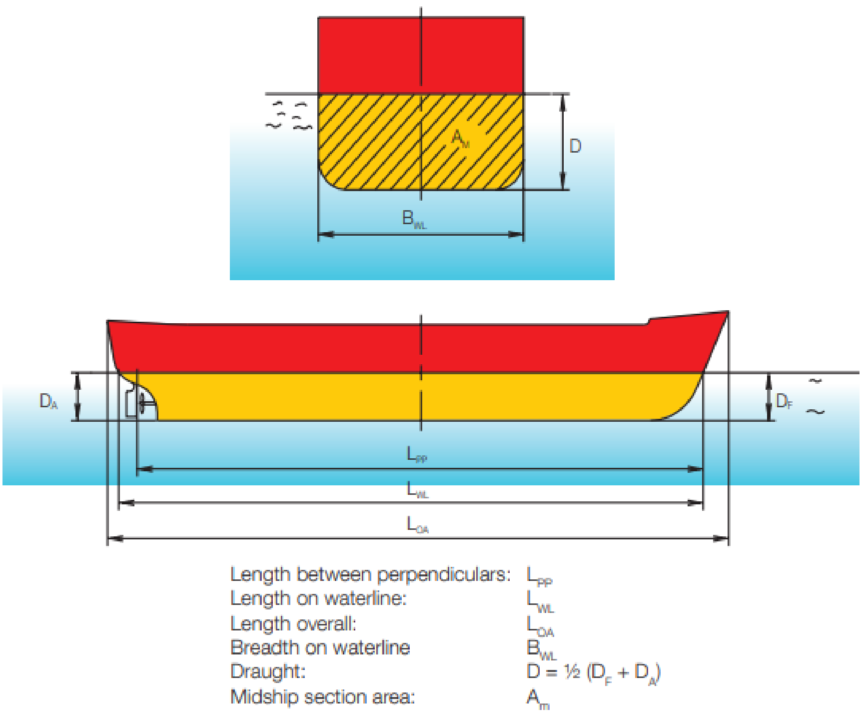

Figure 6: Ship hull and dimension parameters MAN [7]

2.2.5 Ship Resistance

Total ship resistance R_T is the towing force required to overcome the drag force against the motion of a vessel without the effect of the propeller, wind, wave and current, it is calculated using equation 12 where ρ is the density of water, C_T is the total resistance coefficient, V is the ship speed and S is the wetted surface area. In the early stage of the ship design, necessary parameters for calculation of the resistance are not available therefore many methods for estimating ship resistance have been developed over the years. Out of these methods, the most reliable method is achieved by creating a scaled model of the ship and test it in a "Towing tank" then use the scaled model result to predict the full scale ship resistance. For detail on the process of using the model scale to estimate the full scale check Birk [20].

$$R_T = \frac{1}{2}\rho C_T V^2 S \tag{12}$$

Another widely used method is the one published by The International Towing Tank Conference ITTC on its website, with recommended procedure for model testing and CFD calculation of different resistance component which include the model-ship correlation for frictional factor C_F and frictional resistance R_F of a smooth ship which is given in equation 13 and 14 respectively ITTC [35].

$$C_F = \frac{0.075}{[\log_{10} Re - 2]^2} \tag{13}$$

$$R_F = \frac{\rho}{2} V^2 S C_F \tag{14}$$

2.2.5.1 Holtrop and Mennen's Method

In this thesis, the method used for estimation of resistance is "Holtrop and Mennen's" method. it will be used for resistance estimation and for the hull and propeller interaction. Holtrop and Mennen's Method is a regression analysis method based on a vast number of previous model ships which is used for estimating resistance and power of a ship. The method is one of the most widely used methods for resistance estimation Birk [20]. It was first presented in 1978 by Holtrop. and G.G.J [36] and later revised in 1982,1984 and 1988 Birk [20]. The resistance in this method is divided into the following:

- Frictional resistance R_F.
- Appendage resistance R_{APP}.
- Wave resistance R_W.
- Resistance due to bulbous bow near the water surface R_B.
- Pressure resistance due to immersed transom R_{TR}.
- Model-ship correlation R_A.
- Air resistance R_{AA}.

The total resistance is then expressed as given in equation 62. This method requires a long procedure since many different constants and coefficients are required to be calculated first. Since from the introduction of the method some of the variables and constants have been changed over time therefore the procedure presented below is based on all the modification in Holtrop.J [1], Holtrop. and G.G.J [36, 37], Holtrop.J [38]. To calculate these different components of resistance some parameters have to be estimated first, which are Block coefficient $C_{B,WL}$ by rearranging the equation 11. Longitudinal center of buoyancy l_{cb}, if the L_{CB} is not known in the early stage it can be estimated using the suggestion from Guldhammer.H [39] which is given by equation 15 but if the L_{CB} is know then it can be calculated using equation 16.

$$lcb = -(0.44Fn_{design} - 0.094) \tag{15}$$

$$lcb = -\frac{L_{CB}}{L_{WL}} \cdot 100\% \tag{16}$$

The Midship section coefficient C_M can be calculated using method by Jensen [40] in equation 17.

$$C_M = \frac{1}{1 + (1 - C_B)^{3.5}} \tag{17}$$

The prismatic coefficient C_p can be estimated using equation 18 while the block coefficient $C_{B,WL}$ can be estimated by rearranging equation 11 MAN [7].

$$C_P = \frac{C_{B,WL}}{C_M} \tag{18}$$

When the waterline area coefficient C_{WP} is not known it can be estimated using equation 19

$$C_{WP} = \begin{cases} 0.763(C_P + 0.34) & \text{for tankers, bulk carriers, general cargo with } 0.56 < C_P \cdot 0.87 \\ 3.226(C_P + 0.36) & \text{for container ship with } 0.57 < C_P \cdot 0.62 \end{cases} \tag{19}$$

The wetted area surface of the hull S can be estimated using equation 20 and the c_{23} is given in equation 21.

$$S = L_{WL}(2T + B)\sqrt{C_M}\left[0.615989c_{23} + 0.111439C_M^3 + 0.000571111C_{stern} + 0.245357\frac{c_{23}}{C_M}\right] + 3.45538A_T + \frac{A_{BT}}{C_B}\left(1.4660538 + \frac{0.5839497}{C_M}\right) \tag{20}$$

$$c_{23} = 0.453 + 0.4425C_B - 0.2862C_M - 0.003467\frac{B}{T} + 0.3696C_{WP} \tag{21}$$

The half angle of the waterline entrance can be estimated using equation 22 in degree while the a is given by equation 23 Holtrop. and G.G.J [37] and the run L_R is estimated using equation 24 Holtrop.J [38].

$$i_E = 1 + 89e^a \tag{22}$$

$$a = -\left[\left(\frac{L_{WL}}{B}\right)^{0.80856}(I - C_{WP})^{0.30484}[1 - C_P - 0.0225l_{CB}]^{0.6367}\left(\frac{L_R}{B}\right)^{0.34574}\left(\frac{100V}{L_{WL}^3}\right)^{0.16302}\right] \tag{23}$$

$$L_R = L_{WL}\left(\frac{1 - C_P + 0.06 C_P l_{CB}}{4C_P - 1}\right) \tag{24}$$

The Froude number F_n and the Reynolds number R_e are used for the different components of the resistance and they are calculated using equation 25 and 26 respectively.

$$F_n = \frac{V}{\sqrt{g L_{WL}}} \tag{25}$$

$$R_e = \frac{V L_{WL}}{\mu} \tag{26}$$

Frictional Resistance

The frictional resistance R_F in this method uses the ITTC1957 method for estimating the model-ship correlation coefficient C_F given in equation 17 as an input to the resistance as shown in equation 27.

$$R_F = \frac{1}{2}\rho V^2 S C_F \tag{27}$$

When all the resistance component are assembled, the R_F is used in combination with a form factor $(1 + k)$ which increase the accuracy of the total resistance, k uses a constant c_{14} that takes account of the influence of the aft body shape were different form factors for each body shape are given in Table 2 while the equation for calculating the c_{14} and the k is given in equation 28 and 29 respectively.

Table 2: Shapes and constant values

Aft body shape	C_{stern}
Pram with gondola	-25
V-shaped section	-10
Normal section shape	0
U-shaped with Hogner stern	10

$$c_{14} = 1.0 + 0.011 C_{stern} \tag{28}$$

$$k = 0.07 + 0.487118 c_{14}\left[\left(\frac{B}{L_{WL}}\right)^{1.06806}\left(\frac{T}{L_{WL}}\right)^{0.46106}\left(\frac{T}{L_{WL}}\right)^{0.46106}\left(\frac{L_{WL}}{L_R}\right)^{0.121563}\left(\frac{L_{WL}^3}{V}\right)^{0.36486}(1 - C_P)^{-0.604247}\right] \tag{29}$$

Appendage Resistance R_{APP}

To account for the resistance due to the appendage, the equation developed is dependent on the wetted surface area of the appendage S_{APPi} respectively and a form factor $(1+k_2)_{eg}$, a list of possible appendage with factors used in the equation is given in Table 3 and the equation for the $(1+k_2)$ is given in equation 30 for all the appendages present on the vessel.

$$(1+k_2)_{eq} = \frac{\sum_i (1+k_{2i})\, S_{APPi}}{\sum_i S_{APPi}} \tag{30}$$

For a vessel that is equipped with bow thrusters opening, the effect on the resistance can be estimated using equation 31, were $C_{D_{TH}}$ is the drag coefficient of the thruster and the values usually range from 0.003 to 0.012 and it can be estimated from the suggestion of Hollenbach method given in equation 32.

$$R_{TH} = \rho \pi d_{TH}^2 V^2 C_{D_{TH}} \tag{31}$$

$$C_{D_{TH}} = 0.003 + 0.003 \left(\frac{10 d_{TH}}{1} - 1 \right) \tag{32}$$

The appendage resistance R_{APP} is the combination of all the appendage and the thrusters which is calculated in equation 33

$$R_{APP} = \frac{1}{2} \rho C_F V^2 (1+k_2)_{eq} \sum_i S_{APPi} + \sum_i R_{TH} \tag{33}$$

Table 3: Approximated values of different appendages form factor k_2 Holtrop.J [1]

Appendage	k_{2i} value
rudder behind skeg	0.2–0.5
rudder behind stern	0.5
twin screw rudder (slender)	1.5
twin screw rudder (thick)	2.5
shaft brackets	2.0–4.0
skeg	0.5–1.0
strut bossing	2.0–3.0
hull bossing	1.0
exposed shafts (angle with buttocks about 10 degrees)	1.0
(angle with buttocks about 20 degrees)	4.0
stabilizer fins	1.8
dome	1.7
bilge keels	0.4

Wave making resistance R_W

The wave making resistance depends on many coefficient $c_1, c_2, c_3, c_5, c_{15}, c_{16}$ respectively as calculated and the $d = -0.9$ in the equations, the R_W is divided into three resistance depending on the speed of the vessel and it is computed in respect to the Froude number. The variables in the equations changes according to when in slow speed, where the $F_n \leq 0.4$, for medium speed were $0.4 < F_n \leq 0.55$ and for high speed, where $F_n > 0.55$. When the speed is slow ($F_n \leq 0.4$) the resistance can be calculated using equation 34.

$$R_{Wa} = \rho g \nabla c_1 c_2 c_5 exp \left\{ m_1 F_n^d + m_4 \cos(\lambda F_n^{-2}) \right\} \tag{34}$$

For high speed vessels were the $F_n > 0.55$ some of the variables for slow speed have to be changed and therefore the resistance is then calculated using equation 35

$$R_{Wb} = \rho g \nabla c_{17} c_2 c_5 exp\{ m_3 F_n^d + m_4 \cos(\lambda F_n^{-2}) \} \tag{35}$$

For a medium speed where $0.4 < F_n \leq 0.55$ an interpolation between the R_{Wa} and R_{Wb} is done, therefor the resistance can be calculated using equation 36 Birk [20], this means that when calculating R_{Wa} the $F_n = 0.4$ and when calculating the R_{Wb} the $F_n = 0.55$.

$$R_W = R_{Wa}(0.4) + \frac{20F_n - 8}{3} \left[R_{Wb}(0.55) - R_{Wa}(0.4) \right] \tag{36}$$

The different constant used in the R_W are determined as follows: c_7 is determined in accordance with B/L_{WL} as shown in equation 37.

$$c_7 = \begin{cases} 0.229577 \left(\frac{B}{L_{WL}} \right)^{(1/3)} & \text{if } B/L_{WL} \leq 0.11 \\ \frac{B}{L_{WL}} & \text{if } 0.11 < B/L_{WL} \leq 0.25 \\ 0.5 - 0.0625 \frac{B}{L_{WL}} & \text{if } B/L_{WL} > 0.25 \end{cases} \tag{37}$$

The c_1 is determined in accordance with to equation 38 .

$$c_1 = 2223105 c_7^{3.78613} \left(\frac{T}{B} \right)^{1.07961} (90 - i_E)^{-1.37565} \tag{38}$$

$$c_3 = 0.56 \frac{A_{BT}^{1.5}}{\left[BT(0.31\sqrt{A_{BT}} + T_F - h_B) \right]} \tag{39}$$

$$c_2 = e^{(-1.89\sqrt{c_3})} \tag{40}$$

$$c_5 = 1 - 0.8 \frac{A_T}{BTC_M} \tag{41}$$

c_2, c_3, c_5 are estimated using equation 40, 39 and 41 respectively, the coefficient c_2 the accounts for the effect of the wave resistance reduction due to the present of the bulbous bow, while c_3 determines the influence of the bulbous bow, which depends on the transverse bulbous area A_{BT}, the vertical centroid above the baseline h_B and fore draft T_F. The c_5 is the coefficient that accounts for the influence of the transom stern.

$$c_{15} = \begin{cases} -1.69385 & \text{if } \frac{L_{WL}^3}{\nabla} \leq 512 \\ \\ -1.69385 + \frac{\frac{L_{WL}^3}{\nabla^{1/3}} - 8}{2.36} & \text{if } 512 < \frac{L_{WL}^3}{\nabla} \leq 1726.91 \\ \\ 0 & \text{if } \frac{L_{WL}^3}{\nabla} \leq 1726.91 \end{cases} \tag{42}$$

$$c_{16} = \begin{cases} 8.07981 C_P - 13 : 8673 C_P^2 + 6 : 984388 C_P^3 & \text{if } C_P < 0.8 \\ \\ 1.730140.7067 C_P & \text{if } 0.8 \leq C_P \end{cases} \tag{43}$$

$$\lambda = \begin{cases} 1.446 C_P - 0.03 \frac{L_{WL}}{B} & \text{if } \frac{L_{WL}}{B} < 12 \\ \\ 1.446 C_P - 0.03 & \text{if } 12 \leq \frac{L_{WL}}{B} \end{cases} \tag{44}$$

$$m_1 = 0.0140407 \frac{L_{WL}}{T} 1.75254 \frac{\nabla^{1/3}}{L_{WL}} - 4.79323 \frac{B}{L_{WL}} - C16 \tag{45}$$

$$m_4 = c_{15} 0.4 e^{(-0.034 F_n - 3.29)} \tag{46}$$

The rest of the coefficient c_{16,λ,m_1,m_4} can be determined using equation 45,46, 44, and 43 respectively. Using the above mentioned equations and coefficient the wave making resistance R_W can be calculated as given in equation 34, 34 or 36 respectively.

Bulbous bow resistance R_B

The bulbous bow resistance is the resistance due to the pressure near the water surface due to the presence of bulbous bow. This resistance was updated in 1988 by Holtrop.J [1] to account for the effect of the forward sinkage h_F in equation 50 and the wave height at the bow h_w in equation 51 Birk [20]. the resistance can be calculated using equation 47 .

$$R_B = 0.11 \rho g \left(\sqrt{A_{BT}} \right)^3 \frac{F_{ni}^3}{1 + F_{ni}^2} e^{(-3.0 P_B^2)} \tag{47}$$

Where P_B is the coefficient that accounts for the emergence of the bulbous bow in equation 52 while F_{ni} is the froude number based on the h_w and h_F in equation 50 and 51 respectively Holtrop.J [38].

$$c_{17} = 6919.3 C_M^{-1.3346} \left(\frac{\nabla}{L_{WL}} \right)^{2.00977} \left(\frac{L_{WL}}{B} - 2.0 \right)^{1.40692} \tag{48}$$

$$m_3 = -7.2035 \left(\frac{B}{L_{WL}}\right)^{0.326869} \left(\frac{T}{B}\right)^{0.605375} \tag{49}$$

$$h_F = \begin{cases} C_P C_M \frac{TB}{L_{WL}} (136 - 316.3F_n) F_n^3 \\ \text{with a minimum of} \qquad h_F \geq -0.01L_{WL} \end{cases} \tag{50}$$

$$h_W = \begin{cases} \frac{i_E V^2}{400g} \\ \text{with a maximum of} \quad h_W \leq -0.01L_{WL} \end{cases} \tag{51}$$

$$P_B = 0.56 \frac{\sqrt{A_{BT}}}{T_F - 1.5h_B + h_F} \tag{52}$$

$$F_{ni} = \frac{V^2}{\sqrt{g(T_F - h_B - 0.25\sqrt{A_{ABT}+}h_F + h_W)}} \tag{53}$$

Transom resistance R_{TR}

The presence of the immersed transom may influence the resistance and cause additional pressure resistance R_{TR}. This can be estimated as a function of the depth Froude number F_{nT}, which takes into account the immersed transom Birk [20] and can be estimated using equation 54. The transom resistance can be calculated in equation 55.

$$F_{nT} = \frac{V}{\sqrt{\frac{2gA_T}{B+BC_{WP}}}} \tag{54}$$

$$R_{TR} = \frac{1}{2}\rho V^2 c_6 A_T \tag{55}$$

Where c_6 is the coefficient that depends on the F_{nT}.

$$c_6 = \begin{cases} 0.2(1 - 0.2F_{nT} & \text{if } F_{nT} < 5 \\ 0 & \text{if } F_{nT} > 5 \end{cases} \tag{56}$$

Model-ship Correlation Resistance R_A

This correlation resistance is used to account for the difference between the model ship and the full scaled ship, it accounts for the hull roughness and other effect not captured in the model ship Birk [20]. The correlation allowance coefficient is estimated using equation 58 Holtrop.J [1].

$$c_4 = \begin{cases} \frac{T_F}{L_{WL}} & \text{if } \frac{T_F}{L_{WL}} \leq 0.04 \\ \\ 0.04 & \text{if } \frac{T_F}{L_{WL}} > 0.04 \end{cases} \quad (57)$$

Where c_4 coefficient is calculated using equation 57 and c_2 is the same as calculated in equation 40.

$$C_A = 0.00546(L_{WL} + 100)^{-0.16} - 0.002 + 0.003\sqrt{\frac{L_{WL}}{7.5}}C_B^4 c_2(0.04 - c_4) \quad (58)$$

For vessel a with higher hull surface roughness with value above $k_s > 150\mu m$ additional coefficient is used to capture the effect of the higher roughness using equation 59.

$$\Delta C_A = \begin{cases} 0 & \text{if } k_s = 150\mu m \\ \\ \frac{0.105 k_s^{(1/3)} - 0.005579}{L_{WL}^{(1/3)}} & \text{if } k_s > 150\mu m \end{cases} \quad (59)$$

Using the above mentioned coefficient the correlation resistance can be calculated using equation 60.

$$R_A = \frac{1}{2}\rho g V^2 (C_A + \Delta C_A)\left[S + \sum S_{APP}\right] \quad (60)$$

Air Resistance R_{AA}

The Air resistance due to surface area of the moving vessel is calculated according to the ITTC procedure equation 61.

$$R_{AA} = \frac{1}{2}\rho g V^2 C_{DA} V_A \quad (61)$$

Where C_{DA} is the the default air drag coefficient $C_{DA} = 0.8$, ρ is the density of air $\rho = 1.225 kg/m^3$.

Finally, total resistance R_T can be expressed as the additional of combination of all the components resistance and is given in equation 62.

$$R_T = R_F(1 + k) + R_{APP} + R_B + R_W + R_T R + R_A + R_{AA} \quad (62)$$

Propeller Hull interaction

In 1984 Holtrop.J [38] provided different sets of equation for computing the interaction of the propeller for a single and twin screw propeller, which is based on a viscous coefficient in equation 63. The wake and the thrust deduction factor can be computed depending on the screw type equation 70, 71, 72 and 71 respectively, while the relative rotational efficiency is estimated using equation 74 and75.

$$C_V = \frac{(1+k)F_R + R_{APP} + R_A}{\frac{1}{2}\rho g V^2 (S + \sum_i S_{APPi})} \tag{63}$$

$$c_8 = \begin{cases} \frac{S}{L_{WL} D}\left(\frac{B}{T_A}\right) & \text{if } \frac{B}{T_A} \leq 5 \\ \\ \frac{S\left(7\frac{B}{T_A} - 25\right)}{L_{WL} D\left(\frac{B}{T_A} - 3\right)} & \text{if } \frac{B}{T_A} > 5 \end{cases} \tag{64}$$

$$c_9 = \begin{cases} c_8 & \text{if } c_8 \leq 28 \\ \\ 32 - \frac{16}{c_8 - 24} & \text{if } c_8 > 28 \end{cases} \tag{65}$$

$$c_{11} = \begin{cases} \frac{T_A}{D} & \text{if } \frac{T_A}{D} \leq 2 \\ \\ 0.0833333\left(\frac{T_A}{D}\right)^3 + 1.33333 & \text{if } \frac{T_A}{D} > 2 \end{cases} \tag{66}$$

$$c_{19} = \begin{cases} \frac{0.12997}{0.95 - C_B} - \frac{0.11056}{0.95 - C_P} & \text{if } C_P \leq 0.7 \\ \\ \frac{0.18567}{1.3571 - C_M} - 0.71276 + 0.38648 C_P & \text{if } C_P > 0.7 \end{cases} \tag{67}$$

$$c_{20} = 1 + 0.015 C_{stern} \tag{68}$$

$$C_{P1} = 1.45 C_P - 0.315 - 0.0225 l_{CB} \tag{69}$$

For single screw:

$$\begin{aligned} w = {} & c_9 c_{20} C_V \frac{L_{WL}}{T_A}\left[0.050776 + 0.93405 \frac{c_{11} C_V}{1 - C_{P1}}\right] \\ & + 0.27915 c_{20} \sqrt{\frac{B}{L_{WL}(1 - C_{P1})}} + c_{19} c_{20} \end{aligned} \tag{70}$$

For twin screw:

$$w = 0.3095 C_B + 10 C_V C_B - 0.23 \frac{D}{\sqrt{BT}} \tag{71}$$

For single screw:

$$t = \frac{0.25014\left(\frac{B}{LWL}\right)^{0.28956}\left(\frac{\sqrt{BT}}{D}\right)^{0.2624}}{(1 - C_P + 0.0225 l_{CB})^{0.01762}} + 0.0015 C_{stern} \tag{72}$$

For twin screw:

$$t = 0.325 C_B - 0.1885 \frac{D}{\sqrt{BT}} \tag{73}$$

For single screw:

$$n_R = 0.9922 + 0.05908 \frac{A_E}{A_0} + 0.07424(C_P - 0.0225 l_{CB}) \tag{74}$$

For twin screw:

$$n_R = 0.9737 + 0.111(C_P - 0.0225 l_{CB}) - 0.06325 \frac{P}{D} \tag{75}$$

The presented method was used in analysing different ship resistance in this thesis, the method was also implemented in the web based application for estimating the ship resistance.

2.2.5.2 Sea Margin

Sea margin is the additional ship resistance added to the calm water resistance R_T due to the weather condition. This is an important factor to consider when deciding the engine capacity to be installed on the vessel. Typically, 15% of the power delivered to the propeller P_D is is added, for larger container vessels up to 30% can be added when estimating the total install capacity of the engine MAN [7]. The major sea margin factors are Wave , wind, current and roughness of the hull overtime. These effects can be estimated to give the designer a possible range of sea margin value to be added when deciding the engine capacity.

Wave added resistance R_{wave}

The added resistance due to the effect of the wave can be expressed in many ways, in this thesis two method are presented from Iso-1501 [8] and IMO [41] which are shown in equation 76 and 77. They will not consider irregular waves.

$$R_{wave} = 1336(5.3 + V)\left(\frac{B \cdot T}{L_{pp}}\right)^{0.75} \times h_s^2 \tag{76}$$

The method from equation 76 is from IMO guideline which is mainly meant for tankers, bulk carriers and combination carriers IMO [41]. Where R_{Awave} is the added wave resistance, L_{pp} is the length between perpendicular and h_s is the significant wave height and is required to be evaluated for $h_s = 4.0m$.

$$R_{Awave} = \frac{1}{15} \rho s g H_{1/3}^2 \sqrt{\frac{B}{L_{BWL}}} \tag{77}$$

The method presented in equation 77 is from Iso-1501 [8] and is called **STAWAVE-1**. This thesis will use this method for estimation of wave resistance. This method have limitations of $H_{1/3} \leq 2.225\sqrt{L_{pp}/100}$, bow waves, wave from heading 0 to $\pm 45°$. Where $H_{1/3}$ is the significant wave height, and L_{BWL} is the distance from bow to 95% of the maximum breath on the waterline as shown in figure 7

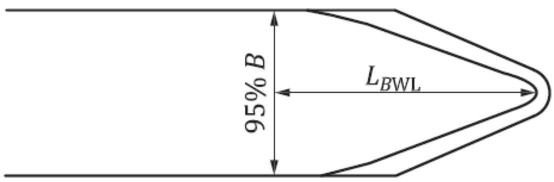

Figure 7: L_{BWL} explanation Iso-1501 [8]

Wind added resistance R_{Awind}

Wind resistance is the extra resistance that is added to the calm water resistance due to the influence of wind and is given in equation 78. Where C_W is the wind resistance coefficient, A_F is the frontal area .

$$R_{Awind} = 0.5\rho C_W A_F v_{wind}^2 - 0.5\rho C_W A_F v^2 \tag{78}$$

2.2.6 Propeller and Thrusters characteristic

Propeller is one of the components that is needed to be estimated in the early phase of the design of a vessel since it influences the propulsion power. The propeller to be selected for a particular vessel is chosen so that the combination of the given hull and the propeller gives a high propulsion efficiency. There are many propeller data series that helps in the process of selecting a propeller. In this thesis the "Wageningen B" series kuiper.G [42], will be used for selecting of a propeller given any particular vessel.

The Wageningen B series is one of the most extensive series of propellers used Troost.L [43, 44], W.P.A van et al. [45], the series has up to 120 different propeller combinations which vary from number of blade Z, expanded ratio A_E/A_0, and the pitch diameter ratio P/D Birk [20]. Table 4 shows the possible combination of propeller for every given Z value, the possible combination of the expanded ratio A_E/A_0 which gives 20 combination, and each of these combination has another possible combination of P/D are 0.5, 0.6, 0.8, 1.0, 1.2 and 1.4.

Table 4: Wageningen B-series different propellers features

Z	expanded area ratios A_E/A_0													
2	0.30													
3		0.35			0.50			0.65			0.80			
4			0.40			0.55			0.70			0.85	1.00	
5				0.45			0.60			0.75				1.05
6					0.50			0.65			0.80			
7						0.55			0.70			0.85		

The Wageningen B series data is given in an open water diagram. Where a typical diagram is shown in Figure 8 containing dimensionless thrust and torque coefficient, K_{Qo}, K_{To}, the open water efficiency η_o and advance coefficient J as a functions of equation 80, 81, 82 and 83 respectively.

$$K_T = \frac{T_p}{\rho n^2 D^4} \tag{79}$$

$$K_{To} = \frac{T_p}{\rho n^2 D^4} \tag{80}$$

$$K_{Qo} = \frac{Q}{\rho n^2 D^5} = \frac{P_p}{2\pi \rho n^3 D^5} \tag{81}$$

$$\eta_o = \frac{J}{2\pi} \cdot \frac{K_{To}}{K_{Qo}} \tag{82}$$

$$J = \frac{v_a}{nD} \tag{83}$$

Where the underscore “o” in the K_{To} and K_{Qo} represent the open water value, n is the propeller speed in s^{-1}, D is the propeller diameter, v_a is the advance speed, J is the advance ratio, T_p is the thrust and Q is the torque. In the early stages of design D can be estimated using equation 84 where T_{max} is the maximum draft.

$$D = 0.395 T_{max} + 1.3m \tag{84}$$

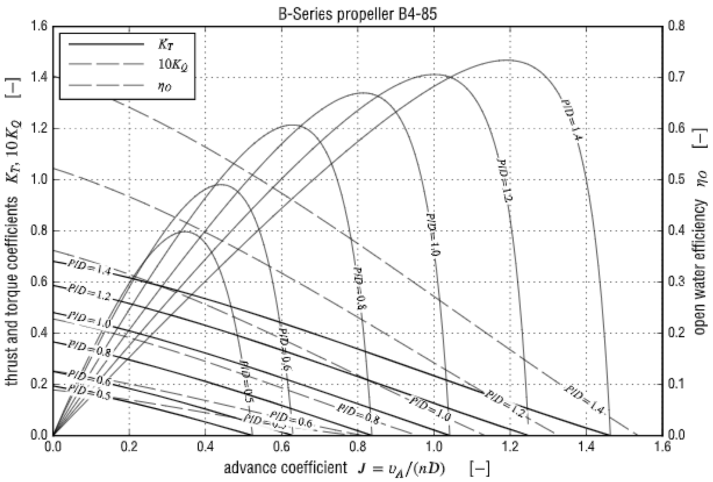

Figure 8: Open water Wangeningen B series chart

In 1975, Oosterveld.M [2] presented the result of regression analysis of multiple open water test data of wageningen B-series in the forming of a polynomial equations for estimation of the thrust coefficient K_{To} and torque coefficient K_{Qo} equation 86 and 85. The equations uses the values of the advance coefficient J, Pitch to diameter P/D, A_E/A_0 and the numbers of blade Z to compute the co efficiencies.

$$K_{To} = \sum_{i=0}^{38} C_{s,t,u,v} \cdot j^s \cdot (P/D)^t \cdot (A_E/A_0)^u \cdot Z^v \tag{85}$$

$$K_{Qo} = \sum_{i=0}^{46} C_{s,t,u,v} \cdot j^s \cdot (P/D)^t \cdot (A_E/A_0)^u \cdot Z^v \tag{86}$$

Where $C_{s,t,u,v}$ are coefficient, and s, t, u, v are shown in Table 5. the result of the polynomials are valid only only when $R_e = 2 \times 10^6$.

Table 5: Coefficient of the polynomial for Wangeningen B-series for $R_n = 2 \times 10^6$ Oosterveld.M [2]

K_T $C^T_{s,t,u,v}$	s (J)	t (P/D)	u (A_E/A_O)	v (Z)
+0.00880496	0	0	0	0
-0.204554	1	0	0	0
+0.166351	0	1	0	0
+0.158114	0	2	0	0
-0.147581	2	0	1	0
-0.481497	1	1	1	0
+0.415437	0	2	1	0
+0.0144043	0	0	0	1
-0.0530054	2	0	0	1
+0.0143481	0	1	0	1
+0.0606826	1	1	0	1
-0.0125894	0	0	1	1
+0.0109689	1	0	1	1
-0.133698	0	3	0	0
+0.00638407	0	6	0	0
-0.00132718	2	6	0	0
+0.168496	3	0	1	0
-0.0507214	0	0	2	0
+0.0854559	2	0	2	0
-0.0504475	3	0	2	0
+0.010465	1	6	2	0
-0.00648272	2	6	2	0
-0.00841728	0	3	0	1
+0.0168424	1	3	0	1
-0.00102296	3	3	0	1
-0.0317791	0	3	1	1
+0.018604	1	0	2	1
-0.00410798	0	2	2	1
-0.000606848	0	0	0	2
-0.0049819	1	0	0	2
+0.0025983	2	0	0	2
-0.000560528	3	0	0	2
-0.00163652	1	2	0	2
-0.000328787	1	6	0	2
+0.000116502	2	6	0	2
+0.000690904	0	0	1	2
+0.00421749	0	3	1	2
+0.0000565229	3	6	1	2
-0.00146564	0	3	2	2

$C^Q_{s,t,u,v}$	s (J)	t (P/D)	u (A_E/A_O)	v (Z)
+0.00379368	0	0	0	0
+0.00886523	2	0	0	0
-0.032241	1	1	0	0
+0.00344778	0	2	0	0
-0.0408811	0	1	1	0
-0.108009	1	1	1	0
-0.0885381	2	1	1	0
+0.188561	0	2	1	0
-0.00370871	1	0	0	1
+0.00513696	0	1	0	1
+0.0209449	1	1	0	1
+0.00474319	2	1	0	1
-0.00723408	2	0	1	1
+0.00438388	1	1	1	1
-0.0269403	0	2	1	1
+0.0558082	3	0	1	0
+0.0161886	0	3	1	0
+0.00318086	1	3	1	0
+0.015896	0	0	2	0
+0.0471729	1	0	2	0
+0.0196283	3	0	2	0
-0.0502782	0	1	2	0
-0.030055	3	1	2	0
+0.0417122	2	2	2	0
-0.0397722	0	3	2	0
-0.00350024	0	6	2	0
-0.0106854	3	0	0	1
+0.00110903	3	3	0	1
-0.000313912	0	6	0	1
+0.0035985	3	0	1	1
-0.00142121	0	6	1	1
-0.00383637	1	0	2	1
+0.0126803	0	2	2	1
-0.00318278	2	3	2	1
+0.00334268	0	6	2	1
-0.00183491	1	1	0	2
+0.000112451	3	2	0	2
-0.0000297228	3	6	0	2
+0.000269551	1	0	1	2
+0.00083265	2	0	1	2
+0.00155334	0	2	1	2
+0.000302683	0	6	1	2
-0.0001843	0	0	2	2
-0.000425399	0	3	2	2
+0.0000869243	3	3	2	2
-0.0004659	0	6	2	2
+0.0000554194	1	6	2	2

$R_n = 2 \times 10^6$

Since the polynomials presented in equation 86 and 85 are only valid for specific Reynolds number, to account for a higher Reynolds number the equations in Table 6 can be used for estimating K_{To} and K_{Qo} Oosterveld.M [2].

The typical process of designing of a propeller using Wageningen B-series data is to use the corresponding data chart as shown in Figure 8, where the corresponding data set is traced on the diagram. This iteration process could be time consuming when optimizing of data but with the help of the polynomials as mentioned above an electronic version of the data could be made to give an easy and fast iteration process of finding the corresponding propeller data. These polynomials are implemented into the web-based application to give a functionality of easy propeller selection on the application.

Table 6: Wageningen B-series polynomial accounting for Reynolds number Oosterveld.M [2]

Polynomials for Reynolds number effect (above $R_n = 2\times 10^6$) on K_T and K_Q

$$
\begin{aligned}
\Delta K_T = &\ 0.000353485 \\
&-0.00333758(A_E/A_o)J^2 \\
&-0.00478125(A_E/A_o)(P/D)J \\
&+0.000257792(\log R_n-0.301)^2(A_E/A_o)J^2 \\
&+0.0000643192(\log R_n-0.301)(P/D)^6J^2 \\
&-0.0000110636(\log R_n-0.301)^2(P/D)^6J^2 \\
&-0.0000276305(\log R_n-0.301)^2z(A_E/A_o)J^2 \\
&+0.0000954(\log R_n-0.301)z(A_E/A_o)(P/D)J \\
&+0.0000032049(\log R_n-0.301)z^2(A_E/A_o)(P/D)^3J
\end{aligned}
$$

$$
\begin{aligned}
\Delta K_Q = &-0.000591412 \\
&+0.00696898(P/D) \\
&-0.0000666654z(P/D)^6 \\
&+0.0160818(A_E/A_o)^2 \\
&-0.000938091(\log R_n-0.301)(P/D) \\
&-0.00059593(\log R_n-0.301)(P/D)^2 \\
&+0.0000782099(\log R_n-0.301)^2(P/D)^2 \\
&+0.0000052199(\log R_n-0.301)z(A_E/A_o)J^2 \\
&-0.00000088528(\log R_n-0.301)^2z(A_E/A_o)(P/D)J \\
&+0.0000230171(\log R_n-0.301)z(P/D)^6 \\
&-0.00000184341(\log R_n-0.301)^2z(P/D)^6 \\
&-0.00400252(\log R_n-0.301)(A_E/A_o)^2 \\
&+0.000220915(\log R_n-0.301)^2(A_E/A_o)^2
\end{aligned}
$$

2.2.6.1 Four Quadrant Operation of Propeller

The open water propeller equations presented in section 2.2.6 for torque and thruster are not valid in all operating possibilities of the propeller. The propeller is expected to be able to operate in four quadrants as given in Table 7 but the given open water equations for the K_Qo and K_To are only valid in the 1st and the 3rd quadrants Luca et al. [46], which suit for a vessel in transit condition. To account for the torque and thruster coefficient in all the four quadrant of the propeller, other equations are employed which are based on the angle of attack β of the propeller. For further details check Luca et al. [46], Miniovich [47], W.P.A.van et al. [48] and yvind Notland Smogeli [21]. The angle of attack of the propeller β is given in equation 87 and the new equations for the coefficients that are valid for all four quadrants are given in equation 88 and 89.

Table 7: Four Quadrants of Propeller Operation

	1^{st}	2^{nd}	3^{rd}	4^{th}
n	≥ 0	< 0	< 0	≥ 0
V_a	≥ 0	≥ 0	< 0	< 0

$$\begin{array}{llll} 1^{st}: & 0^\circ \leq \beta \leq 90^\circ, & V_a \geq 0, & n \geq 0, \\ 2^{nd}: & 90^\circ < \beta \leq 180^\circ, & V_a \geq 0, & n < 0, \\ 3^{rd}: & -180^\circ < \beta \leq -90^\circ, & V_a < 0, & n < 0, \\ 4^{th}: & -90^\circ < \beta \leq 0^\circ, & V_a < 0, & n \geq 0. \end{array}$$

$$\beta = arctan\left(\frac{v_a}{0.7\pi nD}\right) = arctan\left(\frac{v_a}{0.7wR}\right) \tag{87}$$

$$C_T = \frac{T_p}{\frac{1}{2}\rho(v_a^2 + (0.7wR)^2)\frac{\pi}{4}D^2} = \frac{T_p}{\frac{1}{2}R^2\pi\rho V_{0.7}^2} \tag{88}$$

$$C_Q = \frac{Q}{\frac{1}{2}\rho(v_a^2 + (0.7wR)^2)\frac{\pi}{4}D^3} = \frac{Q}{\frac{1}{2}R^3\pi\rho V_{0.7}^2} \tag{89}$$

Where $V_{0.7}$ is the undisturbed incident velocity to the propeller blade at radius of 0.7R and is defined in equation 90 while R = D/2.

$$V_{0.7} = \sqrt{v_a^2 + (0.7wR)^2} \tag{90}$$

The coefficient C_T and C_Q are corresponded to every type of propellers, for any specific propeller the C_T and C_Q are given in equation 92 and 91, which gives a 20^{th} order of Fourier's series in β with range as shown in Table 7 and coefficient $(A_T(k)$ and $B_T(k)$ W.P.A van et al. [45].

$$C_T(\beta) = \sum_{i=0}^{20}(A_T(k)\cos\beta k + B_T(k)\sin\beta k) \tag{91}$$

$$C_Q(\beta) = \sum_{i=0}^{20}(A_Q(k)\cos\beta k + B_Q(k)\sin\beta k) \tag{92}$$

To compute the Fourier's series, the coefficients $A_T(k)$ and $B_T(k)$ for any given Wageningen B-series propeller are presented from an experimental result by W.P.A van et al. [45]. A table for the Wageningen B4-70 with the respective coefficient used for the Fourier calculation is shown in Annex B. The four quadrant equation presented require detailed data that may not be available to be used for the computation or to calculate the torque and thrust coefficient yvind Notland Smogeli [21], therefore a simplified equations are presented by yvind Notland Smogeli [21] as given in equation 93 and 94 respectively.

$$C_{Ts} = A_{T0} + A_{T1}\cos\beta + B_{T1}\sin\beta \tag{93}$$

$$C_{Qs} = A_{Q0} + A_{Q1}\cos\beta + B_{Q1}\sin\beta \tag{94}$$

Finally, the given four quadrant equation for the thrust and torque coefficient presented here can also be written in form of the general propeller equation in equation 79 as given in equation 95 and 96 respectively. For more detail of the four quadrant check yvind Notland Smogeli [21], W.P.A van et al. [45], Luca et al. [46].

$$K_T = C_T\frac{\pi}{8}(J^2 + 0.7^2\pi^2) \tag{95}$$

$$K_Q = C_Q\frac{\pi}{8}(J^2 + 0.7^2\pi^2) \tag{96}$$

2.2.7 Power and efficiencies

Wake and thrust deduction

The effect of the flow into the propeller that is affected by the ship hull is described by the Taylor wake fraction w, which is given in equation 97 while the v_a is given in equation 98.

$$w = \frac{V - v_a}{V} \tag{97}$$

$$v_a = V(1 - w) \tag{98}$$

The effect of the rotation of the propeller which causes water to be sucks back towards the propeller can be described by the thrust deduction factor t and is given by equation 99 while the thrust is given by equation 100

$$t = \frac{(T_p - R_T)}{T_P} \tag{99}$$

$$T_p = \frac{(R_T)}{1 - t} \tag{100}$$

The total power of the vessel depends on all the efficiencies as presented below. The effective power P_E is then described by equation 101.

$$P_E = R_T \times V \tag{101}$$

The thrust power P_T is given by equation 102.

$$P_T = T_p \times v_a \tag{102}$$

Having established the P_T and P_E, the ship hull efficiency can be defined as given in equation 103. For ships with a single propeller is around 1.1 to 1.4 and for two propeller is around 0.95 to 1.05 MAN [7].

$$\eta_H = \frac{P_E}{P_T} = \frac{R_T \times V}{T \times v_a} = \frac{R_T/T_p}{v_a/V} = \frac{1-t}{1-w} \tag{103}$$

The open water propeller efficiency η_O varies from 0.35 to 0.75 and it give in equation 104, where η_O is the propeller efficiency , η_R is the relative rotational efficiency (can be taken as $\eta_R = 1.035$) and P_D is the power delivered to the propeller.

$$\eta_B = \frac{P_T}{P_D} = \eta_O \times \eta_R \tag{104}$$

The propulsion efficiency η_D is given as the ratio of the effective power and the delivered power as given in equation 105.

$$\eta_D = \frac{P_E}{P_D} = \frac{P_E \times P_T}{P_T \times P_D} = \eta_H \times \eta_B = \eta_H \times \eta_O \times \eta_R \tag{105}$$

Shaft efficiency η_S is given as the ratio of the power delivered to the propeller to the break power as given in P_B equation 106.

$$\eta_S = \frac{p_D}{P_B} \tag{106}$$

The total efficiency η_T can then be defined as equation 107. .

$$\eta_T = \eta_H \times \eta_O \times \eta_R \times \eta_S \tag{107}$$

The required engine torque Q_B to be able to delivered the required power can then be define as equation 108. For details of these equation check MAN [7].

$$Q_B = \frac{P_B}{2\pi \times n} \tag{108}$$

The different propeller theories presented in this section will be the basis of the models that will be used for propeller analysis ranging from a vessel in transit to a vessel in DP operation. This model will be used to integrate into the web-based open-source application to give it the capability of analysing a large range of propeller characteristics.

2.2.8 Propulsion system

Propulsion system in this context refers to the different configuration or combinations of machinery used to provide propulsion to a vessel Wikiwand [49]. There are different types of propulsion systems normally used in vessels, in this thesis three propulsion systems are considered which are Mechanical system ME, Diesel electric DE, and hybrid propulsion system. Although details of these propulsion systems are not presented in this thesis, they are presented by Cristian A [9].

2.2.8.1 Mechanical propulsion ME

ME is also called Direct drive because the propeller is directly attached to the diesel engine through a shaft which controls the rotation of the propeller. The diesel engine used for ME propulsion is either slow or medium speed engine, where the difference between them has been discussed in section 2.2.1.1. A typical setup for ME propulsion is shown in Figure 9, where Figure 9a is a ME configuration with a slow speed engine where the propeller is directly connected to the engine and Figure 9b is a configuration with a medium speed engine where the propeller is connected to a gear As shown, one difference between them is that for medium speed engine a gearbox is needed to adjust the speed while for slow speed the shaft is connected directly. R.D. et al. [50].

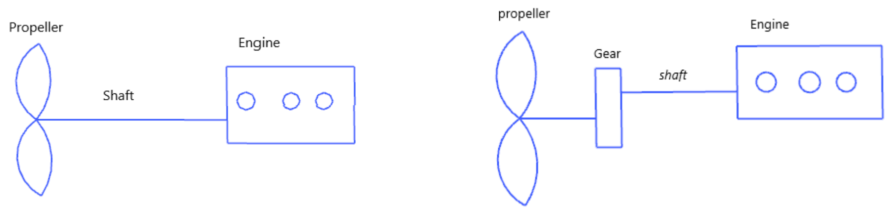

(a) Drive with slow speed engine

(b) Drive with medium speed engine

Figure 9: Direct Drive propulsion with slow speed engine

2.2.8.2 Diesel-Electric propulsion DE

A DE propulsion configuration arrangement is different from a ME system, DE has more complex setup as shown in Figure 10 and they commonly use either medium speed engine or fast speed engine. the prime mover in DE is an electric generator where the electric power produced is distributed and transmitted to the motor which then propeller shaft that is attached to the propeller as shown in the figure Cristian A [9] and R.D. et al. [50].

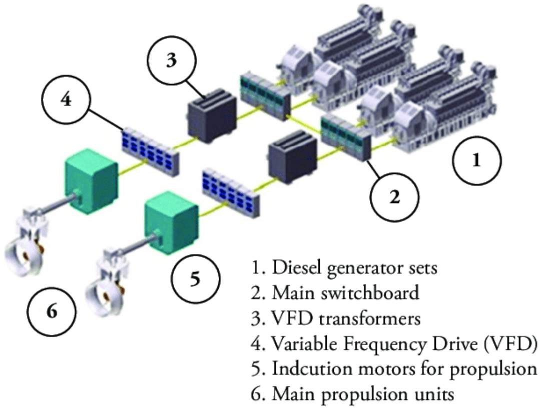

Figure 10: Diesel-Electric Propulsion DE arrangement Cristian A [9]

2.2.8.3 Hybrid Propulsion system

An hybrid propulsion system in this context is the combination of two or more different propulsion systems or power sources, it is a more complex system compare to DE and ME. In Figure 11 typical types of hybrid systems are presented where Figure 11b shows a layout or connection of hybrid system which is a combination of a Mechanical drive and electrical drive. In this system the propeller as shown is directly connected to a gear through a shaft and where the gear can be power through either ME, DE or a combination of both, as shown in the Figure. In Figure 11a an hybrid system layout is shown with a combination of a battery power supply and diesel generator. In this hybrid, the propeller is connected to the motor that is powered by the grid, where power is supplied either through the battery or the generator. The propeller is rotated by motor which is power by the battery or generator. In this system, the battery is usually used for peak shaving or redundancy Cristian A [9].

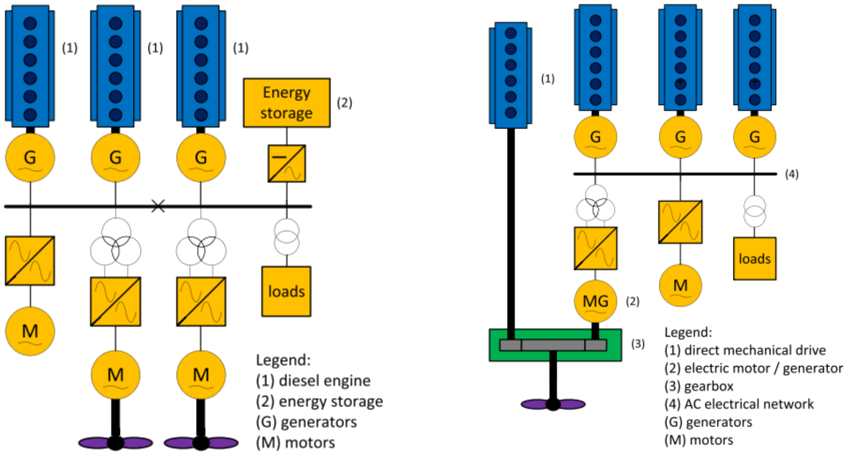

(a) Hybrid : diesel electric and battery **(b)** Hybrid : diesel electric and mechanical

Figure 11: Different hybrid propulsion system

2.2.9 Power management system (PMS)

A Power management system (PMS) is an electronic system in charge of controlling and communicating with the electronic systems. Its major task is to ensure the systems are safe and efficient. In maritime it is usually found on vessels with electric propulsion with operational profile of sea keeping or DP Operation. its major task is to control the power system to minimize blackout and fuel consumption by optimizing the available power supply. Much research has been made and published regarding this topic. For details check the following publication Ingebrigtsen [51], Radan [52], hoglund [53], Halvard Foss [54], T.Lauvdal [55], DAMIR et al. [56].

Functions of Power Management System PMS

PMS has many function on a vessel, the major functions are Ingebrigtsen [51], Radan [52], hoglund [53], Halvard Foss [54]:

- **Power available**: During DP operation it is important that there is always availability of power for the thrusters during operation, the thrusters in a DP system are connected on the same electrical system with other load consumers. This means that other load consumers may increase the energy they consume leaving the total load to be more than the available power which may lead to a blackout. One of the functions of the PMS is to ensure that important load consumers like thrusters are prioritized and ensure other load consumers are checked by the PMS before connecting to the electric grid Radan [52].
- **Load Shedding**: The PMS could be used in some cases to disconnect some of the load consumers completely when needed.

- **Ramp control**: To avoid large step increase on the generator the PMS is used to constraint the increase of load on individual consumers.
- **Automatic Load dependent start/stop**: One of the important function of the PMS is automatically start or turning off a generator when load increases or decreases.
- **Blackout prevention**: PMS is used to prevent blackout depending on the design philosophy.
- **Blackout Recovery**: In an event of blackout the PMS is designed to be able to restart the next available gen-set .
- **Fast Load Reducer (FLR)**: FLR is a system design to be able to reduce the load on the grid within millisecond when the load is greater than the available power. The FLR is a separate system although sometimes it is integrated on the PMS, some vessel with PMS do not have FLR available Radan [52].

2.2.9.1 Power Management System Design

The design of PMS on every system is to achieve the same goal, that is the functions mentioned in section 2.2.9, but the design philosophy to achieve these goals changes with each vessels due to the constraints and operation profile on each vessel. This section will give an overview of implementing of the major functions of PMS. For detail check Ingebrigtsen [51], Radan [52], hoglund [53], Halvard Foss [54].

- **Automatic start and off**: a typical PMS is designed to have the functionality of start and turning off the generator as mentioned, this is done by defining a load limit and timer. When the load reaches the predefined load limit, the timer start counting, when the counter has ended and the load on the grid is still above the predefined limit then a gen-set is started and synchronized to the power bus automatically which takes take about 15 to 30 seconds depending if the gen-set was already on standby mode or not. T.Lauvdal [55]. The corresponding gen-set to be started is determined by a "start up table " which has been predefined. In the Phd work of Damir Ranan Radan [52], T.Lauvdal [55], and DAMIR et al. [56] the equations for the start up table and other details are presented.
- **Blackout prevention**: Many events could lead to blackout on a vessel, in this context, it means the blackout due to overload of gen-set which lead to the shutting down of the gen-set. During a DP operation, there is a dynamic load which may occur very fast, this load my cause the load demand to be greater than the available power, a typical engine have limitations of taking load increase not more than 25% of its rated power and can only accept up to 10% more than its rated power for few seconds SE [57]. Therefore when the dynamic load causes the total load to be greater than the total available power for more than the engine accepted time the engine will shutdown resulting to partial or fully blackout. To prevent this, there are mostly two design philosophies which the PMS could use. The PMS could reduce the load on other consumers, leaving more power to be assigned to the thrusters. This design philosophy does not work in all cases since in some vessel the auxiliary

consumer's load are only fraction of the thrusters load like in the case present by John J.May [58], then this design philosophy will not be suitable since reducing the load from the other consumer will not be enough to take the high dynamic load. The other design philosophy is that when the total load exceeds the available power or predefined load limit a new gen-set should be started according to the start up table or principle.

- **Fast Load Reducer FLR**: Having said that the PMS will prevent blackout by starting a gen-set or reducing the load from other consumers, the dynamic load occur very fast and it requires the engine to act fast. A typical PMS will have a delay or lag in the system leaving it not be fast enough to reduce the loads in some cases, therefore a FLR is used to reduce the load on the thrusters allowing the PMS to either start a new engine or reduce load from other consumers. in an event of Blackout on one of the gen-set, the PMS will receive the signal to start a new gen-set while the FLR will reduced the load to the available power until the PMS start and connect the a new engine to the grid, this process is required by DNVGL [59] to be complete within 45 seconds, for a stand-by engine this is achieved in 30 seconds SE [57] .

In this thesis, a simplified version of the PMS will be design and implemented into the Open source Web-base Application using the typical functions as mentioned here.

2.3 Web-based technologies, Open access

Web-based technologies are those tools that are used in creating or developing a web-based applications, they could be a programming language, library, framework, etc. JavaScript is one of the most important programming languages for web-based development, therefore in this thesis it will be used for the development of the OSS application.

2.3.1 JavaScript

JavaScript is high level programming language that conforms to the ECMAScript specification and is used for client side scripting which gives the ability of dynamic interaction on a web page. JavaScript is one of the mostly widely used scripting languages for development and is support by the web browsers. Like other programming languages JavaScript also uses a concept of object oriented programming (OOP), functional programming, etc. The capability of OOP and client side functionality makes JavaScript a good option for this open-Source project.

2.3.1.1 Object Oriented programming (JavaScript)

OOP is a concept in programming that is based on "Object" instead of functions or logic programming, the following features are included :

- Class.
- Object, method, and property.

- Encapsulation.
- Inheritance.
- Polymorphism.

A “Class” is a blueprint of a set of instructions, methods, data structure used in building an Object while the “Object” is an instance of a class, it contains the methods and properties defined by the class, the object could represent a ”person”, the properties are (age, height, weight etc) where method are set of instructions or the behaviour of the object as shown in Figure 12. Encapsulation is a method which allows the selected properties of the object either to exposed/ hidden or not to be public. Inheritance is the concept that allows an object to share its properties, method with other classes that do not have those properties.

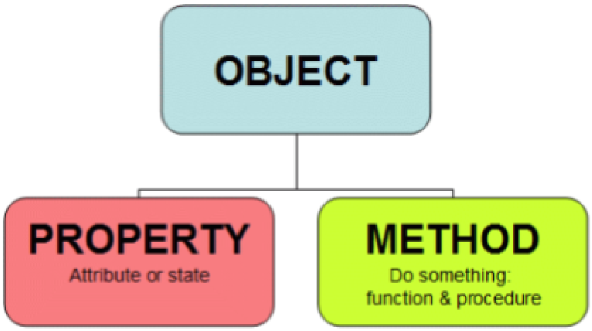

Figure 12: Object representation

This concept gives the ability to represent a real life system in form of “Object” and add properties and methods to it to function as the real system. There are different ways an object could be created in JavaScript. In JavaScript there are different ways an object can be created, an example of a car object with two properties is created using three different ways as show below.

```
// creating Object in different ways
const Car_object = new Object() // creating empty object
Car_object1.color = "red"; // adding //car property
Car_object1.weight_kg = 700; //adding //car property

//second method

const Car_object = {
color : "red", //car property
weight_kg : 700, //car property
}
third method
const Car_object1 = Object.create(Car_object)
```

In Figure 13 an example of a real system is represented using completed OOP method as shown, which shows a battery pack as an object with properties and method represented as a class where the properties are capacity, DOD, C-rate, etc as shown in the figure, typical battery system can be in a charging mode or discharging mode, these modes in OOP are the methods and from the figure the charging mode and discharging mode has been added to the object as a method.

```
class battery_system{
//Object that accept properties from user
  constructor(bat_C_rated, bat_capacity){
    this.c_rate = bat_C_rated;
    this.status = "not used"; // initial status
    this.capacity = bat_capacity;
    this.charging_power = this.capacity*this.c_rate;
    this.scaled_charging_time = 2*60*1000; // charging time
    this.actual_charging_time = (60/this.c_rate)*60*1000;
    this.charging_step =
        (this.actual_charging_time)/(this.scaled_charging_time/500);
        //
     this.charging_step_hours = this.charging_step/(3600*1000); //
    this.discharge_step = this.charging_step_hours;
    this.DOD = bat_DOD;
    this.DOD = this.DOD/100;
  }
 Charge_battery (){"collapse"};
Discharge_battery (){"collapse"};
}
```

Figure 13: Battery pack system represent as class

2.3.2 HTML and CSS

HTML (Hypertext Markup Language) and CSS (Cascading Style Sheet) are the two basis core technologies for enable or building web-based applications, where HTML provides the structure of the web page and CSS is used for describing the how the web page content will be presented .

2.3.3 Open-Source Software OSS

An Open-Source Software OSS is a program whose source code is open to the general public or users and also they have the right to modify the source code, redistribute it, use it without any restriction. OSS is built or developed in a decentralized and collaborative way which depends on the community for development, maintenance, improving the software, thereby letting a wide range of people to contribute to the project. There are many Open source project ranging from individual to organizations, the most relevant to this thesis is the open source library called “Vessel.js” which is developed by the Ship Design and Operation Lab at Norwegian University of Science and Technology Aalesund. The library is used for conceptual ship design to simulate the functionalities and it represents the vessel as an objectVessel.js [60].

For OSS to be opened for collaboration, the software has to be hosted where the general public could be able to access and contribute to it. Today there are many open systems that allows contribution by a community, one of the most popular platforms for hosting and allowing OSS is GitHub, therefore the open application of this thesis will be hosted on GitHub. Where the details the link to code and application can be access in Appendix 6.2.

Chapter 3

Methodology

In this section the methodology used in carrying out the thesis will be presented, which are based on the theories presented in section 2.2.

3.1 Methodology Process Flow

The methodology used in this thesis is shown in a process flow as shown in Figure 14. From the figure, it can be seen that the process is divided into two sections: “Research” and “Web-based Application”, where the first section is the research and development stage of the project and the second section is applying the result of the research to develop the open source application. The figure shows the process and steps of the methodology used in the thesis at a high level, meaning that each step in the process as shown and numbered in the figure may have other smaller processes in it. To understand the steps in the process in detail, each step will be explained using the numbering as reference:

- **1.0 (Start)**, this is the first starting of the project.
- **1.1 (Research)**, the first thing that was done is researching about the topic by reading publications and other related works.
- **1.2 (Gather information)**; after researching is done on necessary publication, the information related to the thesis were gathered to be used in the later stage of the project.
- **1.3 (Establish requirement)**, In this step, the operations that the web-based application will support are established or defined, example are DP and transit operations, resistance estimation, etc.
- **1.4 (Establish machinery)**; in this step, the necessary machinery based on the operations defined in step **1.3** are established, for example propeller, diesel engine, battery storage, etc.

- **1.5 (Machinery information from supplier)**, in this step the data of the machinery established in step 1.4 are collected from the different suppliers website.
- **1.6 (Mathematical model)**; in this step, the mathematical model that represent each machinery are developed based on the collected data. For example, a model engine power, propeller torque , emission etc.
- **1.7 (Test and validate model)**; after developing the different models for the machinery each model result are tested against either data from publication or data from the supplier if available, to ensure the models developed functions as the real system as closely as possible.
- **1.8 (Model result)**; in this step, if the model results that are validated are good enough then proceed to step 1.9; if they not good enough then back to step 1.6.
- **2.0 (Start web-based development)**, when the model established has been validated then proceed to start developing the web-based application using JavaScript where the different models are implemented on the web-based application.
- **2.1 (Machinery as Object)**; in this step, the machinery that has been established in step 1.4 is created in the application using OOP method which are later stored, although at the stage of this open source application there is no external data base yet, every data are stored on the application.
- **2.2 (Method)**, after creating the machinery object, methods are added to the corresponding machinery based on the established models in step 1.6.
- **2.3 (Benchmark result)**, When the machinery Object and methods have been created in the application, each separate machinery is tested and the results are compared to a benchmark.
- **2.4 (Result)**, if the results from step 2.3 are ok then starting design the user interface in step 3.0 if not then back to step 2.1.
- **3.1 (Operations)**; in this step, the operations established in 1.3 are created on the web page of the application to allow users to choose different operation options.
- **3.2 (Choose operation)**, in this step an interface to allow user to choose different operations is created.
- **3.3 (Displaying machinery)**, the different operations created are connected to needed machinery for each operation whereby when a user chooses an operation the information is sent to the data based where all the machinery data are stored, and the data for that specific operation and displayed on the application.
- **3.4 (User input)**, in this step an environment that allows users to create or customize machinery is developed, this machinery is organized and stored like the predefined machinery is stored. This is an important feature to allow people to contribute visually without the need to write any code.

- **3.5 (Perform analysis)**; in this step, an environment that allows performing of analysis of different operations. This also includes the simulation dashboard.

- **3.6 (Data insights)**; after completing the simulation in step 3.5, different data are available for visualization depending on the operation and the KPI that is important to the user regarding the operation that was made.

- **END**, after step 3.6 then the open source application is ready to be used.

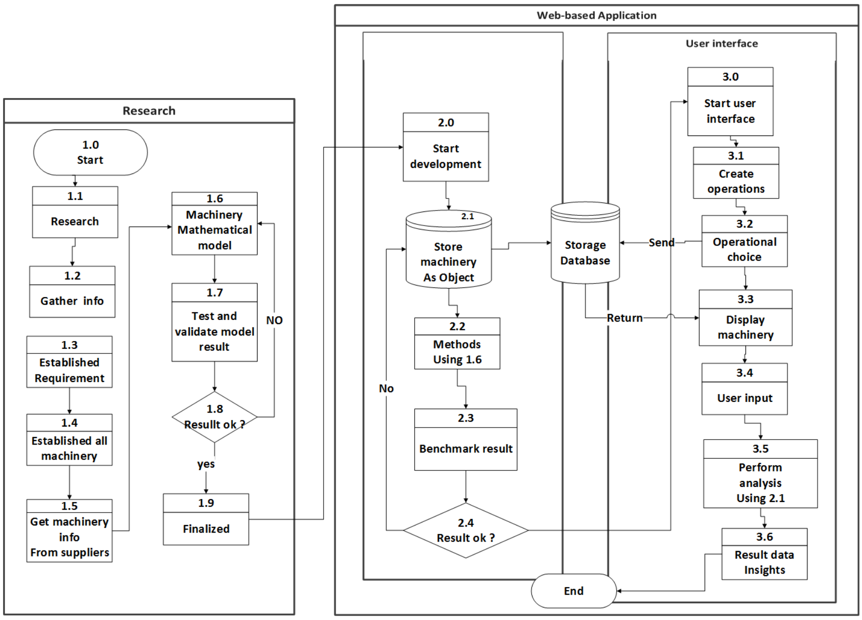

Figure 14: Methodology Process Flow

3.2 Assumptions

To proceed with the method some assumptions are made to either simplify the procedures or to account for data that are mission.

- The thrust on the DP thrusters during simulation is assumed to be governed by the thrust estimated using open water equations as given in equation 79. usually, when considering a DP operation the forces generated are considered in all possible directions of the force.

- SFOC estimation; the method used for the SFOC is based on a model which depends on engine unique value called “based line ” as mentioned. This value varies with engines and are not published on the suppliers websites, therefore the rated SFOC of the engine published on supplier‘s website are used .

3.3 Machinery as an Object

In this section, the step in **2.1** from the process flow is implemented which is to create the machinery as an Object using the method presented in section 2.3.1.1.

3.3.1 Engine as Object

Two diesel engine and two gen-set have been built into the application. To implement this, the process flow as shown was used, which shows that in step 2.1 the machinery is created using the data from the supplier website, in this case they are from Wartsila [61, 62]. With this, a simplified version of engine object with data from the supplier is shown below.

```
 // engine object
const engineData ={
//All engine data
  wartsila:{
     engint_type: "Wartsila 46F",
     Strokes: "4 Stroke",
     speed_type: "Medium-Speed",
     model: "14V46F",
     LHV: "42700 kJ/kg",
     SFOC: "176 g/kWh",
     pistonStroke : "580 mm",
     cylinderBore: "460 mm",
     mean_Presure : "24.9 bar ",
     Engine_Power: "16800 kW",
     Engine_speed:" 600 RPM",
    }
}
```

3.3.2 Engine as Method

After creating the machinery object, the next step is to add methods which are step 2.2 in the process flow chart which is based on step 1.6 (machinery mathematical model), where the models have been presented in section 2.2.1.1 as mathematical equations. The methods are created such that the different engines could use this method by simply passing the engine object or properties to the method functions as shown below.

Listing 3.1: Engine Method

```
function engine_Methods (){
 //methods for use for every engine chosen
   this.torque = function (engine_Object){ // Torque method
   this.mean_p = mean_Presure; // mean effective pressure
   this.cylinderBore = cylinderBore*0.001;// m engine property
   this.pistonStroke = pistonStroke *0.001;//m engine property
   this.speed_RPM = speedRPM; //engine speed
```

```
    this.engineStroke = Strokes;
    if (this.engineStroke === "4 Stroke"){ //engine type
       this.cranshaftRev = 2;
    }
    else if (this.engineStroke === "2 Stroke") {
       this.cranshaftRev = 1
    }
    this.area = (Pi*this.cylinderBore*this.cylinderBore)/4 // area
        of cylinder bore
    this.Volume = this.area*this.pistonStroke*this.cylinderNumber
    this.Torque =
        ((this.mean_p*100000*this.Volume)/(2*3.143*this.cranshaftRev))/1000
}
}
```

3.4 Power management system PMS Design

In section 2.2.9, the basic information regarding PMS has been present in regards to the principles, design of PMS, and how it works. To be able to successfully simulated DP operation a PMS is needed, therefore in this thesis, a simplified PMS will be designed that will be implemented into the software which is based on the concept mentioned in section 2.2.9 and some modifications. Below is the design philosophy.

Failure mode and transient load

In an event of a failure in any of the gen-set, the load that was on the failed gen-set $P_{fail,g}$ is transferred to the rest of the gen-set that are online. In such event, the load shall be shared according to equation 109, which ensured that the transferred load is not greater than the available power online at that instant as stated in section 2.2.9. Where P_{rate} is the rated power of the gen-set. Where $P_{L,v}$ is the available load that has been reduced and $P_{comb,con}$ is the continued allowable power (online generators and battery pack).

$$P_{L,v} \leq P_{comb,con} \tag{109}$$

Where $P_{comb,con}$ is given by equation 110, $P_{g,con,t}$ is the continuous total power of the online gen-set as given in equation 111 , P_b is the battery capacity.

$$P_{comb} = P_{g,con,t} + P_b \tag{110}$$

$$P_{g,con,t} = N_{online} \times P_{g,con} \tag{111}$$

In an event of gen-set failure, the maximum load on each generator shall be 10% above the p_{rate} for not more than ≤ 10 second. This means that within this period, the maximum accepted load shall be according to equation 112

$$P_{comb,max} = N_{online} \times 1.1 \cdot P_{rate} + P_b \tag{112}$$

As stated in section 2.2.9 that the FLR function is to reduce the load in event of failure or peak load, this is done by comparing the load before failure P_{fail} to the maximum available power online $P_{comb,max}$ in equation 113 and ensure the load transferred is not greater the available power.

$$P(L_1, L_2)_{FLR} = P_{FLR}(P_{comb,max}, P_{fail}) \tag{113}$$

The FLR shall reduced the load according to the $P_{comb,con}$ and maximum possible load $P_{comb,max}$ where the reduced load $P_{L,v}$ is given in equation 114.This means that the PMS shall firstly reduced and according to equation 112 and if after 10 second, the load is still greater then it shall be reduced according to $P_{comb,con}$.

$$P_{L,v} = \begin{cases} P(L_1, L_2)_{FLR} = min(P_{comb,max}, P_{fail,g}) & \text{if } t_{a,fail} \leq 10s \\ \\ P(L_1, L_2)_{FLR} = min(P_{comb,con}, P_{fail\_g}) & \text{if } t_{a\_fail} > 10s \end{cases} \tag{114}$$

As stated in section 2.2.9, the gen-set are not only limited by the load on them but also by the transient load transfer to the gen-set. The transient allowable load step on a typical engine or generator is usually 25% to 33% of the rated power P_{rate} SE [57]. Therefore the FLR shall ensure that the transient load transfer to the gen-set in an event of failure is not greater than the maximum allowable transient on the generator and governed as shown in equation 115.

$$P_{g,trans} \leq Pg + \Delta P_{FLR}(P_{g,con}, P_{fail\_g}, t_{FLR}) \tag{115}$$

Where t_{FLR} is the time it takes the FLR to reduce each load step, $\Delta P_{FLR}(P_{g,con}, P_{fail\_g}, t_{FLR})$ is the load added to the generator load and Pg is the generator load before FLR reduced the load. for more detail check Radan [52], DAMIR et al. [56]

Start/Stop generator set

As mentioned, one of the functions of the PMS is to start and stop the gen-set when the criteria in section 2.2.9 are met.

In the publication of Radan [52], DAMIR et al. [56], the methodology that was presented for starting a generator is based on a predefined start up table as mentioned in section 2.2.9, in this thesis, a start up table will not be implemented but a different approach was implemented which allows the PMS to evaluate the situation based certain criteria that are given and automatically decide the next gen-set to be started or the load to assign to each gen-set in order to achieve the optimal performance of the engines putting safety into consideration.

The governed algorithm for deciding the numbers of generator set to be started is based on the restriction given in equation 116, where $P_{L,A,g}$ is the load that will be assigned to each generator set when online.

$$P_{L,A,g} = \begin{cases} 0.3 \cdot P_{rate} \leq P_{L,A,g} < 0.6 \cdot P_{rate} & \text{if } N_{online} \geq 2 \;\; \& \;\; P_b = 0 \\ \\ 0.3 \cdot P_{rate} \leq P_{L,A,g} < 0.8 \cdot P_{rate} & \text{if } N_{online} \geq 2 \;\; \& \;\; P_b > 0 \end{cases} \tag{116}$$

The actual value of $P_{L,A,g}$ will vary and when other power sources like battery pack are available then the upper limit power can be increase as shown in equation 116 but this will depend on:

- Safety; in an event of failure of gen-set the remaining gen-set should be able to supply enough power to keep the vessel without drifting from its position in a DP operation, which will also influence the blackout possibility. This means that when the PMS is deciding the numbers of gen-set to be online it considered the fact that in an event of failure on one of the gen-set, the remaining gen-set should be able to carryout operation until the next gen-set is started. This is important when during DP operation to avoid drift of the vessel from the current location due to insufficient power to the thrusters.

- FC; the combined fuel consumption of all the online gen-sets should be optimal enough while pitting the first point into consideration.

This means that the value of $P_{L,A,g}$ will vary depending on the trade-off between the two points mentioned above. The PMS using the method presented is shown in a high level block diagram in Figure 15 and the structure of the code as class is shown in 3.2. From the diagram **1:** $P_{L,v}$ is the total load is sent to **3**, where the load and the power are compared as given in equation 109 and if the load is greater then two signal are sent out, one is to **2: start algorithm** to start new gen-set while other is to reduce the load by the FLR in **4** according to equation 114 before sending it to **6: Power Plant**. As shown the **4** and **6** sends signals back and fort, where the power plant sends information's regarding gen-sets status while FLR send the reduced load. While **2** estimate the optimal numbers of gen-set according to equation 116 and sends the corresponding number to the power plant to be turned ON. In an event gen-set failure or blackout it is detected in **5**, if there is failure then **3** is activated and also sends a signal to **2** start a new gen-set. This PMS is implemented into the web-based application. To understand more details on the code check the code that is hosted on GitHub whose link is give in the Appendix 6.2.

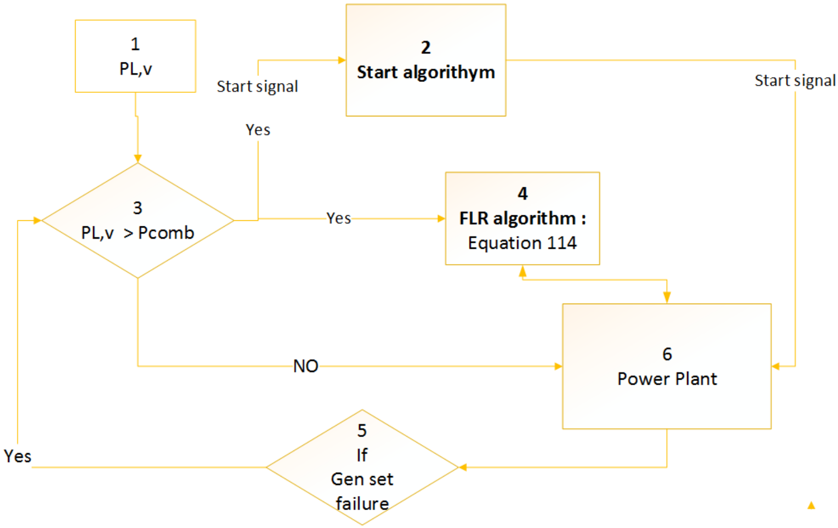

Figure 15: High level block diagram of the PMS

Listing 3.2: PMS

```
class PMS {
    constructor(engine_nums,engine_power,operation,Aux_load,bat_SOC){
       //constructors
    }
    start_off_engine(){
      //initialized and estimate number of gen-set to be online
    }
     update(){
      // check for update
  }
  optimized_engine_load(step){
     //optimized the load on each engine to have a better
          performance
  }
  turn_on_new_engine(){
       //start new gen-set in the event of blackout or peak peaks
            load
    }
  FLR(){
         //Fast load reducer, to reduce to load on the gen-set
        }
    blackOut_prevention(){
       //Ensure blackout never happen
    }
    blackOut_recovery(){
```

```
      // In the case of a blackout restart all system.
    }
    charge_battery(){
     // Activate battery charging
    }
    discharge_battery(){
     // Activate discharging of batter
    }
    Test_blackout(blackOut_type){
      //Test system by creating blackout
    }
    Monitor_system(){
    //monitor all system status and detect blackout
    }
}
```

3.5 Software Hierarchy

In the previous section, different theories and methodologies have been presented which are the basis for developing the application. To understand the application a software hierarchy is presented in Figure 16. As shown the 2nd level is divided into 7 which represent the major sections of the application where each of them is divided into sub-level as shown in the figure, the numbers are used to refers to each module when explaining below :

1. **(Ship Resistance)**; one of the features of the application is the ability to used for ship resistance estimation. From the hierarchy structure, it is divided into 1.1 which is the calm water resistance, and 1.2 which is the added Resistance. Where 1.1.1 is the method implemented into the application for calm water resistance estimation which is based on Holtrop and Mennen method presents in section 2.2.5.1. The Added Resistance 1.2 is divided into 1.2.1 resistance due to wave and 1.2.2 Resistance due to Wind where the respective equation are presented in equations 78 and 76 respectively.

2. **(Engine performance)**; a key indicator of engine performance is the SFOC which is usually presented in SFOC VS load curve. The application also has a feature that allows user to test different engine performance, this is implemented using equation 6.

3. **(Power Source)**; 3.0 is the possible power source that a vessel can have and it is divided into 3.1 (Engine) and 3.2 (battery storage). The 3.1 is further divided into a sub level, 3.1.1 which is the fuel consumption of the engine and is given by equation 8 while 3.1.2 is the power produced and 3.1.3 is the torque given in equation 4.

4. **(Propeller)**; 4.0 is the propeller analysis of the application, this section allows users to perform propeller analysis of the wageningen B series, which is according to the principle and different equations presented in section 2.2.6.

5. **(Simulation)**; 5.0 represents the different simulation the web-based application can perform, it is divided into sub level of 5.1 which is the section of the application for DP simulation equipped with PMS while 5.2 is the section on the application that allows Transit simulation and is divided into sub level of 5.2.1, 5.2.2 and 5.2.3 which represent the different propulsion system a user can choose while in transit mode (ME , DE, and Hybrid).

6. **(PMS)**; 6.0 is the power management system, whose details have been presented in section 3.4 and block diagram shown in Figure 15.

7. **(Data Insights)**; 7.0 represents the section use for analysis data generated after a simulation is made. It is divided into sub level of 7.1.1 which is the emission emitted during a simulation, 7.1.2 is the fuel consumption during an operation which is further divided into the different fuels, and 7.1.3 is the engine performance. Each engine during operation stores its operating data as an object which users can use it determine the performance of an engine over the other or for different analysis.

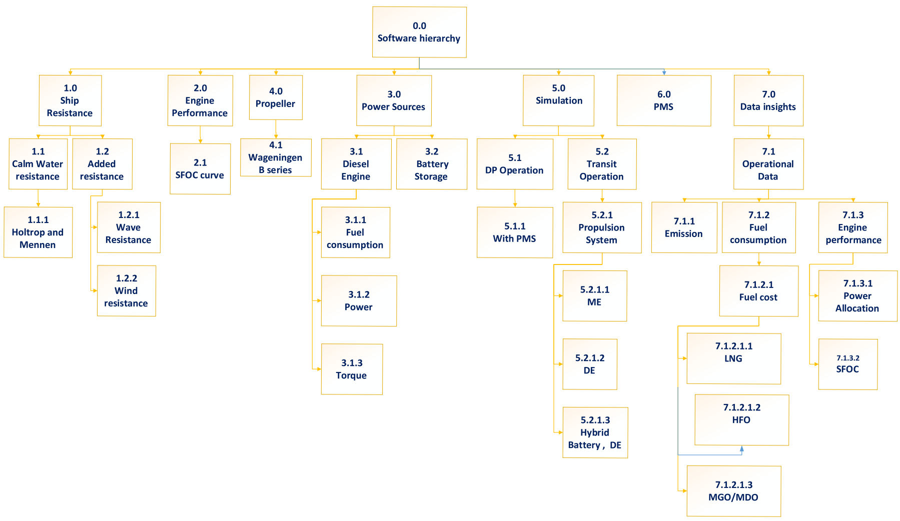

Figure 16: Software hierarchy

3.6 General Methodology

In the previous sections the methodology and equations regarding the web-based application have been presented, To Further understand the application a block diagram and a logic diagram showing how the application works and how the modules in the Hierarchy Figure 16 interact with each other are presented.

3.6.1 Block Diagram representation

The block diagram shown in Figure 17 shows the flow of data in the application. It can be explained as follows:

1. **(Input)**; from the diagram, the input section as shown, are required input that are given to the application which are vessel properties, weather condition and propeller dimension .

2. **(Resistance)**, the second block as shown is the resistance which takes the input from block 1 and estimated the calm water resistance and the added Resistance where the added resistance is sent to 4 and 6 while the calm water resistance is sent to 3.

3. **(Propeller)**, In block 3, the data from the user input (vessel properties) in block 1 is sent to block 3 and the resistance from block 2. Using the vessel data, a corresponding propeller size with the resistance, the power delivered to the propeller is estimated and send to block 5.

4. **(Machinery configuration)**; in block 4, the machinery configuration that are available on the application be can be chosen, which are depending on the propulsion system. Where the chosen information is sent to block 5.

5. **(Power plant)**; in block 5, the required engine power and the numbers of engines are determined, this is done by either using the already built in engine library or creating a customized engines using the information from block 2, 4 and block 3. where the engines powers and the number installed are sent to block 8 (PMS).

6. **(Operation and simulation)**, in block 6 the user can choose the type of operation that is needed to be simulated (DP or Transit).

7. **(Vessel performance KPI)**; after the simulation is complete, the user can have insights of the data generated during the simulation. Depending on the user KPIs.

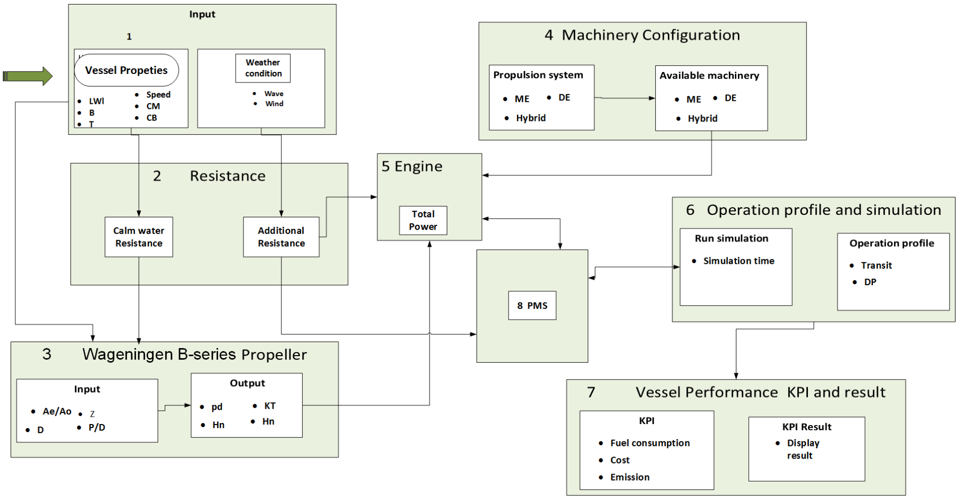

Figure 17: Block diagram of the web-based application

3.6.2 Propeller and Power estimation Logic

The Logic behind the propeller and power estimation in the application is shown in Figure 18. As shown on the figure, the user is required to input the vessel properties, with the input data an initial propeller diameter based on the maximum draught is estimated using equation 84 and the Wageningen B Series propeller properties are also automatically chosen. The vessel resistance is estimated using Holtrop and Mennen method. With these automatically estimated results, the user can review the propeller diameter D and the chosen Wageningen data, if they are not Ok then the data can be adjusted to meet the user needs. If the data are ok then a function uses the data and the input data from the user input to estimate the wake, thrust andK_T, K_Q as shown on the figure. The wake is based on Holtrop method using equations 70 and 71 respectively, the thrust function is also based on Holtrop method using 72 and 73 while K_T and K_Q function uses the Wageningen B series polynomial on Table 6 . These results are used in estimating the hull and propeller efficiency and if these efficiencies are not good enough the user can go back to adjust the Wageningen B series propeller data until the efficiencies meet their needs as shown on the figure. After that, the efficiencies and the resistance are passed to function to estimate the required power for the vessel using combination of different equations as shown on the logic figure.

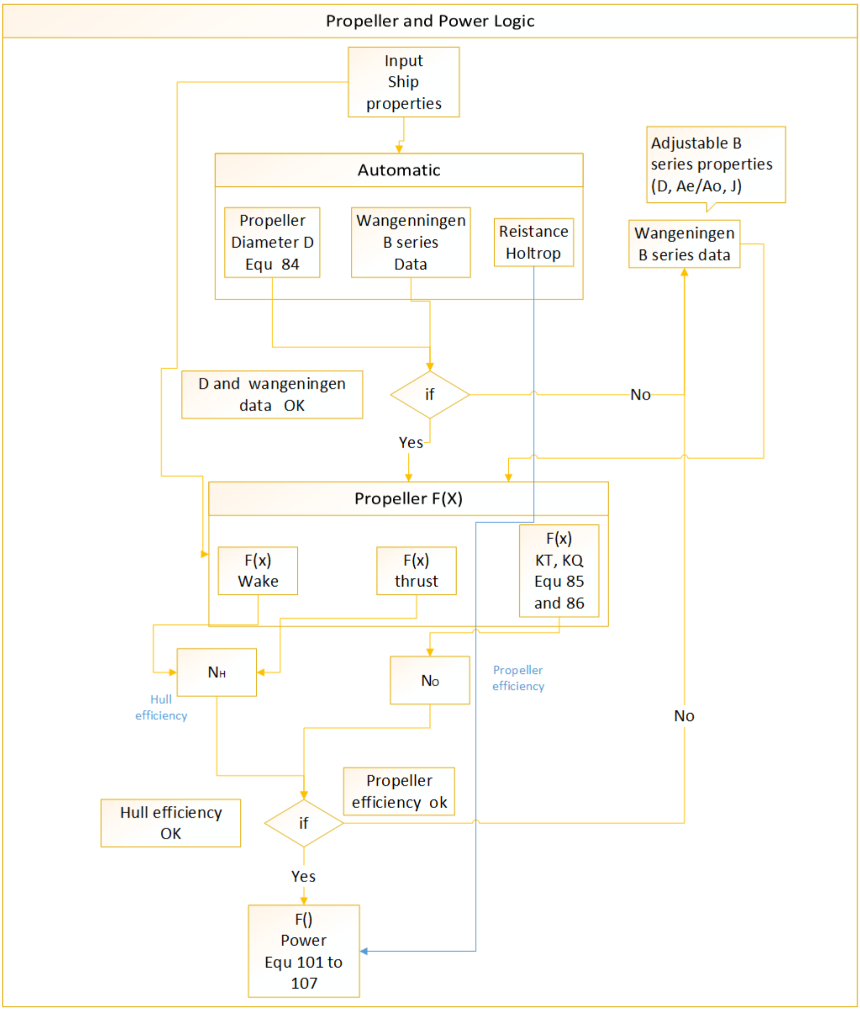

Figure 18: Propeller and power logic

3.6.3 DP Operation Simulation Logic

In this section, the basic logic used during a DP simulation is present, for detailed steps of the logic, check the GitHub page where the code is hosted as shown in appendix 6.2 . In Figure 19 the logic during DP operation is shown, from the figure before starting the simulation, the required power needed is estimated using the method in the power logic in section 3.6.2. Section 2.2.6.1 discussed on how the open water equations are not applied to the four quadrants of the propeller and different equations based on the angle of attack of the propeller was presented. During the DP operation, the thrusters are running in a manner that the open water equation does not apply therefore the equations in 2.2.6.1 should have been used. However, due to the fact that some data required to used these equations are missing it assumed that the required power as shown in Figure 19 will follow open water propeller equations which were used to implement the power estimation logic in section 3.6.2.

After estimating the power, the user decides the gen-set they want to be installed by choosing from the data base or creating its own desired gen-set. Then the chosen gen-set data is pass to an algorithm which based on equation 116 which check if installed power is enough ($P_{L,V} > P_{com}$). If the expected load will be greater then a message will be displayed asking the user to choose a new set of gen-set with a recommendation on the minimum required installed power. If the chosen gen-sets are ok, then the data of the gen-sets are sent to the **Power Plant** as shown.

To start the simulation, the user inputs weather conditions which are the maximum possible significant wave height and the maximum possible wind speed of the location, where these are passed to an algorithm called Environmental load which will be discussed in section 3.6.4. The algorithm keeps generating wave and wind causing dynamic load on the system. When the simulation is on going the PMS algorithm presented in section 3.4 is responsible for controlling the power plant, environmental loads and the thruster load as shown in the figure. The environmental loads are the loads that are caused by waves and wind. During a simulation, these loads are used to create dynamic load on the thruster. To understand the environmental loads check section 3.6.4 and Figure 20. As shown on the figure, the power plant can be a combination of battery storage and gen-set. The gen-set power is given by equation 1 while the battery power and capacity is given by equation 9. When the gen-sets are online or being used, fuel is being consumed and the performance of the gen-set is represented by SFOC. Where the emission emitted from the gen-set can be estimated using the equation as shown in the figure.

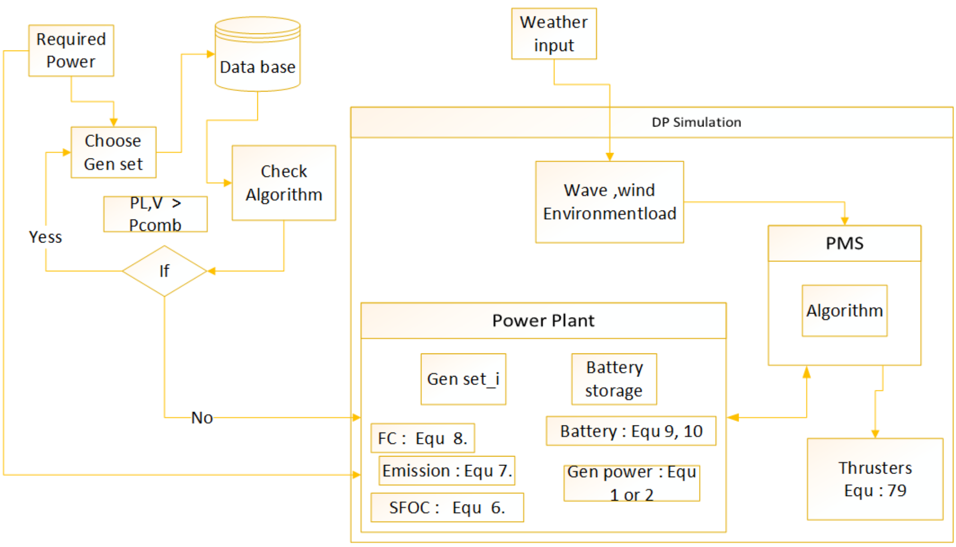

Figure 19: DP operation simulation logic

3.6.4 Environmental loads

During a simulation, it is expected that the vessel should have a dynamic load resulting from the wave and wind in that environment, this is done using the algorithm as shown Figure 20, where a user is expected to input the maximum possible wind speed and maximum possible significant wave height which they are passed to algorithm as shown. These are called “max significant wave height” and “max wind speed” as shown in the figure. As long as simulation is ongoing the algorithm keeps creating a new wave and speed randomly in a way that it Will never be above maximum speed input (wind_input) and maximum wave height input (wave_input) by the user. The output of the new generated wave and wind speed are passed to a function to calculate the load caused by the waves and wind which are then applied as the dynamic load and passed to the PMS as shown. The load generated by the algorithm is based on equation 77 and 78 respectively.

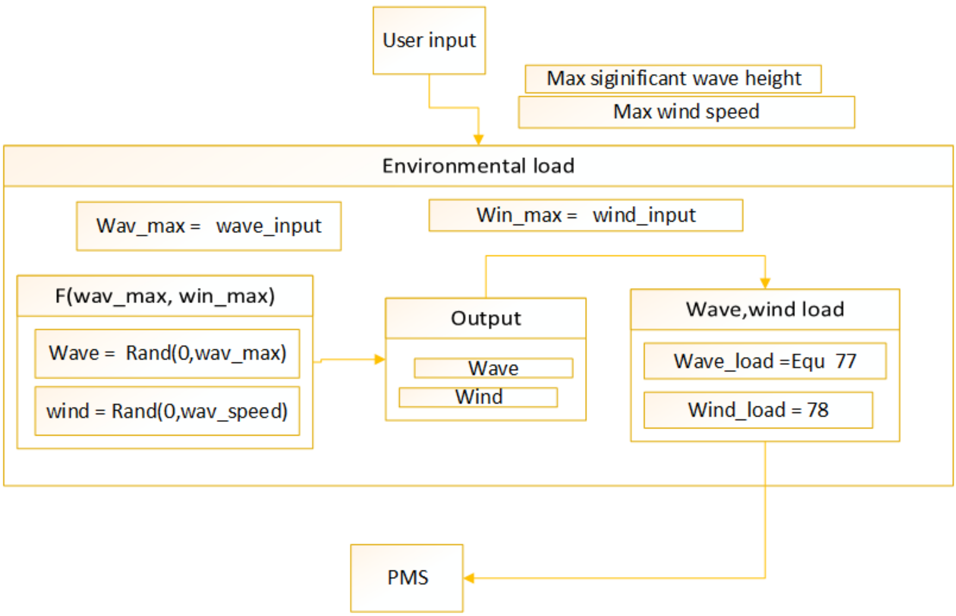

Figure 20: Environmental loads Logic

3.6.5 Verification

As mentioned in the methodology, different machinery methods will be tested and compared to existing results to ensure that the software is functioning as it should. In this section the verification will be presented.

3.6.5.1 Resistance Benchmark

The vessel resistance section on the application was built with the Holtrop and Mennen method. To ensure that there is no error in the implementation and the result is within the accepted range, the software was used to estimate the resistance of a vessel, where the details of the vessel data are shown in Figure 21. This vessel was chosen because the author's of this method Holtrop.J [38] uses this method to analyzed the vessel resistance, where the result are shown in the paper. The results can be see in Figure 22b. this serves as a verification benchmark to compare the result of the application to the result presented in the publication.

length on waterline	L	205.00 m
length between perpendiculars	L_{pp}	200.00 m
breadth moulded	B	32.00 m
draught moulded on F.P.	T_F	10.00 m
draught moulded on A.P.	T_A	10.00 m
displacement volume moulded	∇	37500 m^3
longitudinal centre of buoyancy	2.02% aft of ½L_{pp}	
transverse bulb area	A_{BT}	20.0 m^2
centre of bulb area above keel line	h_B	4.0 m
midship section coefficient	C_M	0.980
waterplane area coefficient	C_{WP}	0.750
transom area	A_T	16.0 m^2
wetted area appendages	S_{APP}	50.0 m^2
stern shape parameter	C_{stern}	10.0
propeller diameter	D	8.00 m
number of propeller blades	Z	4
clearance propeller with keel line		0.20 m
ship speed	V	25.0 knots

Figure 21: Reference vessel data for the verification

In Figure 22a a screenshot of the result from the application with different component of the resistance are shown. Each individual value was compared to the result estimated from the publication, but the major comparison are highlighted in red. When comparing the result of the benchmark and the result from the application as shown in Figure 22b, it can seen that the Frictional resistance R_F from the application is $868.09kN$ while the benchmark result is $869.6kN$, the Appendages resistance R_{APP} from the application is $8.63kN$ while from the benchmark is $8.83kN$, the frontal area of the vessel was not given so the air resistance is considered zero on both side, the pressure due to bulbous bow was estimated to be $0.001kN$ while from the benchmark it is about $0.049kN$, wave making resistance R_W from the application is $559.6kN$ while from the benchmark is $557.11kN$, the transom resistance R_{TR} are both $0kN$, the mid-ship correlation resistance R_A is $219.92kN$ from the application while the benchmark is $221.98kN$. The addition of these components, which is the total resistance R_T given by equation 62, is $1825.49kN$ from the application while the benchmark gives 1793. The difference in total resistance is due to fact that the total resistance uses a form factor $(1 + k_1)$ which has been modified according to the updated version in Holtrop.J [1], as shown in equation 62.

DIFFERENT RESISTANCE	
RESISTANCE	KN
Frictional	868.09
Wave making	559.57
Appendages	8.62914
thruster resistance	0
pressure bulbous bow	0.001
pressure at Transom	0
Mid-ship Correlation	219.92
Air resistance	0
Wind resistance	0
Fouling Resistance	0
Wave resistance	1058.88
Calm water resistance	1825.49
Extrem condition Resistance	1825.49

(a) Application analysis result

F_n	= 0.2868	F_{nT}	= 5.433
C_P	= 0.5833	R_{TR}	= 0.00 kN
L_R	= 81.385 m	c_4	= 0.04
lcb	= −0.75% (relative to ½ L)	C_A	= 0.000352
c_{12}	= 0.5102	R_A	= 221.98 kN
c_{13}	= 1.030	R_{total}	= 1793.26 kN
$1 + k_1$	= 1.156	P_E	= 23063 kW
S	= 7381.45 m²	C_V	= 0.001963
C_F	= 0.001390	c_9	= 14.500
R_F	= 869.63 kN	c_{11}	= 1.250
$1 + k_2$	= 1.50	C_{P1}	= 0.5477
R_{APP}	= 8.83 kN	w	= 0.2584
c_7	= 0.1561	c_{10}	= 0.15610
i_E	= 12.08 degrees	t	= 0.1747
c_1	= 1.398	T	= 2172.75 kN
c_3	= 0.02119	A_E/A_O	= 0.7393
c_2	= 0.7595	η_R	= 0.9931
c_5	= 0.9592	$c_{0.75}$	= 3.065 m
m_1	= −2.1274	$t/c_{0.75}$	= 0.03524
c_{15}	= 1.69385	ΔC_D	= 0.000956
m_2	= −0.17087		
λ	= 0.6513	From the B-series polynomials:	
R_W	= 557.11 kN		
P_B	= 0.6261	K_{Ts}	= 0.18802
F_{ni}	= 1.5084	n	= 1.6594 Hz
R_B	= 0.049 kN	K_{Qo}	= 0.033275
		η_o	= 0.6461
		P_S	= 32621 kW

(b) Verification benchmark result Holtrop.J [38]

Figure 22: Benchmark result and analysis result

3.6.5.2 Engine performance analysis

One of the components from the software hierarchy in Figure 16 shows the ability for the application to be used for engine performance analysis. The method implemented into the application is based on IMO [3], Hassan and Hassan [5] and the accuracy of this method depends on a "baseline value" that is unique to every engine, where a typical range of values can be seen in Figure 3. When the exact values for the engine models are not published in the engines suppliers websites, I adopted the value ranges recommended in the figure when implementing the mathematical models. Since these recommended values are used in estimating the SFOC, the accuracy of the SFOC will also influence the fuel consumption, emissions and fuel cost. Although this model was not fully tested to confirm its accuracy.

3.6.5.3 Propeller open water characteristic

An important part of the application is the estimation of the propeller open water characteristics. To ensure that the results of this estimation are accurate, they are compared to an existing Wageningen B series B4-85 chart as shown in Figure 8. The results of K_Q and K_T where manually checked against the data on the chart. Another comparison is shown in Figure 23, where the existing results for different propellers dimensions are shown in Figure 23b Birk [20]. To ensure that the propeller analysis result from the application are good enough, these different propeller parameters as shown in the figure are input to the application respectively. The result of the different propellers from the application are approximately the same with the existing results. Where an example of the propeller's data inputted and the result is shown in figure 23a, Which the result of the K_Q and K_T as shown are the same are approximately.

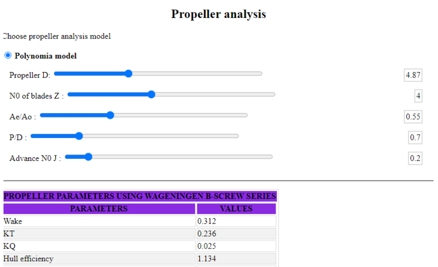

(a) Application result

Prop 1	$Z = 4, P/D = 0.7000, A_E/A_0 = 0.5500$					
J:	0.000000	0.200000	0.400000	0.600000	0.800000	1.000000
K_T:	0.293034	0.235922	0.163956	0.080357	−0.011655	−0.108858
$10K_Q$:	0.314941	0.265489	0.202513	0.125021	0.032021	−0.077478
Prop 2	$Z = 5, P/D = 0.7000, A_E/A_0 = 0.5500$					
J:	0.000000	0.200000	0.400000	0.600000	0.800000	1.000000
K_T:	0.304817	0.247985	0.173682	0.084871	−0.015485	−0.124422
$10K_Q$:	0.325948	0.279672	0.218642	0.138134	0.033421	−0.100223
Prop 3	$Z = 4, P/D = 0.9000, A_E/A_0 = 0.5500$					
J:	0.000000	0.200000	0.400000	0.600000	0.800000	1.000000
K_T:	0.382545	0.327866	0.258221	0.176763	0.086647	−0.008971
$10K_Q$:	0.502623	0.442389	0.366125	0.273048	0.162376	0.033326
Prop 4	$Z = 5, P/D = 0.9000, A_E/A_0 = 0.7000$					
J:	0.000000	0.200000	0.400000	0.600000	0.800000	1.000000
K_T:	0.413463	0.353818	0.276834	0.186159	0.085442	−0.021668
$10K_Q$:	0.550275	0.483373	0.396737	0.290990	0.166755	0.024655

(b) Verification benchmark result Birk [20]

Figure 23: Propeller benchmark result and analysis result

3.7 Simulation environment and workflow

In this section, a high level diagram of a possible work flow of the application for simulation will be presented as shown in Figure 24. To follow the process, the vessel data presented in Figure 21 will be used as a case study to go through the steps. More details will be shown when explaining the flow chart.

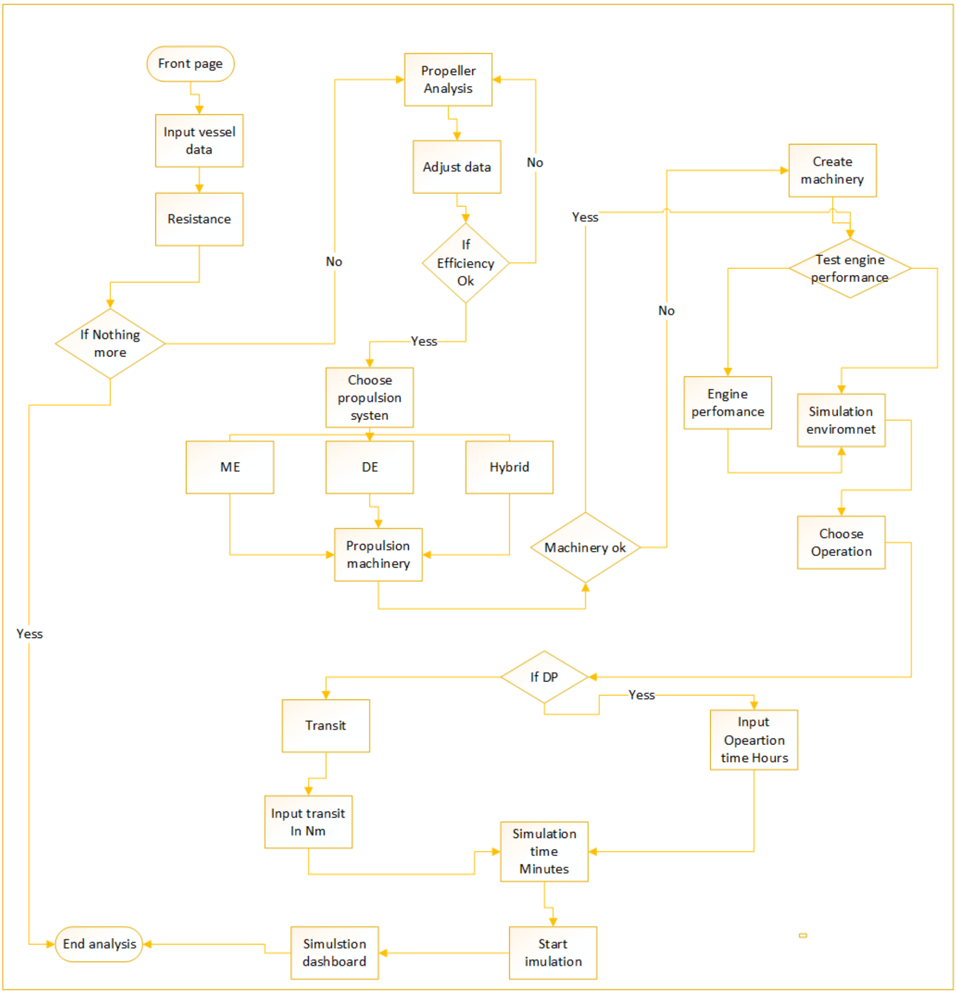

Figure 24: Simulation work flow

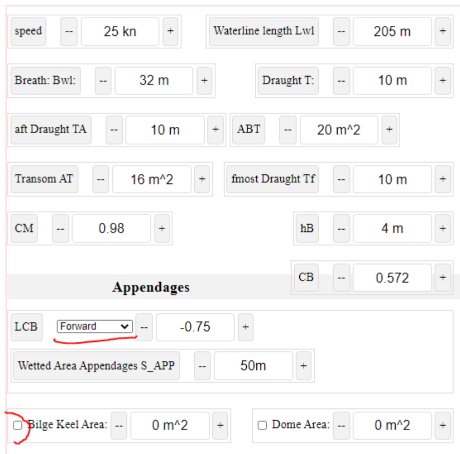

Figure 25: Vessel data input for resistance estimation

From the Figure shown, when you are on the front page, the first thing to do is to input the vessel data. In this case the data used for the case study is shown in Figure 21. The application accepts input of different dimensions and vessel data, as shown in Figure 25. For a vessel with different appendages, in order for the application to account for that you need to activate it by clicking the check button as shown. When inputting the lcb, an option is given to choose either $forward$ or aft, the $+$ is used to increase the values, while the $-$ is used to decrease the values. The user may also opt to simply type the values in.

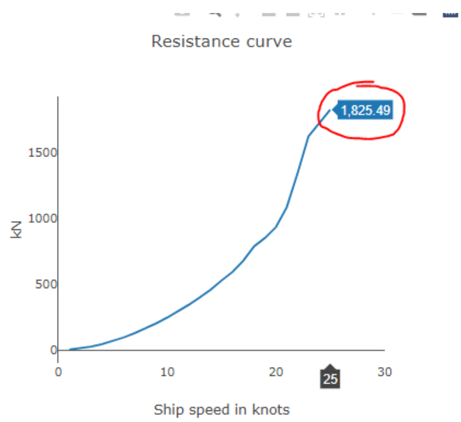

Figure 26: Vessel estimated resistance curve result

From the flow chart, after the vessel data is inputted, the resistance will automatically be calculated. Taking the reference vessel shown in Figure 21 as an example. the result of the resistance after the input is given in a curve of total resistance vs. speed, as shown in

Figure 26, while other results are given with respect to the different resistance components, as shown in Figure 22b. As shown in the flow Figure 24 if the user is only interested in the vessel resistance, then the process ends there.

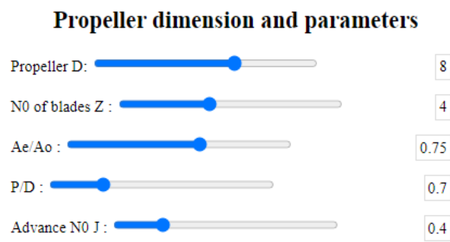

Figure 27: B series propeller adjustable input section

The next stage as shown from the flow chart is deciding the propeller that gives the best performance to the vessel based on the data that was input using the Wageningen B series. To do this a section on the application allows users to choose propeller combinations based on the Wageningen B series propeller data mentioned in section 2.2.6 and the propeller section on the application is shown in Figure 27. As shown in the process chart this involves an iterative process until the user is satisfied with the result.

PROPELLER PARAMETERS USING WAGENINGEN B-SCREW SERIES	
PARAMETERS	VALUES
Wake	0.276
KT	0.160
KQ	0.020
Hull efficiency	1.105
Open water efficiency	0.520
Thrust factor	0.20
advance propeller speed	9.31 m/s
propeller speed rps	2.91s^-1
Thrust T	2276.93 kN
Thrust Power	21245.6 kW
Power delivered to propeller	41224.54 kW
Effective power	23475.8 kW
Break Power: Calm water	42065.86 kW
Break Power: extrem condition	42065.86 kW

Figure 28: Estimated power and efficiency output

The result of the selected propeller are different output data which can be seen in Figure 28. Each time the user adjusts any of the propeller parameters as shown in Figure 27 the output is automatically updated based on the new data.

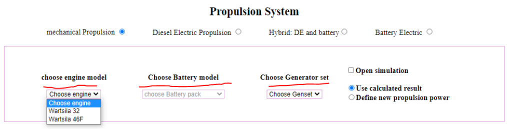

Figure 29: Propulsion system on the application

From the flow chart, after the user is satisfied with the efficiency output as shown in Figure 27, then they proceed to choosing the propulsion system of the vessel. The application allows users to choose different propulsion systems, as shown in Figure 29. When a propulsion system is selected, only the corresponding machinery for that system are available to be chosen. For example, as shown on the figure shows, when the ME propulsion was chosen, the battery pack becomes unavailable to be selected because a ME setup doesn't use a battery pack.

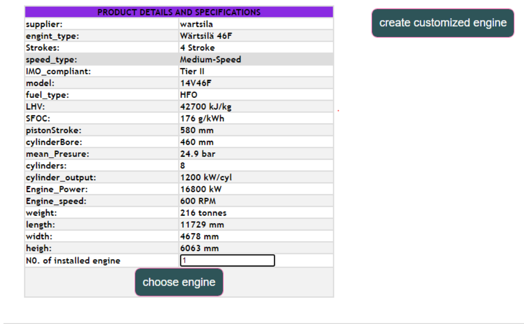

PRODUCT DETAILS AND SPECIFICATIONS	
supplier:	wartsila
engint_type:	Wärtsilä 46F
Strokes:	4 Stroke
speed_type:	Medium-Speed
IMO_compliant:	Tier II
model:	14V46F
fuel_type:	HFO
LHV:	42700 kJ/kg
SFOC:	176 g/kWh
pistonStroke:	580 mm
cylinderBore:	460 mm
mean_Presure:	24.9 bar
cylinders:	8
cylinder_output:	1200 kW/cyl
Engine_Power:	16800 kW
Engine_speed:	600 RPM
weight:	216 tonnes
length:	11729 mm
width:	4678 mm
heigh:	6063 mm
NO. of installed engine	1

Figure 30: Engine properties

For each propulsion system chosen, different machinery types are available. Taking the case for ME propulsion, two Diesel engine models from Wärtsilä have been built into the application allowing users to choose from list. By choosing any of the machinery models, the details of the engine are displayed as shown in Figure 30.

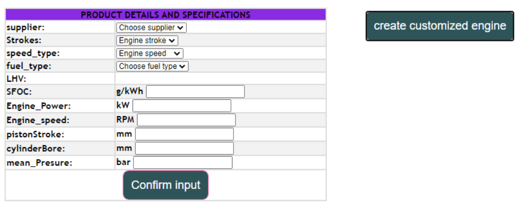

PRODUCT DETAILS AND SPECIFICATIONS	
supplier:	Choose supplier
Strokes:	Engine stroke
speed_type:	Engine speed
fuel_type:	Choose fuel type
LHV:	
SFOC:	g/kWh
Engine_Power:	kW
Engine_speed:	RPM
pistonStroke:	mm
cylinderBore:	mm
mean_Presure:	bar

Figure 31: Create a customized engine

From the flow chart, after the propulsion machinery is displayed and if the predefined machinery did not meet the user's needs, an option to customized machinery is available which will allow the user to create its own machinery, as shown in Figure 30, by clicking the “create customized engine” button a new window opens and allows users to input the machinery properties, as shown in Figure 31. The input field was designed to only accept engine models engine from MAN, Wärtsilä and CAT. This is due to the model used for engine performance (SFOC). When the user confirms the input, the created engine is stored as the predefined engine.

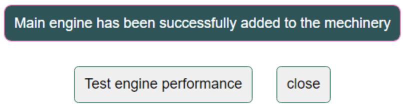

Figure 32: Engine installation confirmation

If the engine properties displayed are ok then the user can click the “choose engine” button as in Figure 30 to install the engine on the vessel. If creates its own engine then the “confirm input” button and installed the engine on the vessel. This will open a new window confirming that the engine has been successfully added to the machinery, shown in Figure 32.

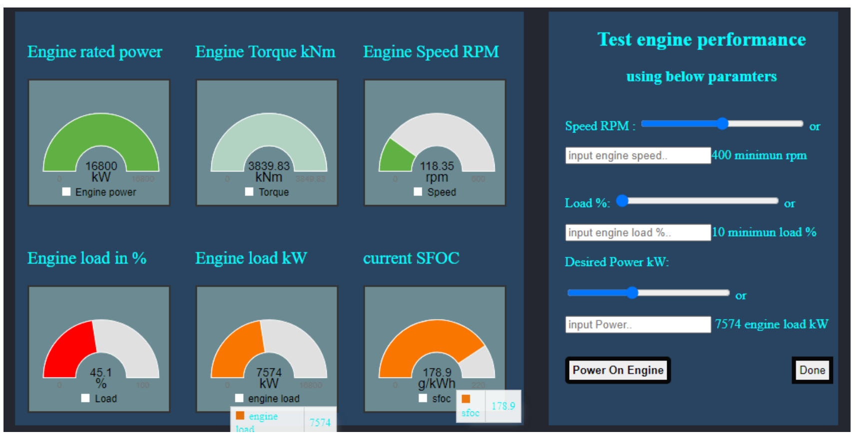

Figure 33: Engine dashboard for performance analysis

For users interested in engine performance analysis, the “Test engine performance” button shown in Figure 32 can be clicked, which will open a new window that containing a dashboard of engine parameters as shown in Figure 33. The dashboard figure shows the rated power, torque, speed, load in percentage, load and SFOC of the engine, while on the right side of the figure the user can adjust any of these parameters to see the performance of the engine as shown. For example, a user could increase the engine speed to see what power or SFOC the engine will produce at that speed. For every adjusted parameter, the effects are shown on the dashboard. Below the dashboard, is a section that is also displaying the engine performance by plotting a performance curve of load vs the SFOC as shown in Figure 34. When the user has completed the engine analysis, then the "Done" button can be clicked as shown on Figure 33 to close the dashboard and curve.

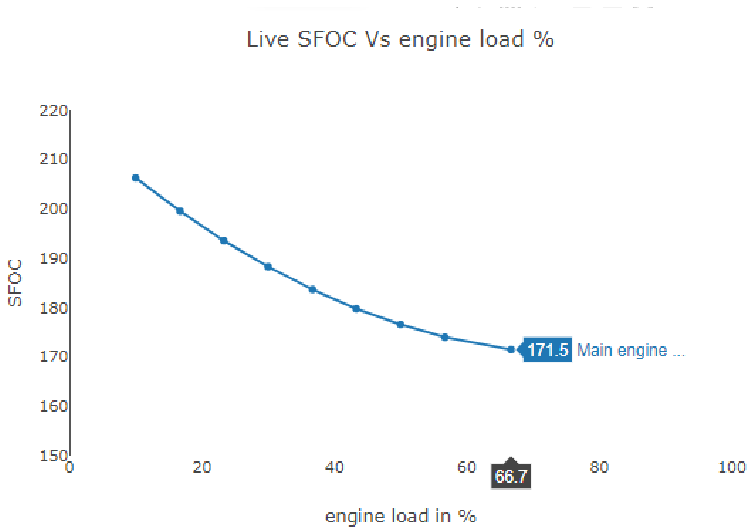

Figure 34: Engine performance analysis result: Load vs SFOC curve

The next step after the engine performance is completed is to start the simulation. To do that, the user should click the "open simulation" button shown in Figure 29, which will open a new window that allows users to choose the operation they want to simulate, as shown in Figure 35. In this case the Transit operation was chosen. The figure shows that, besides the Transit, an input called "Voyage nautical miles" is shown, while at the DP there is nothing shown. This is because the Transit operation have been chosen. If the DP operation is chosen, then that will close and a new input field will appear beside the DP, as shown on the flow chart.

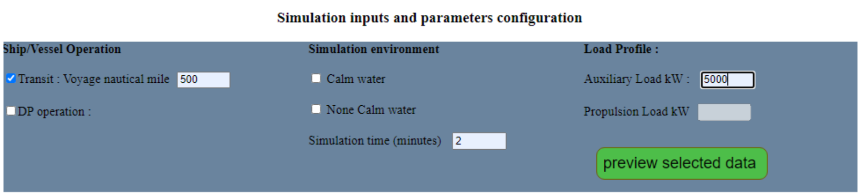

Figure 35: Engine dashboard for performance analysis

For a Transit simulation the voyage distance in Nautical miles is required as an input. In the example shown 500 Nautical miles was inputted. Another input is the auxiliary load. The simulation time as shown on the figure is the time that will take the application to complete the simulation. After the required input has been filled, as shown in Figure

35, then the “Preview selected data” button can be clicked, which will analyse the possible loads that the vessel could face and compare it to the installed power, then a new window will open showing the different engines that have been installed on the vessel (Figure 36), if the installed power is not enough, the a warning will appear telling you the minimum expected power.

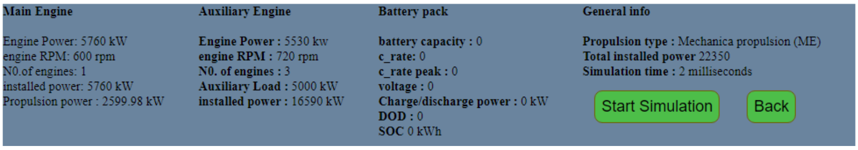

Figure 36: Preview of information for simulation

To start the simulation, the “start simulation” button is clicked as shown in Figure 36. This will open the main simulation dashboard, which is designed to mimic the bridge on a vessel as shown in Figure 37. The figure shows that the dashboard is divided into 7 sections, where **Propulsion system** is showing the installed power for propulsion, load, number of installed engines and active engine, fuel consumption of the propulsion system, and SFOC. The section **Auxiliary systems** shows the same things as shown in the **Propulsion system** but for the Auxiliary system . As shown, the Auxiliary systems shows that 4 gen-set are installed and two are online. The **Battery pack** section shows the battery capacity and different status when using the battery, like the SOC and capacity. One of the sections displays the ETA, vessel speed, wave height, remaining distance in nautical miles as shown. The **Power** section captures all the powers and loads that are generated and the loads that are on each engine online. From this section, you could see the available power installed and the total load, it also tracks the load on each of the engines that the PMS has assigned from the beginning of the simulation to the end.

Figure 37: Simulation Dashboard

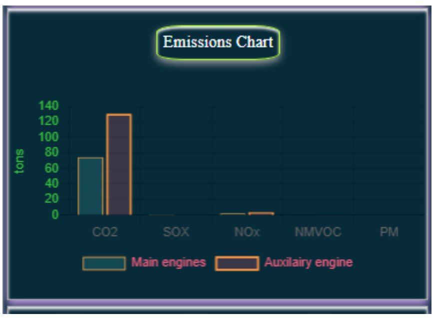

(a) main dashboard emission section

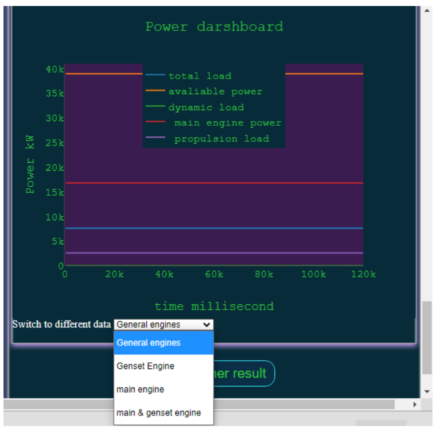

(b) main dashboard power section

Figure 38: Sections from the main dashboard

The power section on the simulation dashboard also allows users to change the type of power and load being displayed, as shown in Figure 38b. From the figure, it can seen that the possible drop down which allows users to choose either gen-set engine or main engine. The drop down list also changes with the type of propulsion system. For example, if it is a DE propulsion then there will be no main engine drop down, if battery packs are installed, it will also appear on the list. Another section on the main dashboard is **emission**. During a simulation, it shows the emissions from the engines and can be seen in a cut out section in Figure 38a. From the figure, it shows the emissions from the main engine and auxiliary engine. Simulations are always started in a calm water environment, which means no wave and wind are applied. A section on the dashboard **Update parameters** is used to activate different environmental conditions as shown. It allows adjusting the speed during an ongoing simulation, with the changes being applied to the simulation immediately. It also allows activating wave and wind as shown.

From the dashboard figure, a button called "check other results" can be clicked during or after a simulation. It will open a new window for operational data insights of the simulation and the new window has button for emissions, fuel cost, fuel consumption, and return to the main dashboard, as shown in Figure 39. When the emission button is clicked, a histogram of possible emission is shown, the user can choose different fuels and then it estimates different possible emissions if that fuel was used for the operation (Figure 39a). When the user clicks the "fuel cost" button, the display will change to a histogram of the estimated cost comparing different fuels (Figure 39b).

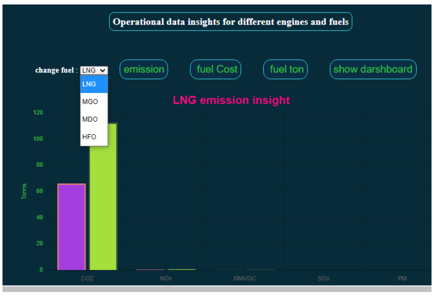

(a) Further emission insights

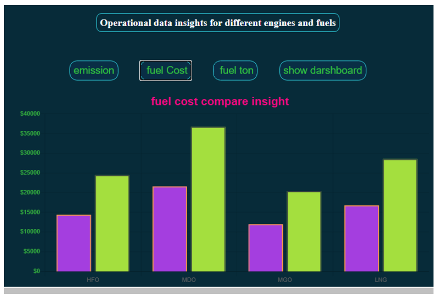

(b) Fuel cost insight

Figure 39: Operation data insights

Chapter 4

Analysis and Simulation

In this section two case studies will be analyzed using the application.

4.1 Case study: NTNU Gunnerus research vessel

The first case study involves NTNU research vessel "Gunnerus". The aim of the case study is to plan a transit operation with the vessel using the web-application in order to have an insight of the possible data that will be generated during the transit.

Gunnerus is a diesel electric propulsion (DE) vessel equipped with dynamic position system. A model view is shown in Figure 40. The main dimensions of the vessel are shown in Figure 41b, while some other dimensional data are shown in Annex C 6.2. The vessel is equipped with 3 Nogva-Scania generators with 450 kW, where the performance data of the generator from the supplier is shown in Annex C, Figure 64.

Figure 40: Gunnerus model from ShipLab (Vessel.js)

Machinery: Diesel electric propulsion

Main electric propulsion	1000 kW (Siemens 2 x 500 kW)
Main generators	3 x Nogva-Scania 450 kW
Bow tunnel thruster	1 x Brunvoll 200 kW
Speed at 100% MCR	12,6 kn
Cruising speed	9,4 kn
Gear	2 x Finnøy
Rudder	2 x Rolls-Royce, Ulstein Hinze Rudder FB-H 1200
Steering gear	2 x Rolls-Royce, Tenfjord SR562-FCPX2

(a) Gunnerus main machinery

Main dimensions

Length over all	(Loa)	31.25 m
Length between pp	(Lpp)	28.90 m
Length in waterline	(Lwl)	29.90 m
Breadth middle	(Bm)	9.60 m
Breadth extreme	(B)	9.90 m
Depth mld. Main deck	(Dm)	4.20 m
Draught, mld	(dm)	2.70 m
Mast height / antenna		14.85 / 19.70 m
Dead weight		107 t

(b) Gunnerus main dimensions

Figure 41: Gunnerus vessel dimensions and machinery NTNU [10]

4.1.1 Simplifications and assumptions

Some necessary data required as an input to the web-based application are not available for the Gunnerus vessel, therefor some assumptions, simplifications, and estimations had to be made to perform the analysis. One of the data required as an input to the application is the lcb which is based on the LCB, where the $LCB = 15.193$ is provided in the Annex C 63 and it be written in respect to the L_{WL} as $LCB = 15.193 - L_{WL}/2$ With value of the LCB and equation 16 the lcb is estimated to be 3.5 aft.

$$lcb = -\left(\frac{15.193 - \frac{29.9}{2}}{\frac{29.9}{2}}\right) \times 100 = -3.5\% \tag{117}$$

To estimate the power delivered to be propeller, the application uses a model based on the Wageningen B-series as described in section 2.2.6, but in the paper Sverre et al. [63], it is stated that Gunnerus is fitted with 19A type duct propeller, which is a K-series propeller. Therefore the application can not be used to estimate the K_T and K_Q of Gunnerus. In order to solve this, one of the files regarding gunnerus shows an analysis of the propeller installed on it as shown in Annex C Figure 65. This shows a curves of K_T and K_Q of the propeller, therefore a model was built based on these results to be used for estimating the properties of the propeller K_T and K_Q. Where the model is given in equations 119 and 118 respectively, X in the equation is the J. These models where integrated into the application to be able to estimate the K_T and K_Q of gunnerus.

$$K_{T,gun} = -0.0657X^3 + 0.177X^2 - 0.6979X + 0.8227 \tag{118}$$

$$10K_{Q,gun} = -0.104X^3 - 0.110X^2 - 0.022X + 0.873 \tag{119}$$

In Sverre et al. [63], the actual power consumption of Gunnerus is presented in a speed vs power curve shown in Figure 66, where the measured data was used to create a model for direct estimation of the vessel power based on the existing power consumption of the vessel. The model for the power estimation is given in equation 120, where $P_{actual,gun}$ is the actual power consumption on the vessel and X is the vessel speed in knots.

$$P_{actual,gun} = 3.973X^3 - 84.90X^2 + 669.1X - 1754.4 \tag{120}$$

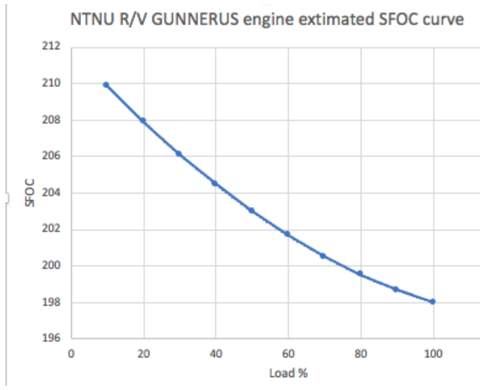

Figure 42: Gunnerus engine estimated SFOC curve

To be able to estimated the required fuel consumption or the possible emission for a voyage the application estimate the SFOC of the gen-set at every given load. At this stage of the application, the model used for estimation of the SFOC engine/gen-set is based on the major engine suppliers like MAN, Wärtsilä and CAT as mentioned earlier, therefore the model can not predict the SFOC for any engine out of this range.

From the Gunnerus data as shown in Figure 41, the gen-set is supplied by nogva [13], which is outside the model range for SFOC estimation. The supplier of the gen-set have provided some performance data of the engine as shown in Annex C Figure 64. Where it can be seen that at 100% of the engine load, the SFOC is given to be $198g/kWh$, at 75% the SFOC is $200g/kWh$ and at 50% of the engine load the SFOC is $203g/kWh$. From the given information a model was developed that is integrated into the application to allowing estimation of the SFOC of the engine at any given load, where the model is based on equation 121 and the X in the equation is the percentage of the load on the engine. Using the model, a SFOC vs load curve of the Gunnerus vessel is created as shown in Figure 42.

$$SFOC_{gun} = 0.0008X^2 - 0.22X + 212 \tag{121}$$

In order to estimate the resistance of the vessel, the application also required the dimension of the transom and the bulbous bow. From the data of the vessel provided these dimensions are not given but they are gotten from an external source.

The vessel will transit from Trondheim to Aalesund. The details of the voyage route are determined using ports.com [11] as shown in Figure 43. From the figure, it shows that the total voyage distance is 130 nautical miles and this will be the basis for the analysis.

4.1.2 Simulation steps

In this section, procedures used for the analysis on the application will be presented. The procedures are the same with the application work flow presented in section 3.7, but in this case Gunnerus data will be used.

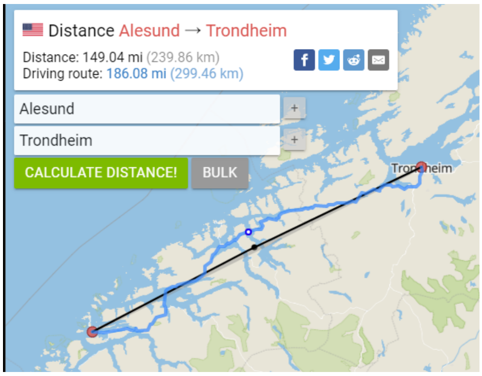

Figure 43: Gunnerus transit route to Aalesund ports.com [11]

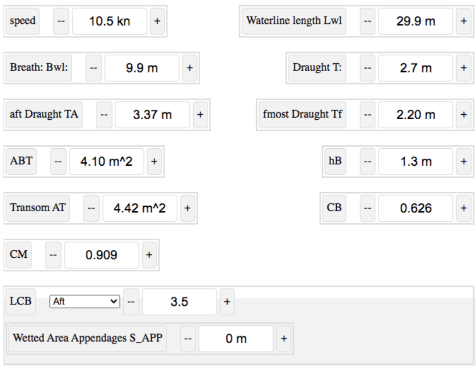

Figure 44: Input parameters for speed estimation

4.1.2.1 Gunnerus resistance

The estimation of the Gunnerus resistance was performed by inputting its dimensions to the respective field on the application. The dimensions that where input are shown in Figure 44. They are the data shown in Figures 41b and 63. While the ABT and AT are gotten from external source, other dimension like the appendages where not possible to obtained. The speed of 10.5 knots was used because Figure 41a shows that 9.4 knots is used during cruising speed and 12.6 is 100% MCR.

4.1.2.2 Propeller characteristic and power

To estimate the power of the vessel, the properties of the propeller are required to be inputted, as shown in Figure 45. These properties are used to estimate the efficiency of the propeller and the engine brake power. In section 4.1.1, it was established that the propeller on Gunnerus does not follow the model implemented in the application, therefore the estimated η, K_T and K_Q of the propeller are based on the new model that was integrated, as discussed.

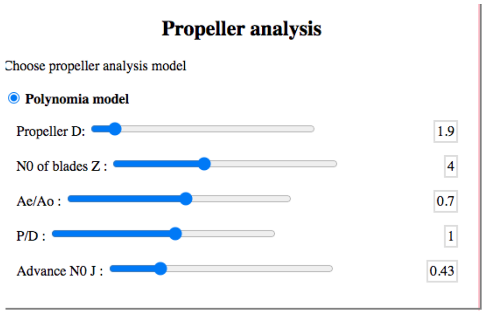

Figure 45: Input parameters for speed estimation

4.1.2.3 Propulsion system

After inputting propeller characteristics and estimating power, the next stage in the application is to choose the propulsion system and the engine to be installed on the vessel. The different possible propulsion systems are shown in Figure 46. From the figure it can be seen that diesel electric propulsion was chosen because Gunnerus also operates on that. When installing a generator set on the vessel, an option is shown allowing the user to choose a predefined generator or to create a customized one. The properties of the generator will be used to estimate the SFOC at any load. In section 4.1.1 a separate SFOC model for Gunnerus was created as discussed. This model was integrated into the application for SFOC estimation when the vessel is sailing.

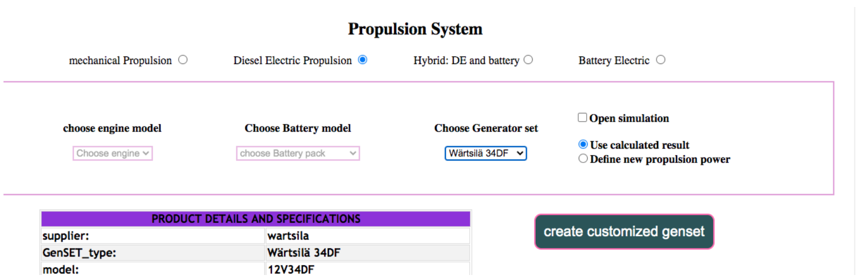

Figure 46: Gunnerus propulsion system

4.1.2.4 Operation details

After the propulsion step is done, the next step is to choose the operation the vessel will perform and to input the operational data. In previous sections, it has been stated that the case study will involve a transit condition with a voyage of 130 nautical miles. In Figure 47, the transit operation and the voyage distance that is used for the application is shown. The 3 minutes shown in the figure is the time the application will use to complete the simulation where the 20 kW is a random value of the auxiliary power since the application is expecting an input.

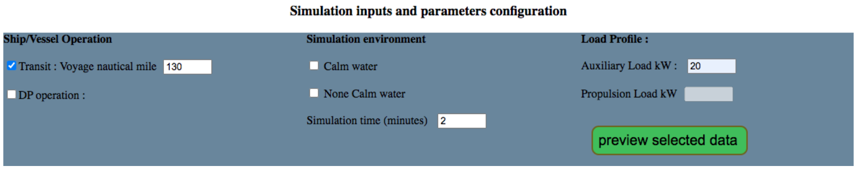

Figure 47: Gunnerus transit condition input

Having installed the generator set and defined all inputs, the summary of the machinery and other information are shown in Figure 48. From the figure, all the gen-set are considered as "Auxiliary engine" and the engines are considered as main engines by the application. Therefore, it can be seen that everything in the main engine is 0 except the propulsion power $712,47kW$ which is the estimated power from the inputs. In the auxiliary section as shown engine power is $450kW$ and the number of engines is 3. The battery pack capacity is 0 because no plant was chosen. The general section shows the propulsion system, which is DE, and the total installed power on the vessel, which is $1350kW$. The summary of the machinery is consistent with the machinery on Gunnerus, therefore the simulation can be performed.

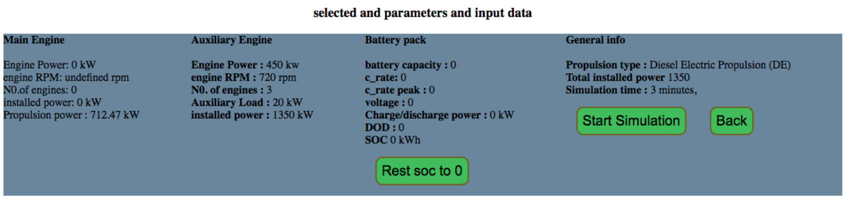

Figure 48: preview installed machinery

4.2 Result and Analysis

In this section, the result of the analysis from the application will be presented.

4.2.1 Gunnerus estimated resistance

In section 4.1.2.1, the available data of Gunnerus dimensions were input to the application. The resistance of the vessel was estimated based on those provided data and the result is shown in Figure 49. Figure 49b shows the resistance curve at 10.5 knots which gives a total resistance of $93.76kN$. From the resistance curve shown, it can be seen that the resistance increases steadily until $9knots$, at which point the result was about $33kN$, and at $10.5knots$ the resistance jumps to $93.76kN$. This nature of increase does not seem to be realistic. The reason for this might be the fact that some data of the dimension are mixed up or not correct since they are gotten from different sources. Figure 49a shows the different components of resistance respectively, from the figure, the $frictional\ resistance$ as shown is estimated to be $10.5kN$, the $bulbous\ resistance$ as shown is $3.113kN$, the $wave$

making resistances is estimated to be 65.07 kN. Other components of the resistance are shown in Figure 49a.

DIFFERENT RESISTANCE	
RESISTANCE	KN
Frictional	10.5
Wave making	65.065
Appendages	0
thruster resistance	0
pressure bulbous bow	3.113
pressure at Transom	6.8
Mid-ship Correlation	3.7
Air resistance	0
Wind resistance	0
Fouling Resistance	0.94
Wave resistance	186.77
Calm water resistance	93.76
Extrem condition Resistance	93.76

(a) Gunnerus component resistance

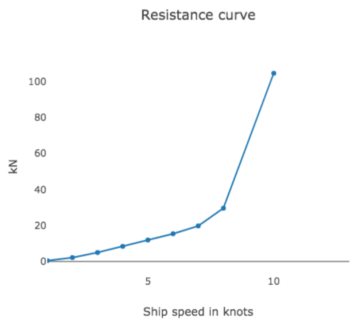

(b) Gunnerus resistance curve

Figure 49: Gunnerus estimated resistance based on the available data

4.2.2 Gunnerus estimated propeller characteristic and power

In section 4.1.2.2, the propeller properties were inputted and analyzed with $D = 1.9m$, $P/D = 1$ and $J = 0.61$ as estimated by the application. With this data and the model for the Gunnerus propeller as explained in section 4.1.2.2, the propeller K_T, K_Q and η are estimated as shown in Figure 50. In Annex C, Figure 65 the actual values of Gunnerus propeller characteristics are shown, comparing this to the estimated values at $J = 0.61$ the K_T, K_Q and η are approximately the same.

PROPELLER PARAMETERS USING WAGENINGEN B-SCREW SERIES	
PARAMETERS	VALUES
Wake	0.351
KT	0.420
KQ	0.078
Hull efficiency	1.272
Open water efficiency	0.566
Thrust factor	0.1747
advance propeller speed	3.5 m/s
propeller speed rps	2.8s^-1
Thrust T	123.73 kN
Thrust Power	398.24 kW
Power delivered to propeller	698.22 kW
Effective power	506.42 kW
Break Power: Calm water	712.47 kW
Break Power: extrem condition	712.47 kW

Figure 50: Propeller characteristic and power

From the results, the w is estimated to be 0.351, which seems higher than expected but no data to verify this, the reason for this higher value is because it is estimated using the Holtrop method, which depends on the actual dimension and some component resistance of the vessel as shown from equation 63 to 73 and some of the dimensions may be incorrect or mission as mentioned earlier. The result of the estimated Gunnerus power is $712.47kW$ as shown. Comparing this to the actual measured result of the vessel power, which gives about $450kW$ at 10.5 knots as shown in Annex C Figure 120) the difference in the two powers is due to the high resistance that was estimated.

4.2.3 Simulation dashboard

After previewing the machinery, choosing an operation, and starting the simulation, a dashboard is displayed as shown in Figure 51. The dashboard is used to monitor the current state of the operation which is updating every 500 milliseconds. From the dashboard in the auxiliary section, it can be seen that the total installed power is $1350kW$, the total load is $732.47kW$. If there is an increase due to waves, this will be updated instantly. In this simulation, the load is expected to be constant since it is assumed to be a calm water. The 3 is the total numbers of gen-sets installed on the vessel, the 2 is the current active gen-set online and if the PMS starts a new gen-set due to failure or dynamic loads this will update. The $199.39g/kWh$ is the SFOC of each gen-set online. The emission section on the dashboard shows the emissions of the operation at the current time. The section below the "emission" monitors the environment conditions, like the wave height if is activated. In this case it is $0m$ because the vessel is in a calm water. It also measures the current speed of the vessel, where is 10.5 knots is the current speed of Gunnerus. Finally, it calculates the ETA to the destination based on the inputted voyage distance and is updated based on the current speed. The power section monitors the loads and generators power as shown respectively.

Figure 51: Simulation dashboard

4.2.4 Operational data insight

The application analyze different data of the operation, therefore in this section the operational insights that may be relevant to the voyage preparation will be presented.

The dashboard in Figure 51 shows a summary of operational data insight, but it is possible to have more insights of each data separately as explained and shown in section

24. A separate window is open as shown in Figure 54. From the figure, it can be seen that it is possible to have an insight of different fuel data. by Clicking on the emission button, the emissions insights regarding the voyage for different types of fuels are available and can be visualized by choosing the fuel type as shown in figure 53a. The results of these different fuels assumes that the SFOC of the gen-sets are the same if they are used as fuel.

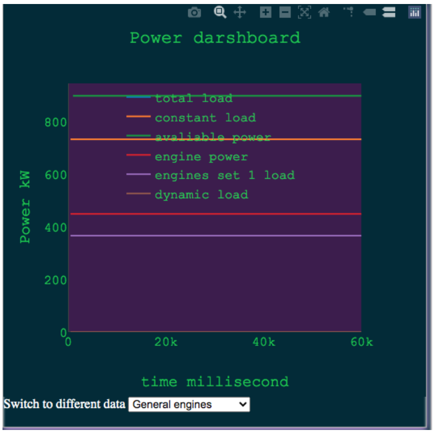

(a) Power and load insight

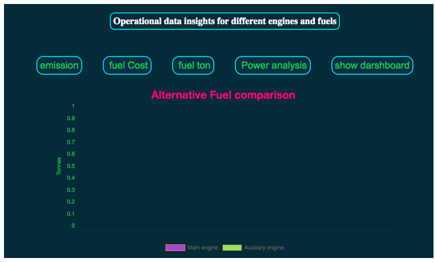

(b) Result data insight

Figure 52: Gunnerus voyage data insight

Figures 53b and 53a shows the result for emission for LNG and MGO, other fuel like HFO and MDO are possible to be displayed as shown in the drop-down menu in Figure 53a.

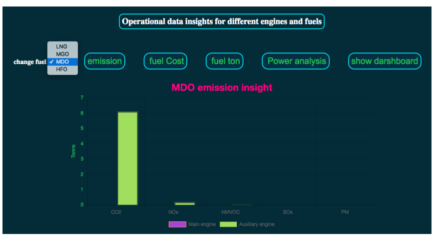

(a) MGO emission

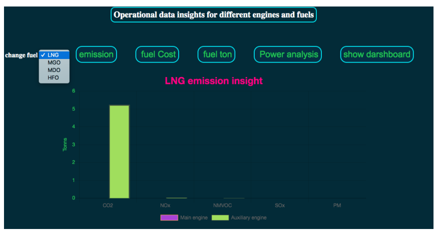

(b) LNG emission

Figure 53: Gunnerus voyage emission data insights

To have the insight on the fuel consumption of the voyage, the ”fuel ton” button is clicked, which will open the estimated fuel consumption of the voyage as shown in Figure 54b. From the figure, the total estimated fuel consumption of Gunnerus from Trondheim to Aalesund is about 3.5 tonnes.

Another important insight is the cost of operation, this can be accessed with the ”fuel cost” button, which shows a comparison between the estimated cost of different fuels, as in Figure 54a.

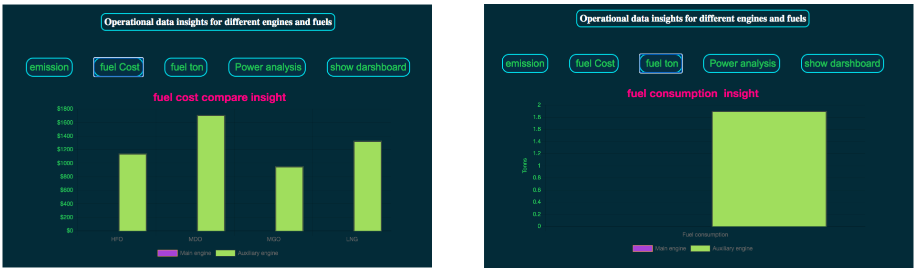

(a) Cost insights of different fuel types

(b) LNG emission

Figure 54: Gunnerus voyage emission data insights

4.2.5 Gunnerus Battery installation: PMS insights

Battery installations on vessels have increased recently due to the tight regulations from IMO and other concerns, as mentioned earlier. One of the major reasons for installing a battery on a vessel is to be used as a means for peak shaving, by setting the battery pack to take the peak loads that are supposed to affect the engine.

In this section, the designed PMS will be used to analyze the dynamic load the gen-set on Gunnerus is exposed to in a rough water environment with and without a battery pack installed. The analysis will not focus on the emission or fuel consumption during this period or the emission that can be saved by installing a battery pack, but the effect on the gen-set which will either result in an increase of emission or fuel consumption. Therefore it is assumed that Gunnerus has a PMS with the functionality as the one designed in this thesis.

Except for vessels that moves in a predefined route like ferries that could operations on completely on battery propulsion system while most other vessels, it is common that a battery pack is installed as either for a backup system or used for peak shaving of the dynamic loads MO [28]. In this analysis, it is assumed that the battery pack that will be installed is just for the purpose of peak shaving.

This case study will use one of the battery packs that has already been built into the application, which is from Energy [12]. To install a battery pack on the application, all the steps from the previous case study are the same, except that instead of choosing DE as shown in Figure 46, a hybrid propulsion will be chosen as shown in Figure 55. This will give the user access to the different battery packs available on the application, where the result of the chosen battery pack is displayed as shown in Figure 56.

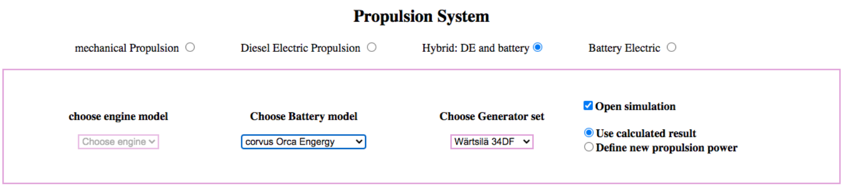

Figure 55: Hybrid: battery diesel electric propulsion

PRODUCT DETAILS AND SPECIFICATIONS	
supplier:	corvus
model:	Orca Energy
battery_Type:	Lithoum-ion
c_Rate_peak:	6 C
c_Rate:	3 C
lifeCycle:	800
DOD:	80 %
voltage:	1100 VDC
capacity:	125 kwh
SOC:	100 kWh
cont_charging_power:	375.0
peak_charging_power:	750.0
nor_Voltage:	980 VDC
weight:	1620 kg
heigh:	2200 mm
width:	645 mm
depth:	705 mm
choose battery pack	

Figure 56: Battery pack specification Energy [12]

Having installed the battery pack on Gunnerus, the machinery on the vessel can be previewed as shown in Figure 57. From the figure it can be seen that a battery pack with a capacity of 125 kWh and SOC of 100 kWh has been installed, while other conditions like speed, resistance, etc., are the same as the first case study. Before starting a simulation with the battery pack, a simulation case study without the battery in section 4.2.1 will be perform again, but in this case the function on the dashboard that allows tuning on different environments will be used to activate waves, leading to dynamic loads on the gen-set.

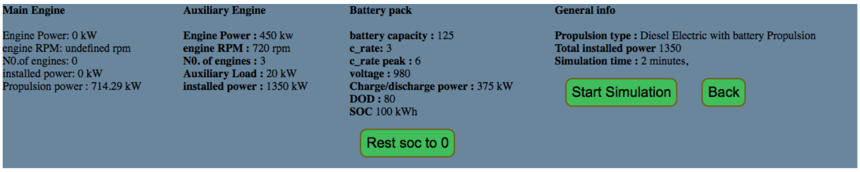

Figure 57: Preview of installed machinery

To understand the effect of the dynamic load, the data log by the PMS which is related to the load on each gen-set will be analyzed. The PMS controls the operation of every installed power system, including deciding the load on each gen-set as explained in section 3.4. Figure 58 shows a cut-out section from the main dashboard showing the power and load logs from the PMS during the rough weather simulation without battery installed.

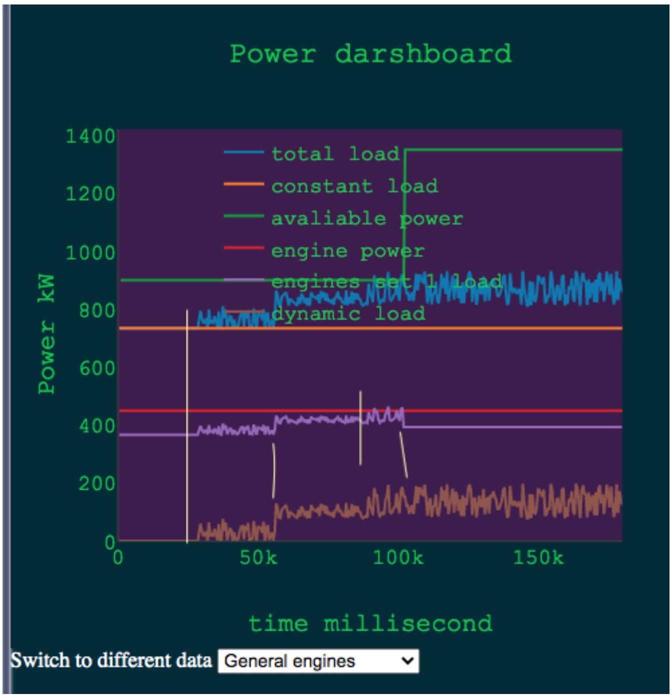

Figure 58: General PMS insights on power

From the figure, the legend with colors is used to show the different types of loads and power on the system. Where the total load is color coded as blue, constant load is coded as dark orange, the available power is coded as green, engine power is coded as red, load on the engine is code as purple and dynamic load is coded as brown. These colors may change when changing the layout.

When the simulation started, the conditions are the same as in Figure 51. Where PMS decides that 2 gen-set should be online and keeps the remaining gene-set as a backup as shown on the figure. After some seconds into the simulation, immediately after the first vertical line shown in Figure 58, the wave environment was activated as mentioned and the load became dynamic. The generated waves keeps increasing until after the third vertical line, then it reaches about 2 meters significant wave height. At this point, the total dynamic load on the two gen-set reaches the maximum accepted load on the combined engine, then a signal was sent to start the 3rd engine, which was on backup. It normally takes about 20 seconds for the generator to be ready to accept loads as shown, which corresponds to the fourth vertical line. Looking at the available power at that point, it went from about 900 kW which is the power for two gen-set to 1350 kW indicating the new gen-set has been turned online and is ready to accept load. At that same point, the load on one of the gen-set that was running on a full load was reduced and has a constant. This is because when the new gen-set was turned On, then the PMS reassigns and reallocates the loads on the gen-sets. To understand the effect of the dynamic loads on each individual engine, the button "switch to different data" as shown in Figure 58 was used to navigate through different gen-set. The results are shown in Figures 59a and 59b. One could see that both gen-sets follow the same pattern until the 3rd vertical line. This is because, before the 3rd vertical line, only two gen-set were online and running on the same load until the new gen-set was turned on. After that, the PMS assigned one of the first online gen-set and the new gen-set to running as one category, which means that they will have the same amount of load on them and they are called "set 1 engine" as shown in Figure 59a. From the figure, the load in the category remains constant even when there is a dynamic load on the whole system. This is because the PMS decides that the "set 1 engine" should have a constant load at about 80% of the engine rated load to reduce the dynamic loads on all systems. While the remaining gen-set is categorized as "set 2 engine" as shown in figure 59b, which is used for taking the dynamic load. This results in the gen-set to run on very low percentage of load.

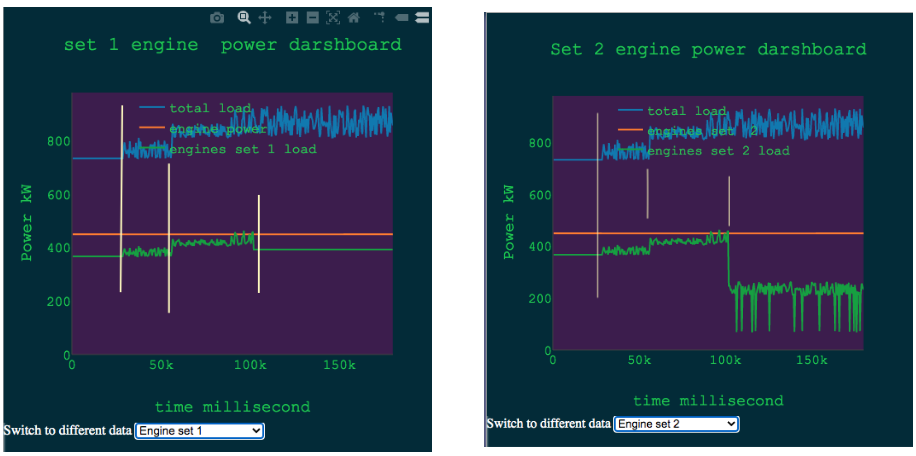

(a) Effect on gen-set 2

(b) Effect on gen-set 2

Figure 59: Dynamic effect insights on the Gunnerus gen-set

From Figure 59b, the low percentage of load and the dynamic loads on "gen-set 2" lead to the gen-set to run very low performance efficiency, which will result in higher SFOC, fuel consumption and emission on the gen-set, as explained by shi et al. [64]. This behaviour displayed by the gen-set is the result of how the PMS was designed, for other PMS this result might be different.

4.2.5.1 Battery storage effect

To analyze the effect of installing a battery pack, the same conditions, significant wave height, speed as in the simulation without battery is done in section 4.2.5 is carried out again with battery pack installed. Where the result of the simulation is shown in Figure 60, which is a cutout section from the main dashboard. from the figure, the simulation started in calm water which the load was constant until the wave environment was activated from the main dashboard at the first vertical line shown. To have better insight on what is happening, the dashboard was switch to focus only battery system as shown in Figure 60b. From the figure, when the simulation started there was no load on the battery as shown, until when the wave environment was activated at the first vertical line shown, this is because the PMS uses battery pack only for dynamic load. After the first vertical line, the load on the battery was the same as the dynamics load, indicating that dynamic loads are not affecting any of the gen-set since the battery is taking the load. At the second vertical line, the waves have reached the point where the 3rd gen-set was turned ON in the simulation done without the battery pack installed in section 4.2.5. Looking at this point only two gen-set are online as shown in Figure 61, and the gen-sets are still running on constant load as the battery pack takes the dynamic load. At the 3rd vertical line on battery dashboard Figure 60b, the SOC of the battery reaches 0, indicating the battery have discharged all its energy and can no longer take the load and the load on the battery dropped to $0kw$, this also corresponds to $50k$ millisecond as shown. The actual energy consumed by the battery is not represented by the simulation time, since the application simulation long operation in few minutes, that is why it seems like the battery pack discharged faster than expected.

(a) General power and load insight

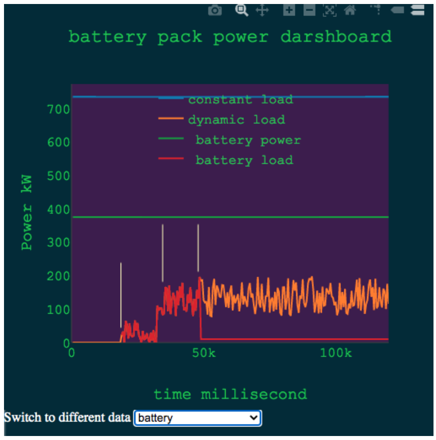

(b) Battery operation insights

Figure 60: PMS insights on engines and battery

Looking at the online gen-set at time $50k$ milliseconds (Figure 61), they started experiencing dynamic load on the two gen-set because the PMS has transferred the dynamic load that where on the battery pack to the gen-sets, which immediate reached the max possible accepted load. The request for starting the third gens-set was made at the 3rd vertical line shown in Figure 61b, and it takes around 20 seconds for the gen-set to be ready to take the load. After that, the get-sets now have the same behavior as the simulation without battery pack, where two gen-set are in operation at constant load while one of the gen-set is used for dynamic load.

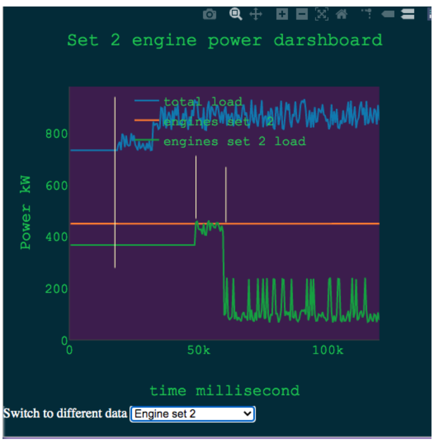

(a) Gen-set 2 insight

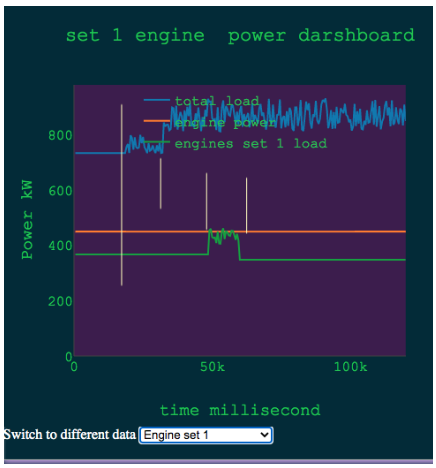

(b) Gen-set 1 insight

Figure 61: Insights on engine with battery and dynamic loads

From the insight of the two simulations performed, one could see that the simulation without battery pack uses all 3 the gen-sets, in which one gen-set is dedicated for the dynamics and was running on a low performance efficiency which will result in high emission and fuel consumption and even early maintenance on the gen-set. Comparing this to the simulation where a battery pack was installed, At the same dynamic loads only 2 get-sets were online and using the battery to take dynamic loads, allowing the two gen-sets to operate at its optimal efficiency. When the battery finishes discharging, the third get-set was turned on. In this case. The PMS should have used part of the power in charging to battery, which will cause the 3rd gen-set to run at a better efficiency even if the battery pack was not taking the dynamic load.

caro Arago Fonseca Henrique M. Gaspar

Chapter 5

Discussion

In this section, the results of this thesis will be discussed. The discussion will be divided into two sections, where one section will focus on the developed application while the other section will discuss the case study that was simulated using it.

5.1 Open source application

The aim of this thesis was to develop an open source application for ship machinery configuration analysis that will serve as a basis for more a complex system to be built upon.

The open source application is divided into sub-models as shown in Figure 16, where they can function individually or in interaction with one another to achieve the desired result. From the result of the verification in section 3.6.5, the ship resistance estimation from the application gives a total ship resistance of $1825kN$ while the result from the publication Holtrop.J [38] gives $1793.26kN$. The reason for this difference is the update made to equations as explained earlier. The effect of the updated equations is that the calculated value of the $(1 + k_1)$ from the benchmark as shown in Figure 22b is 1.156 while the value from the application is 1.193, which resulting in the difference of the total resistance. With this, it is safe that the resistance estimation section of the application is good enough for simulation or estimating of resistance in accordance to Holtrop and Mennen method.

The model that enables propeller analysis was built based on the Wageningen B-Series propeller. From the verification made, it shows that the result from the application gives approximately the same result with the existing data for a B series as shown in Figure 23. Since the support for other propeller series has not been included in the application, this means that the required power or open water characteristics of a vessel with a propeller that is not Wageningen B-Series can not be estimated at this stage of the application. This was the case when Gunnerus vessel was used for the case where a separate model was developed and integrated to estimate the open water characteristic. The main reason of integrating Wageningen B-Serie propeller first is that, is one of the most used propeller series Troost.L [43]. Based on the result of the verification of the propeller, it is safe to say that the application gives result that is good enough for Wageningen B-Serie propeller analysis.

On the application where a user is allowed to choose or create a customized engine, it only allows 3 main suppliers of engine models to be chosen. This constraint is due to the fact that the model for the engine SFOC is based on those 3 suppliers. In order to allow all engines to be used, another method which is not updated in this thesis has been implemented. The method uses a curve fitting method, where a polynomials equation is derived for each engine. The method uses a minimum of 3 data point on x and y to create a model based on these points. Since most engine suppliers provides the SFOC of the engine at 3 different load rates, these points could be inputted to the application where a model will be generated for estimating the SFOC of that specific engine. A typical example of how this works is the Gunnerus case study, where the engine supplier provides SFOC of the engine for 3 different loads. With this. a model was created for estimating the SFOC at any given time, as shown in equation 121.

The PMS that was designed in this thesis and implement into the application has not been compared to an existing model. From case study done, the performance of the PMS has been displayed by showing how it handles the different power sources by deciding how many engines to turn on, the load amount to assign each engine, turning off and on an engine, and load sharing among different power sources (diesel engine and battery). With the help of the PMS logs, the different engine performances are analyzed. Therefore it is safe to say that the basic functions of a PMS have been designed and integrated into the application.

During a simulation, the user can activate and control different weather environment features from the main dashboard, for example wave an wind. The waves that are generated by the system might not really represent the actual wave acting, this is because the algorithm for generating the wave uses the maximum expected significant wave height input by the user and generates waves from 0 up to that input wave height. This means that waves could jump from 0 m to max input value, this might result in a larger fluctuation in the dynamic loads than is supposed to be. To prevent this, a better algorithm for creating waves and wind could be implemented in the future.

On the application, it is shown that it is possible to perform a simulation of DP operation. As mentioned in section 3.6.3, the open water equations can not be used to estimate the actual power during DP. The method present for DP power estimation also lacks some data required to be implemented in the application. To account for the forces acting on the vessel during a DP operations, the force has to be considered in all directions, but this was not covered in this thesis. Therefore the DP simulation on the application at this stage will not give the actual result for a DP operation.

5.2 Case study

From the case study done with the application, the resistance curve of Gunnerus as shown in Figure 49b, gives a curve that is different than what was expected, which supposed to be a steadily increasing curve. However, as shown it has a jump from 9 to 10.5 knots. The actual main reason for this jump or high result can not accounted for, but this might be from the dimension of the vessel, since they where obtained from different sources.

Another reason could have been that the application gives a wrong result but since the resistance section of the application has been verified that option is ruled out, leaving only the dimensions to be the issue.

The Gunnerus power that was estimated with the application at 10.5 knots as shown in Figure 50 shows that the power is 714.29 kW. Comparing this to the existing power vs speed curve as shown in Annex C figure 66 which gives power about 450 kW at 10.5 knots. The difference for this due to the high resistance that was estimated . A possible reason could have been that the value of the open water characteristics are not correct, but these values have been compared to the existing result and they are approximately the same. Therefore the only possible issue that could cause the higher is the resistance as shown in the curve.

From the analysis of Gunnerus, the comparison between the effect of operating in wave condition first without and then with a battery pack installed. The result shows that the gen-set could experience a high dynamic load if subjected to the same weather condition used in the simulation when battery pack was not installed. This made one of the gen-sets to run in a very low efficiency, which will result in higher SFOC, high fuel consumption, emission and even shorten the life span of the gen-set or result in earlier maintenance due to the engine dynamics. From the analysis, installing a battery pack will reduce this high dynamics, thereby reducing the SFOC, and also preventing a new gen-set to be turned by the PMS

As shown on the application, different machinery has been built into the application. With this machinery, different configuration can be achieved, although this thesis did not consider every possible machinery configuration.

5.3 Possible analyses

In section 4, the application that was developed in this thesis was used to perform simulation with different machinery configurations. The simulations made are just few of the possible simulations that can be done with the application. Other possible analyses or simulations include:

- Simulation with direction propulsion.
- Simulation with DE propulsion, which is down with Gunnerus.
- Hybrid simulation; this simulation is shown when the DE and battery pack were simulated during the case study.
- Engine performance analysis during dynamic loads. This analysis can be seen in the case study where a simulation was one in rough weather condition.
- Effect of installing a battery pack; this analysis was also demonstrated during the case study.
- Blackout analysis; with logs on the PMS. It is possible to analyze the possibility of a blackout given a set of engine configuration.

Chapter 6

Conclusion and Further Work

6.1 Conclusion

In conclusion, this thesis was able to answer the research questions by using web technologies such as JavaScript, object and methods to represent vessel machinery as a mathematical model. These models are made to interact with each other to create the behaviour of the vessel machinery. Finally, this machinery has been used to created a simulation environment for vessel machinery configuration. Where some of the capability of the simulation environment were displayed by performing a simulation using the Gunnerus vessel. This allowed different machinery configurations to be analyzed in the case study.

6.2 Further Work

One of the aims of open source software (OSS) development is the continuous development and improvement of the system. As a basis for OSS, this application presents many areas that need to be improved. These include the models used and structure of code. Some of the major areas for future improvement are:

- DP operation simulation: as mentioned in the discussion, the DP simulation will not give an actual DP operation result. To solve this issue, a method to handle the forces in all directions of the vessel should be integrated into the system.

- Four propeller quadrants and other series: as mentioned, at this stage only Wageningen B series propellers are integrated to the application. To extend the range of this application, other propeller series should be integrated. Another area of the propeller section that needs to be improved is the extension of the model to include the four quadrants of the propeller.

- Machinery configuration: new machinery can be integrated into the application to allow users to create different configurations. The system could be extended to include machinery configurations such as, for example, a hybrid system for ME propulsion with power take in and power take out.

- Today ship energy efficiency is a key factor in IMO agenda, where requirement are made for a new vessel to achieved a certain Energy Efficiency Design Index (EEDI). The guideline made by IMO on how to estimated the EEDI should be integrated into application to allow the application to measure the EEDI of vessel.

Bibliography

[1] Holtrop.J. A statistical resistance prediction method with a speed dependent form factor. In *Scientific and Methodological Seminar on Ship Hydrodynamics (SMSSH'88)*, Varna Bulgaria, 1988. P. 1-7.

[2] Oossanen.P Oosterveld.M. Further computer-analyzed data of the wageningen b-screw series. *INTERNATtONAL SHIPBUILDING PROGRESS*, 22: 251 - 261, 1975. doi: 10.3233/ISP-1975-2225102.

[3] IMO. Third imo ghg study 2014 executive summary and final report, 27.08.2020. URL http://www.imo.org/en/OurWork/Environment/PollutionPrevention/AirPollution/Documents/Third%20Greenhouse%20Gas%20Study/GHG3%20Executive%20Summary%20and%20Report.pdf. (accessed data : 12.09.2020).

[4] power equipment direct. Two-stroke vs. four-stroke. URL https://www.powerequipmentdirect.com/stories/116-How-2-Cycle-and-4-Cycle-Engines-Differ.html. Accessed date : 01. 09. 2020.

[5] Zakerdoost Hassan and Ghassemi Hassan. Application of a variable-fidelity hydrodynamic optimization strategy in fuel-efficient ship design. *SAGE Jounals*, 233: 6293–6306, 2018. doi: 10.1177/0954406218792574.

[6] J.-P Jalkanen, Lasse Johansson, Jaakko Kukkonen, Anders Brink, Juha Kalli, and Tapani Stipa. Extension of an assessment model of ship traffic exhaust emissions for particulate matter and carbon monoxide. *Atmospheric Chemistry and Physics*, 12, 03 2012. doi: 10.5194/acp-12-2641-2012.

[7] MAN. Basic principles of ship propulsion. URL https://spain.mandieselturbo.com/docs/librariesprovider10/sistemas-propulsivos-marinos/basic-principles-of-ship-propulsion.pdf?sfvrsn=2. (accessed data : 17.09.2020).

[8] Iso-1501. Guidelines for the assessment of speed and power performance by analysis of speed trial data first edition, 2015. Accessed date : 30. 09. 2020.

[9] Morales Vsquez Cristian A. Evaluation of medium speed diesel generator sets and energy storage technologies as alternatives for reducing fuel consumption and exhaust emissions in electric propulsion systems for psvs. *Ship Science and Technology*, Vol.9 No.18:49, 2016. doi: doi.org/10.25043/19098642.128.

[10] NTNU. Gunnerus detail. Accessed date : 08. 11. 2020
https://www.ntnu.edu/oceans/gunnerus/spesifications.

[11] ports.com. Sea route distance. Accessed date : 15. 11. 2020
http://ports.com/sea-route/.

[12] Corvus Energy. Corvus orca energy. Accessed date : 20. 11. 2020
https://corvusenergy.com/products/corvus-orca-energy/.

[13] nogva. Di16 074m. Accessed date : 15. 11. 2020
http://www.nogva.no/en/products/auxiliary/scania/di16-074m.

[14] Tiedo Tinga, Wieger Tiddens, F Amoiralis, and M Politis. Predictive maintenance of maritime systems: Models and challenges. pages 68–68, 06 2017. doi: 10.1201/9781315210469-56.

[15] Riviera. Electric propulsion key to a zero-emissions future in cruise. Accessed date : 20. 11. 2020
https://www.rivieramm.com/expert-views/expert-views/electric-propulsion-key-to-a-zero-emissions-future-in-cruise.

[16] Siri Solem, Kjetil Fagerholt, Stein Erikstad, and yvind Patricksson. Optimization of diesel electric machinery system configuration in conceptual ship design. *Journal of Marine Science and Technology*, 20, 02 2015. doi: 10.1007/s00773-015-0307-4.

[17] Sandbakken Egil Christoffer. Marine machinery systems - tools and architecture. Master's thesis, 2010. institution: Norwegian University of Science and Technology.

[18] Bendik Voldnes. Simulation of marine hybrid machinery systems based on vessel operational data. Master's thesis, 2017. institution: Norwegian University of Science and Technology.

[19] Gaspar Henrique M., . Fonseca Icaro A, and de Oliveira Felipe F. Virtual prototyping and simulation of multibody marine operations using web-based technologies. In *proceedings of the ASME 2019 38th International Conference on Ocean Offshore & Arctic Engineering (OMAE 2019)*, Glasgow, Scotland, UK, 2019.

[20] Lothar Birk. *Fundamentals of Ship Hydrodynamics : Fluid Mechanics, Ship Resistance and Propulsion*. John Wiley & Son Ltd, University of New Orleans, USA, 2019. ISBN 9781118855515.

[21] yvind Notland Smogeli. ***Control of Marine Propellers From Normal to Extreme Conditions***. PhD thesis, 2006. ISBN 82-471-8147-9, Institution: Department of Marine Technology Norwegian University of Science and Technology.

[22] Lammeren Van, Manen D.van, Oostervel M. W. C., and W P A J. The wageningen b-screw series. In *Transactions of SNAME*, 1969.

[23] Chris Woodford. Diesel engines. URL https://www.explainthatstuff.com/diesel-engines.html. Accessed date : 01. 09. 2020.

[24] marinediesels. marinediesels.info. URL http://www.marinediesels.info/. Accessed date : 01. 09. 2020.

[25] wartsila. Wrtsil encyclopedia of marine technology: Diesel engine. URL https://www.wartsila.com/encyclopedia/term/diesel-engine. Accessed date : 01. 09. 2020.

[26] APEX INNOVATIONS. Engine theory and calculations. URL https://www.apexinnovations.co.in/pdf/Engine_theory_and_calculations.pdf. Accessed date : 10. 09. 2020.

[27] x Engineer. What is the mean effective pressure (mep) of an engine ? URL https://x-engineer.org/automotive-engineering/internal-combustion-engines/ice-components-systems/mean-effective-pressure-mep/. Accessed date : 10. 09. 2020.

[28] OLVE MO. Whats the point of installing batteries on marine vessels if the batteries are charged by electricity from their diesel generators?, 2019. URL https://blog.sintef.com/sintefenergy/why-install-batteries-on-ships/. Accessed date : 12. 09. 2020.

[29] Ovrum E and T.F. Bergh. Modelling lithium-ion battery hybrid ship crane operation. *Applied Energy*, 152:162–172, 2015. doi: doi.org/10.1016/j.apenergy.2015.01.066. DNV GL NO-1322 Hvik Norway.

[30] Tremblay Olivier, Dessaint Louis-A., and Dekkiche Abdel-Illah. A generic battery model for the dynamic simulation of hybrid electric vehicles. In *2007 IEEE Vehicle Power and Propulsion Conference*, Arlington, TX, USA, 2007. doi: 10.1109/VPPC.2007.4544139. institution : Electrical Engineering Department, Ecole de Technologie Superieure,
ISSN :1938-8756.

[31] Electropaedia. Battery management systems (bms). URL https://www.mpoweruk.com/bms.htm. Accessed date : 16. 09. 2020.

[32] DNVGL. Dnv gl handbook for maritime and offshore battery systems. 2016. Revision: V1.0.

[33] DNV GL. Part 6 additional class notations chapter 2 propulsion, power generation and auxiliary systems. URL http://rules.dnvgl.com/docs/pdf/DNVGL/RU-SHIP/2016-07/DNVGL-RU-SHIP-Pt6Ch2.pdf. Edition : July 2016, Accessed date : 16. 09. 2020.

[34] Molland Anthony F., Turnock Stephen R., and Hudson Dominic A. *Ship Resistance and Propulsion : Practical Estimation of Propulsive Power*. Cambridge University Press, University of Southampton, 2011. ISBN 9780511974113. doi: https://doi.org/10.1017/CBO9780511974113.

[35] ITTC. 1978 ittc performance prediction method. In *Recommended Procedures and Guidelines - ITTC, 7.5-02 03-01.4*, 2017. Revision 04.

[36] J Holtrop. and Mennen G.G.J. A statistical power prediction method. In *International Ship building Progress*, volume 25(290) : 253-256, Rotterdam Netherlands, 1978. Revision 04.

[37] J Holtrop. and Mennen G.G.J. An approximate power prediction method. In *International Shipbuilding Progress*, volume 29(290) : 166 - 170, Copenhagen Danmark, 1982. Revision 04.

[38] Holtrop.J. Statistical re-analysis of resistance and propulsion data. international shipbuilding progress. In *International Ship building Progress*, volume 31(363): 272276, 1984. Revision 04.

[39] Harvald.S Guldhammer.H. Ship resistance - effect of form and principal dimensions. *Akademisk Forlag : Copenhagen Danmark*, 1974. revised.

[40] G Jensen. *Moderne Schiffslinien*, volume XXXII : page 93 - 110. Handbuch der Werften, 1994. Hansa.

[41] IMO. Draft revised guidelines for determining minimum propulsion power to maintain the manoeuvrability of ships in adverse conditions : 71/inf.28 28 april 2017 english only, 2017. URL http://www.iacs.org.uk/media/4419/mepc-71-inf28-draft-revised-guidelines-for-determining-minimum-propu pdf. Accessed date : 30. 09. 2020.

[42] kuiper.G. The wageningen propeller series. *Maritime Research Institute Netherlands :Wageningen, the Netherlands*, publication no : 92 - 001, 1992.

[43] Troost.L. Open water test series with modern propeller forms, part 2. *Transactions of North East Coast Institute of Engineers and Shipbuilders*, publication No. 42 : PP 91, 1940. N.S.M.B.

[44] Troost.L. Open water test series with modern propeller forms, part 2. *Transactions of North East Coast Institute of Engineers and Shipbuilders*, publication No. 33 : 321, 1938.

[45] Lammeren W.P.A van, Manen J.D.van, and M.Oosterveld. The wageningen b screw series. *Transactions of SNAME*, 77: 269-317, 1969.

[46] Pivano Luca, Johansen Tor Arne, and Smogeli yvind N. A four-quadrant thrust estimation scheme for marine propellers: Theory and experiments. *IEEE TRANSACTIONS ON CONTROL SYSTEM TECHNOLOGY*, XX :Y, 2008.

[47] I.Ya. Miniovich. Investigation of hydrodynamic characteristics of screw propellers under conditions of reversing and calculation methods for backing of ships. *Buships Translation 697*, 1960.

[48] Lammeren W.P.A.van, Manen J.D.van, and Oosterveld M.W.C. The wageningen b-screw series. 1969.

[49] Wikiwand. Marine propulsion. Accessed date : 30. 09. 2020.

[50] Geertsma [a,b,*] R.D., Visser [a,b] R.R, Negenborn [b]and K., and Hopman [a] J.J. Design and control of hybrid power and propulsion systems for smart ships: A review of developments. *Applied Energy*, 194:30–54, 2017. doi: https://doi.org/10.1016/j.apenergy.2017.02.060. institution: [a]Department of Maritime and Technology, Delft University of Technology, The Netherlands
[b] Faculty of Military Sciences, Netherlands Defence Academy, The Netherlands.

[51] Torstein B Ingebrigtsen. *Scenario- and OptimizationBased Control of Marine Electric Power Systems*. PhD thesis, 2016. ISBN 978-82-471-6647-5. Institution: Department Of Cybernetics Norwegian University of Science and Technology.

[52] Damir Radan. *Integrated Control of Marine Electrical Power Systems*. PhD thesis, 2008. ISBN 978-82-471-6647-5. Institution: Department of Marine Technology Norwegian University of Science and Technology.

[53] hoglund. Power management system (pms). URL https://hoglund.no/solutions/marine-automation/power-management-system-pms. Accessed date : 30. 09. 2020.

[54] John May Halvard Foss. Power management system for the ”deepwater horizon” a dynamically positioned all weather semisubmersible. In *Dynamic Positioning Conference*, 2000. URL https://dynamic-positioning.com/proceedings/dp2000/power_foss.pdf.

[55] A.K.dnanes T.Lauvdal. Power plant pms with fast acting load reduction for dp vessels. In *Dynamic Positioning Conference*, 2000. URL https://dynamic-positioning.com/proceedings/dp2000/power_lauvdal.pdf.

[56] RADA DAMIR, JOHANSEN TOR A., SRENSEN ASGEIR J., and DNANES ALF KRE. Optimization of load dependent start tables in marine power management systems with blackout prevention. In *WSEAS Transactions on Circuits and Systems*, volume 4(12), pages 1861–1866, 2005.

[57] MAN Diesel SE. Project guide for marine plants, diesel engine 48/60b, 2006. Accessed date : 30. 09. 2020.

[58] PE John J.May. Improving engine utilization on dp drilling vessels. In *Dynamic Positioning Conference*, 2003. URL https://dynamic-positioning.com/proceedings/dp2003/power_may.pdf.

[59] DNVGL. Offshore stabdard dnv-os-d201electrical installations, 2011. DNV GL: Oslo, Norway.

[60] Vessel.js. Introduction. URL https://shiplab.github.io/vesseljs/. Accessed date : 4. 10. 2020.

[61] Wartsila. Wrtsil 46f product guide, . URL https://www.wartsila.com/marine/build/engines-and-generating-sets/diesel-engines/wartsila-46f. Accessed date : 10. 10. 2020.

[62] Wartsila. Wrtsil 32 product guide, . URL https://www.wartsila.com/marine/build/engines-and-generating-sets/diesel-engines/wartsila-32f. Accessed date : 10. 10. 2020.

[63] Steen Sverre, Savio Luca, Selvik rjan, and Vahid Hassani. Experience with rim-driven azimuthing thrusters on the research ship gunnerus. *MARINTEK,NTNU*.

[64] w shi, Robert van de Ketterij, Douwe Stapersma, Hugo Grimmelius, and Benny Mestemaker. The effect of dynamic load on fuel consumption and exhaust emissions of tshd during dredging process. 09 2010.

Annex

Annex A: Fuel data

Table 8: Fuel and there emission factor IMO [3]

Emission type	Fuel type	emission factor
CO_2	LNG HFO MGO	2.750 3.114 3.206
SO_X	LNG HFO MGO	0 0.025 0.010
NO_X	LNG HFO MGO	0.0140 0.0903 0.0961
PM	LNG HFO MGO	0.00018 0.00728 0.00097
$NMOCV$	LNG HFO MGO	0.003 0.00308 0.00308

Annex B: Wangeningen B Series

k	A_T	B_T	A_Q	B_Q
0	2.5350E-02	0.0000E-00	2.4645E-03	0.0000E-00
1	1.7820E-01	-7.4777E-01	2.6718E-02	-1.1081E-01
2	1.4674E-02	-1.3822E-02	1.6056E-03	1.5909E-04
3	2.8054E-02	1.0077E-01	6.5822E-03	1.6455E-02
4	-1.6328E-02	-1.1318E-02	-2.2497E-03	-2.0601E-03
5	-5.3041E-02	4.7186E-02	-7.8062E-03	8.5343E-03
6	6.0605E-04	1.0666E-02	2.4126E-04	8.7856E-04
7	3.6823E-02	-9.0239E-03	6.1475E-03	-3.1327E-03
8	-2.5429E-03	-7.8452E-03	-1.6065E-03	-9.6650E-04
9	-1.7680E-02	2.3941E-02	-3.3291E-03	4.3190E-03
10	2.7331E-03	8.0787E-03	1.2311E-03	1.2453E-03
11	2.1436E-02	-1.4942E-04	3.1123E-03	9.5986E-05
12	-2.4782E-03	-3.1925E-03	-1.2559E-03	-7.9986E-04
13	1.2317E-03	9.2620E-03	1.3948E-03	1.5073E-03
14	5.0980E-03	1.5527E-03	8.8397E-04	2.4595E-04
15	7.8076E-03	-6.5683E-03	5.0358E-05	-1.6918E-03
16	-3.7816E-03	-6.1655E-04	-7.9990E-04	5.1603E-04
17	3.5353E-03	5.1033E-03	1.3345E-03	1.1504E-03
18	5.3014E-03	-6.0263E-04	1.1928E-03	-4.7976E-04
19	2.1940E-03	-8.2244E-03	-1.3556E-04	-1.4566E-03
20	-2.8306E-03	-6.3789E-04	-7.0825E-04	2.3280E-04

Figure 62: Fouries series Coefficient for Wangeningen B4-70 propeller

Annex C: Gunnerus Vessel Data

DATA-CHECK PROPERTIES	ENCL. 1)
	REPORT
	DATE 2020-11-13
	REF

Run name:

Ship name: inputHVL.mgf (imported)
Loading condition description: Design water line after elongation

ShipX exported data
Main dimensions (from input):

Length between perpendiculars	(m)	33.900
Breadth	(m)	9.600
Draught, midship	(m)	2.786
Sinkage	(m)	0.000
Trim, + = aft	(deg)	0.000

Coefficients for data check etc.:

Type		Specified	Calculated
Displacement	(tonnes)	584.15	579.59*
Vertical center of bouyancy,	KB		1.657*
Vertical center of gravity,	VCG	2.786*	
Longitudinal center of bouyancy,	LCB		15.193*
Longitudinal center of gravity,	LCG	15.188	15.193*
Block coefficient,	Cb	0.626	0.624
Water plane area coefficient,	Cw	0.846	0.869
Prismatic coefficient,	Cp		0.724
Mid section area coefficient,	Cm	0.906	0.861*
Longitudinal metacentric height,	GMl		38.583*
Transverse metacentric height,	GMt		2.290*
Roll radius of gyration,	r44	3.300*	
Pitch radius of gyration,	r55	8.475*	
Yaw radius of gyration,	r66	8.475*	
Roll-yaw radius of gyration,	r46	0.000*	

* - Applied in the hydrodynamic calculations

ShipX - 16.11.2019 - 12.22.38 - Licensed to: NTNU (NTNU)

Figure 63: Gunerus data from NTNU computer folder

Rated power and fuel consumption		
RPM / Hz	***1500 / 50***	***1800 / 60***
Generator effect	450 kW	511 kW
Torque	2865 Nm	2711 Nm
Fuel Consumption 100%	198 g/kWh	202 g/kWh
Fuel Consumption 75%	200 g/kWh	203 g/kWh
Fuel Consumption 50%	203 g/kWh	207 g/kWh
Emission ratings	EU Stage IIIa US Tier 2 and IMO Tier II	

Figure 64: Gunnerus engine performance datanogva [13]

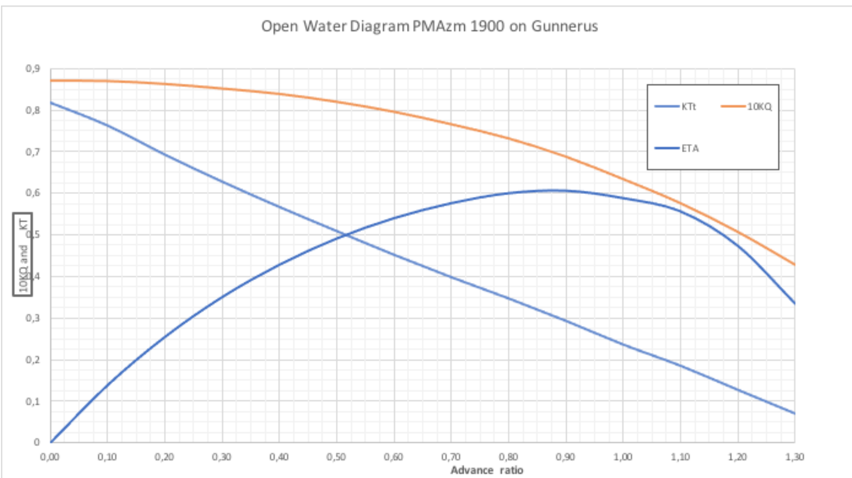

Figure 65: Gunnerus engine performance data

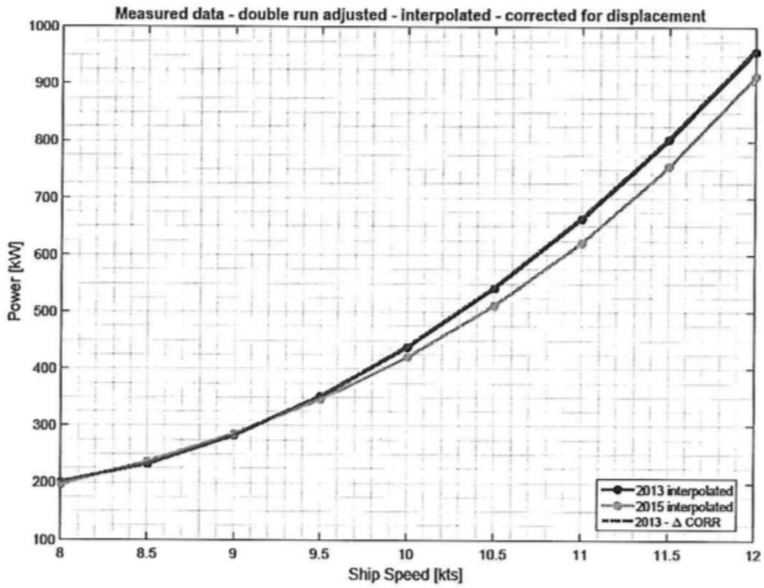

Figure 66: Existing gunnerus power curve

Appendix

Appendix A: GitHub Details

The software is hosted on GitHub page and the code is also on GitHub to allow developers collaborate.

To access the code on GitHub use this link: open code here or use this link https://github.com/osain-az/Vessel-Machinery-Configuration

To access the application use the Link provided here : open application here or use this link
https://osain-az.github.io/Vessel-Machinery-Configuration